

Evidence for periodicity in 43-year-long monitoring of NGC 5548

E. Bon^{1,2}, S. Zucker³, H. Netzer⁴, P. Marziani⁵, N. Bon^{1,2}, P. Jovanović^{1,2}, A. I. Shapovalova⁶, S. Komossa⁷, C. M. Gaskell⁸, L. Č. Popović^{1,2}, S. Britzen⁷, V. H. Chavushyan⁹, A. N. Burenkov⁶, S. Sergeev¹⁰, G. La Mura¹¹, J. R. Valdés⁹ & M. Stalevski^{1,12,13}

ABSTRACT

We present an analysis of 43 years (1972 to 2015) of spectroscopic observations of the Seyfert 1 galaxy NGC 5548. This includes 12 years of new unpublished observations (2003 to 2015). We compiled about 1600 H β spectra and analyzed the long-term spectral variations of the 5100 Å continuum and the H β line. Our analysis is based on standard procedures, including the LombScargle method, which is known to be rather limited to such heterogeneous data sets, and a new method developed specifically for this project that is more robust and reveals a

¹Astronomical Observatory, Volgina 7, 11060 Belgrade, Serbia;

²Isaac Newton Institute of Chile, Yugoslavia branch, Serbia;

³Department of Geosciences, Tel-Aviv University, tel-aviv 6997801, Israel;

⁴School of Physics and Astronomy and the Wise Observatory, The Raymond and Beverly Sackler Faculty of Exact Sciences, Tel-Aviv University, tel-aviv 6997801, Israel;

⁵INAF, Osservatorio Astronomico di Padova, Padova, Italia;

⁶Special Astrophysical Observatory of the Russian AS, Nizhnij Arkhyz, Karachaevo-Cherkesia 369167, Russia;

⁷Max-Planck-Institut für Radioastronomie, Auf dem Hügel 69, 53121 Bonn, Germany

⁸Department of Astronomy and Astrophysics, University of California at Santa Cruz, Santa Cruz, CA 95064.

⁹Instituto Nacional de Astrofísica, Óptica y Electrónica, Apartado Postal 51, CP 72000, Puebla, Pue, Mexico, Mexico;

¹⁰Crimean Astrophysical Observatory, P/O Nauchny, Republic of Crimea 298409, Russia;

¹¹Dipartimento di Fisica e Astronomia “G. Galilei”, Università degli Studi di Padova, Vicolo dell’Osservatorio 3, 35122 - Padova, Italy

¹²Departamento de Astronomía, Universidad de Chile, Camino El Observatorio 1515, Casilla 36-D Santiago, Chile

¹³Sterrenkundig Observatorium, Universiteit Gent, Krijgslaan 281-S9, Gent, 9000, Belgium

~ 5700 day periodicity in the continuum light curve, the $H\beta$ light curve, and the radial velocity curve of the red wing of the $H\beta$ line. The data are consistent with orbital motion inside the broad emission line region of the source. We discuss several possible mechanisms that can explain this periodicity, including orbiting dusty and dust-free clouds, a binary black hole system, tidal disruption events, and the effect of an orbiting star periodically passing through an accretion disk.

Subject headings: galaxies: active — galaxies: interactions — (galaxies:) quasars: individual (NGC 5548) — galaxies: Seyfert — black hole physics

1. Introduction

Despite much progress in recent years, many fundamental questions about the structure and kinematics of the innermost material in active galactic nuclei (AGNs) remain unanswered. Two key features of thermal AGNs are (i) that the IR to X-ray continuum is highly variable and (ii) that they have a broad-line region (BLR). Because the wavelengths of emission lines are well known the effective line-of-sight velocity of line-emitting gas is known. Line profiles of broad lines are thus an important constraint on models of the inner regions of AGNs. Furthermore, the ratios of intensities of different lines depend on the physical conditions of the environment of the gas such as the density and radiation field.

Variability of AGNs on short and long timescales potentially provides valuable insights about the physics of accretion, mechanisms of fueling nuclei and the growth of supermassive black holes. Because the BLR gas is close to the center of the AGN, it readily responds to continuum variability. Cross correlating the variability of broad lines with variability of the continuum readily gives the sizes of line-emitting regions (Cherepashchuk & Lyutyi 1973; Gaskell & Sparke 1986). In addition, the velocity-dependence of a line's response to continuum variability provides information about the kinematics and dynamics of the line emitting gas (see e.g., Gaskell 1988; Maoz et al. 1994; Netzer & Peterson 1997; Peterson 1997; Netzer 2013).

Because of its brightness, NGC 5548 was among the first Seyfert galaxies to be studied. It was the first galaxy to have optical variability reported (Deuch 1966). Between 1966 (Dibai et al. 1968) and 1970-71 (Anderson 1971; Ulrich 1972) there was a large change in the profile of the broad $H\alpha$ line. The optical continuum was also highly variable (Lyutyi 1973). The first reverberation mapping of NGC 5548 (Peterson & Gaskell 1986) showed that $H\beta$ responded to continuum changes with a delay of only a few weeks. Because its brightness, reliable variability, and convenient broad-line region (BLR) size, NGC 5548 was recognized as an

easy target for reverberation mapping. It has therefore been the subject of much monitoring for several decades (see e.g., Peterson & Gaskell 1986; Netzer et al. 1990; Koratkar & Gaskell 1991; Clavel et al. 1991; Peterson et al. 1991, 1992; Dietrich et al. 1993; Korista et al. 1995; Peterson et al. 1999; Kaspi et al. 2000; Dietrich et al. 2001; Peterson et al. 2002; Shapovalova et al. 2004; Sergeev et al. 2007; Bentz et al. 2007; Popović et al. 2008; Bentz et al. 2009; Denney et al. 2009; Denney 2010; De Rosa et al. 2015; Li et al. 2016, and references within). Studies at radio, visible, UV, and X-ray wavelengths indicate violent processes including ejection of gas, (e.g., Kollatschny & Zetzl 2013a; Kaastra et al. 2014).

According to Sergeev et al. (2007), inspection of individual broad $H\beta$ profiles over a 30-year period reveals that the broad emission line profiles can undergo dramatic changes (from a typical single-peaked profile centered near the systemic redshift of the galaxy, to profiles that show prominent blue or red peaks. Descriptions of blue and red peaks are presented in many papers (see e.g. Anderson 1971; Ulrich 1972; Ptak & Stoner 1973; Peterson et al. 1987; Sergeev 1992; Shapovalova et al. 2004, 2006; Popović et al. 2008; Li et al. 2016).

AGN variability is detected at essentially all wavelengths (Netzer 2013) and on all time scales (the light crossing time of the system, the rotational period of the central power-house with the associated line emitting gas, and the viscous time of the central accretion disk, see Czerny 2006; Netzer 2013). The light crossing time of the broad line region (BLR) of more than 60 sources has been used to characterize the dimension of the system (R_{BLR}) and to estimate black hole (BH) mass (see e.g. Gaskell & Klimek 2003; Kaspi et al. 2000; Bentz et al. 2013; Du et al. 2015, and references therein). While most AGN vary by a factor of a few in the optical band, there have been a few examples with systematic long-term trends, like Mrk 590, which shows: a) an overall long-term decrease by a factor 100, along with b) a change in Seyfert type (Denney et al. 2014), suggesting a significant decrease in accretion rate. Despite many searches for semi-periodic variations in the AGN lightcurves, few convincing candidates have been found so far (see e.g. Sillanpaa et al. 1988; Lehto & Valtonen 1996; Fan et al. 1998; Rieger & Mannheim 2000; Valtaoja et al. 2000; De Paolis et al. 2003; Sudou et al. 2003; Guo et al. 2006; Gezari et al. 2007; Guo et al. 2014; Liu et al. 2015; Bon et al. 2012; Graham et al. 2015a,b; Shapovalova et al. 2016).

Periodic variations could be produced various ways, including binary black hole (BH) systems, tidal disruption events (TDE) and more (e.g. Gaskell 1983; Sillanpaa et al. 1988; Komossa 2006; Bogdanović et al. 2008; Gaskell 2009; Eracleous et al. 2012; Popović 2012; Bon et al. 2012; Valtonen & Ciprini 2012; Bogdanović 2015; Komossa et al. 2016; Komossa 2015, and references therein). Distinguishing between scenarios requires extremely long monitoring, that is only available for a handful of sources. While AGN variability has been documented for many decades, only a few light curves span a time interval as long as

100 years [e.g., NGC 4151, from 1906 (Oknyanskij & Lyuty 2007), 3C273, from the 1880s (Smith & Hoffleit 1963), and OJ287, from 1891 (Valtonen & Sillanpää 2011) to the present. Therefore, well-covered long-term lightcurves of nearby AGN are required to search for the presence or absence of periodic signatures. This paper presents the analysis of very long duration light curves of NGC 5548 that span over 43 years and 1600 optical spectra, including 12 years of new data. The aim of this paper is to search for periodicity in the continuum light curve, the emission-line light curves, and the radial velocity curves. The structure of our paper is as follows. In §2 we present information about the new observations. In section §3 we explain our methods of calibrations in section §4 light and radial velocity curves. Various possible interpretations are given in section §5. Finally, in §6 we summarize our results and present the conclusions.

2. Observations and data reduction

We analyzed over 1600 spectra of NGC 5548 in the $H\beta$ spectral interval, covering over 43 years: (a) archival spectra obtained by K. K. Chuvaev from 1972-1988 (Sergeev et al. 2007) prior to the *International AGN Watch* (IAW) campaigns. These early spectra were recorded on photographic plates acquired with an image tube at the 2.6 m Shajn Telescope of the Crimean Astrophysical Observatory. (b) the intensive, 13-year study from 1988 to 2002 of the IAW program (Peterson et al. 2002). This provided 1530 optical continuum measurements and 1248 $H\beta$ measurement¹. (c) a spectral monitoring program with the 6-m and 1-m telescopes of the Special Astrophysical Observatory (SAO) in Russia from 1996 to 2002, and the 2.1 m-telescope of Guillermo Haro Observatory (GHO) in Cananea, Mexico from 1996 to 2003 (Shapovalova et al. 2004). (d) more recent, unpublished observations of the same program covering 2003 - 2013, observed at SAO (see Table 1) and a continuation of the monitoring campaign presented in Shapovalova et al. (2004), (e) spectra from the new IAW campaign obtained at Asiago observatory in 2012, 2013 and 2015² and (f) new unpublished observation from 2013 from the Asiago observatory (also given in Table 1).

Details of the additional optical spectra obtained at INOAE and Asiago are as follows. The SAO and INOAE spectra were obtained with the 6-m and 1-m telescopes at

¹The IAW data could be obtained in the digital format from the following link: <http://www.astronomy.ohio-state.edu/~agnwatch/data.html>

²with kind permission of PI Bradley Peterson to use IAW data published in Peterson et al. (2013) and unpublished data from 2012, 2013 and 2015, observed at Asiago, as there is no publication based on those data yet.

SAO and with the INAOE 2.1-m telescope at the Guillermo Haro Observatory (GHO) at Cananea, Sonora, Mexico. In all cases observations were made with long-slit spectrographs equipped with CCDs. The typical wavelength range covered was from 4000 Å to 7500 Å, the spectral resolution was 4.5-15 Å, and the S/N ratio was > 50 in the continuum near $H\alpha$ and $H\beta$. Spectrophotometric standard stars were observed every night. The logs of these new observation are presented in the Table 1. We also include a set of unpublished spectra observed at the 1.22-m telescope of the Asiago Astrophysical Observatory, configured in long-slit spectroscopy mode. The total exposure time was 3600s, divided in multiple runs of 600s or 1200s each, in order to prevent saturation of the strongest emission lines. The spectrograph used a 300 lines/mm grating with a 300 μm slit width, achieving a spectral resolution $R \simeq 600$ between 3700 Å and 7500 Å. Wavelength calibration was obtained using FeAr comparison lamps, while the flux calibration was performed with the observation of the spectro-photometric standard stars Feige 34 and Feige 98. Cosmic rays were identified and masked out through the combination of the different short exposures.

3. Methods of analysis

With the goal to analyse NGC 5548 spectra from 43 years of monitoring campaigns, we performed full spectrum fitting analysis using ULySS code (Koleva et al. 2009)³ that we adopted for fitting Sy1 spectra with models representing a linear combination of non-linear model components – emission lines, Fe II templates, AGN continuum and the stellar population of the host galaxy. This is the first time the package has been used to analyze spectra of broad lines in AGNs, while before it was used for (i) determining stellar atmospheric parameters using the models of stellar atmosphere (Wu et al. 2011) and (ii) studying the history of stellar populations (Bouchard et al. 2010; Koleva et al. 2011, 2013). Recently, Bon et al. (2014) tested the accuracy of the code in recovering stellar population and gas parameters in Type 2 AGNs.

We obtained light curves and radial velocity curves for all spectra and searched them for possible periodicities. We used standard methods for treating unevenly spaced data, and a new method specially developed for this purpose tailored for our specific special conditions of very few cycles and very specific sampling characteristics of here obtained data series (see section 4.1).

³The ULySS full spectrum fitting package is available at: <http://ulyss.univ-lyon1.fr/>

3.1. Line and continuum fittings

Since ULySS gives us a choice of defining and including components, we adjusted it to analyze simultaneously all components that contribute to the flux in the wavelength region around $H\beta$. For analyzing variability of NGC 5548 we defined the model, $M(x)$, as follows:

$$M(x) = P(x) ([T(x) \otimes G(x)] + C(x) + N(x) + B(x) + \sum_{i=1}^4 FeII_i(x) + \sum_{j=1}^n S_j(x)), \quad (1)$$

where $M(x)$, represents bounded linear combination of non-linear components – stellar template spectrum $T(x)$ convolved with a line-of-sight velocity broadening function, an AGN continuum model $C(x)$, a sum of narrow $N(x)$ and semi-broad components $B(x)$ of [O III] emission lines, respectively, a sum of Gaussian/Gauss-Hermit functions $\xi(x)$, accounting for other AGN emission lines in analyzed spectral domain, and Fe II template consisting of four groups of Fe II lines.

A multiplicative polynomial $P(x)$, that represents a linear combination of Legendre polynomials, was included in a fit, in order to eliminate overall shape differences between the observed stellar and galactic spectra. The introduction of this polynomial in the fit ensures that results are insensitive to the normalization, Galactic extinction and the flux calibration of a galaxy and stellar template spectra (Koleva et al. 2008). For simplicity, we assumed a Gaussian velocity broadening function $G(x)$, but it is possible to use also Gauss-Hermite polynomials (Rix & White 1992; van der Marel 1994). The contribution of the components to the total flux can be obtained from their weights which are determined at each Levenberg-Marquardt (Marquardt 1963) iteration, using a bounding value least-square method (Lawson & Hanson 1995).

For the stellar population model we used grid of PEGASE.HR single stellar populations, computed with the Elodie.3.1 library and a Salpeter IMF (Le Borgne et al. 2004). The model $M(x)$ is generated at the same resolution and with the same sampling as the observation and the fit is performed in the pixel space. The fitting procedure performs the Levenberg-Marquardt minimization (Marquardt 1963). In modeling the integrated spectra of NGC 5548 we added the powerlaw to the stellar population base to represent an AGN featureless continuum ($f_\lambda \sim \lambda^\alpha$). The spectral index α , depends on the continuum slope, and represents the free parameter in the fit. In order to tie the parameters of the [O III] lines, we defined two separate components of the model: a narrow component and a semi-broad component. In this way we tied the widths, shifts and intensities of [O III] components (intensity ratio was kept to 3:1). The rest of emission lines in the domain $\lambda\lambda[4430, 6400]$ were fitted with a sum of Gaussians - we fitted He II 4686 Å with two components, while we used four components in the fit of $H\beta$ line - narrow, broad blueshifted, broad redshifted and very broad component.

As proposed by Kovačević et al. (2010), we defined four groups of Fe II lines to fit the Fe II multiplets around the H β line - Fe II s, p and f group and I Zw1 template. Since it is very difficult to fit stellar population in the spectra of Sy1 galaxies with broad emission lines, in the first step we fitted spectra of NGC 5548 in the minimum of activity with all free parameters of the model (defined with equation 3.1), and with multiplicative polynomials of the 15th order (as in Bon et al. 2014). We find that a single stellar population with age of 7200 Myr and metallicity [Fe/H]=0.2 fits the best spectra in the minimum. In fitting the rest of the spectra from monitoring campaigns of this galaxy, we fixed age and metallicity at best fitted values from the first step, and used the multiplicative polynomial of the first order, to minimize the effects of this polynomial on the fit of emission lines. Free parameters associated with the stellar population were kinematic parameters - mean stellar velocity and dispersion. Examples of best fit spectra at the minimum and maximum activity are presented in Fig. 1.

All the results presented below are based on the assumption that the luminosity of the [O III] 5007 line, and all other narrow emission lines, do not change in time (see for example Peterson et al. 2002; Shapovalova et al. 2008). We assumed that the slit width and position angles used in the various campaigns were not affected with the O III region size in the NGC 5548, which appeared to be very compact (see Schmitt et al. 2003). For that reason we made a simple test to estimate light loss for smallest slit used (see the appendix). The spectra were scaled to a constant flux of $F([\text{O III}]\lambda 5007) = 5.58 \cdot 10^{-13} \text{ ergs s}^{-1} \text{ cm}^{-2}$, and we constructed host galaxy subtracted continuum light curves of continuum flux measured at 5100Å and broad H β emission line. The 5100Å continuum light curve and the H β light curve are presented in Fig. 2.

From the set of 1494 “IAW” spectra, we remove 128 spectra of the H α region only, 109 spectra with poor spectral resolution and 48 spectra which did not cover large enough range to measure the 5100Å continuum. This left us with 1209 IAW spectra, that combined with 249 spectra from Crimean Astrophysical observatory, 83 spectra from SAO/GHO observatories, and 7 spectra from Asiago, make in total 1548 spectra. After careful inspection of the fits, we have removed ten additional spectra, leaving 1538 spectra for further analysis (Table 2).

The zero point error in the radial velocity has been measured from the scatter of the difference between the peak, v_r of [O III] $\lambda 5007$ and the narrow component of H β , $\delta v_r = v_r(H\beta) - v_r(OIII) \approx 35 \text{ km/s}$. We note that there is a known small systematic offset of $\delta v_r \approx +19 \text{ km/s}$, frequently found in [O III]-strong AGN (e.g., Eracleous & Halpern 2003; Hu et al. 2008; Komossa et al. 2008; Marziani et al. 2016, and references therein). The velocity zero point was set on the peak wavelength of [O III] $\lambda 5007$, as [O III] $\lambda 5007$ is a very

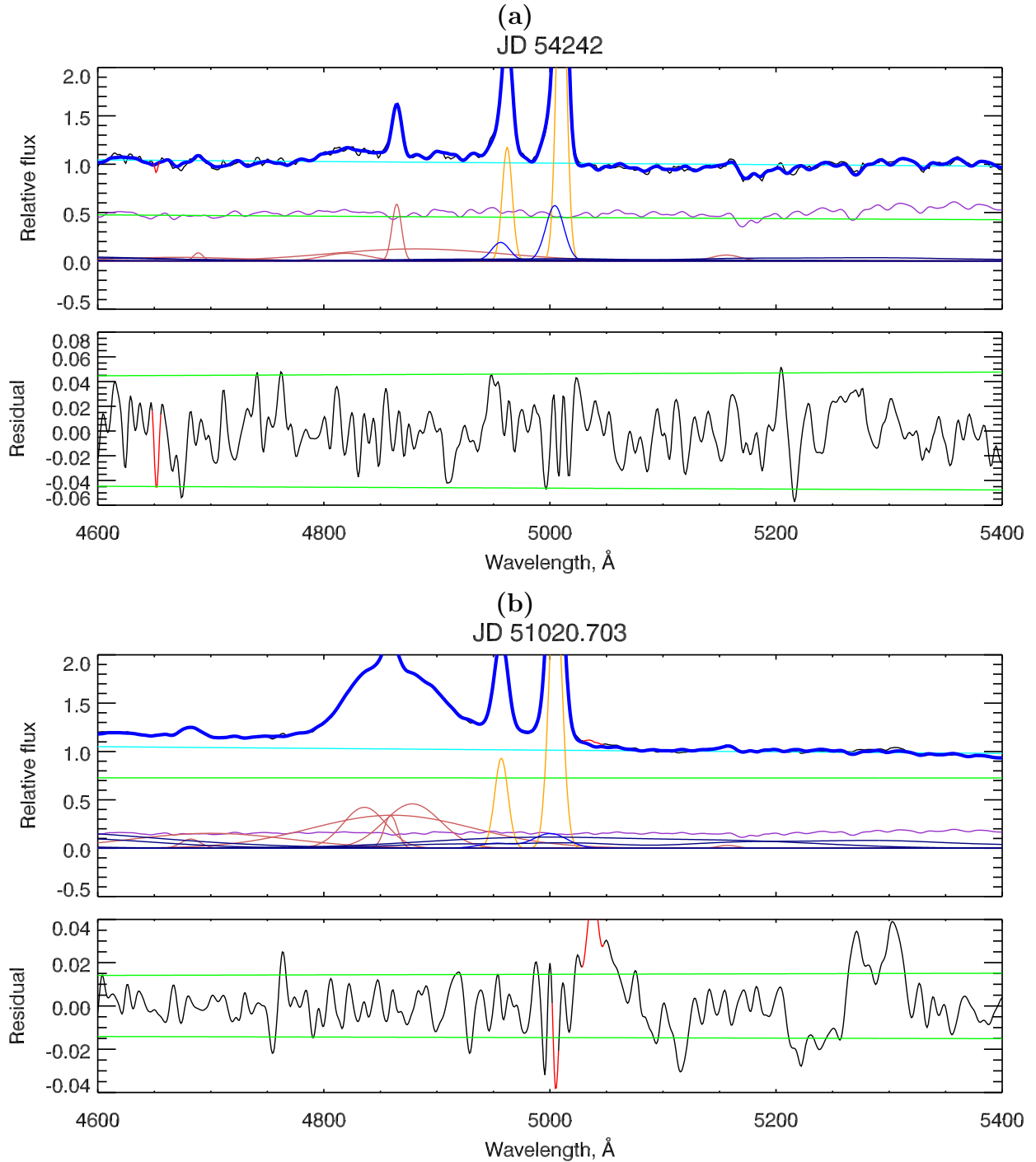


Fig. 1.— Examples of best fit spectra at minimum (a) and maximum (b) activity. The black line in the upper panels of both (a) and (b) represents the input spectrum, the blue line represents the best-fit model, and the cyan line represents the multiplicative polynomial, while red, yellow, blue, dark blue and violet lines represent components of the best-fit model: violet – stellar population, red– components of He II and $H\beta$ lines, yellow – narrow [O III] lines, blue – broad [O III] lines, dark blue – Fe II multiplets and green – the AGN continuum. The bottom panel shows residuals from the best fit (black line). The green solid line shows the level of the noise.

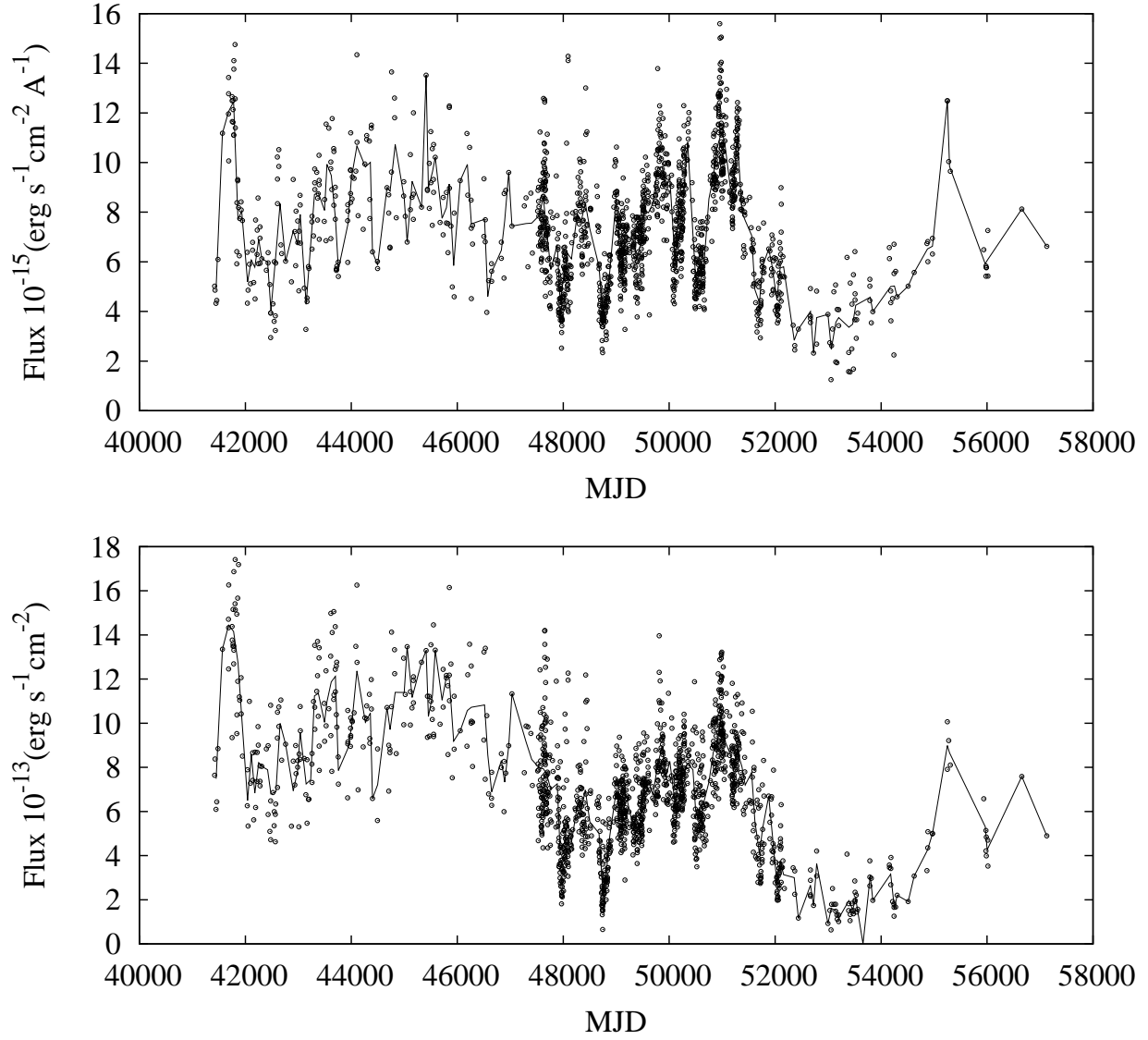


Fig. 2.— Top: Continuum 5100 Å light curve (dots) and 80 day binned continuum light curve (slashed line). Bottom: The same as in the top panel, but for H β .

sharp feature of high S/N, less influenced by the underlying broad H β profile.

Typical errors on light and radial velocity curves have been estimated from the dispersion of the measured parameters on short time intervals (< 20 days), in cases multiple spectra are available (5 for the continuum light curve). Since 20 d is a period long enough to include possible significant intrinsic variations, we considered the time behavior of the *minimum* dispersion value around the average of a given parameter (for example, FWHM, HWs) computed over 20 d as a function of time. Typical rms errors for H β seem to be around $5 \cdot 10^{-13}$ erg s $^{-1}$ cm $^{-2}$, while for the typical rms scatter for the 5100Å continuum flux is 10^{-16} erg s $^{-1}$ cm $^{-2}$ Å.

Recently, a paper by Li et al. (2016) discusses a large part of a similar data set in a somewhat similar way. The main differences between Li et al. (2016) and our analysis is in our unified approach and in the quantity of data used. In our study this was achieved using a more robust method and taking into account some important components that were not considered by Li et al. (2016) (the galactic host emission, Fe II multiplets and He emission and two components of each [O III] narrow line in spectral fit). As mentioned above, 1538 spectra were analyzed (with the new spectra covering the last 12 years), instead of only about 850 used by Li et al. (2016), with a large gaps in the last 12 years of their time series.

4. Results

4.1. Variability Analysis

Light and radial velocity curves were analyzed for possible periodicity using standard methods, such as Lomb-Scargle (Lomb 1976; Scargle 1982), and also with the new method for unevenly sampled data tailored to this specific case, with the specific special conditions of our data series. Besides light curves, we constructed curves using measurements of different fractional intensities of blue side (blue dots) and red side (red dots) H β broad emission line at 25%, 50%, 75% and 90% as a function of time. They behave as half widths radial velocity curves at these fractional intensities. We calculated line centroids⁴, and full widths⁵ as well. Half widths and centroid radial velocity curves are presented in Fig. 3. Full widths of the line are also calculated and their curves are presented in the Fig. 4. We applied different methods to test for possible periodicities, similarly as for light curves.

⁴Centroids are calculated as $\lambda_c = (\lambda_{red} + \lambda_{blue})/2$

⁵Full widths are calculated as $\lambda_{FW} = (\lambda_{red} - \lambda_{blue})$

4.2. Lomb-Scargle periodicity analysis

Using Lomb-Scargle (Lomb 1976; Scargle 1982) analysis (LS method), we analyzed light and radial velocity curves, with previously removed linear trends. Results could be seen in Table 3.

To avoid the problem of very different sampling, we analyzed rebinned curves. With rebinning we also eliminate shorter variations that correspond to the light crossing time scale of the system. We rebinned the radial velocity curves to the 80 day average bins, since the variability lags of $H\beta$ to continuum variations were under 30 days (Zu et al. 2011; Peterson et al. 2002; Kaspi et al. 2000; Koshida et al. 2014). According to Czerny et al. (1999) there are two clearly distinct physical mechanisms of variability in NGC 5548 curves, with two different timescales, one under 30 days and another with order above hundred days. The short timescale variability is connected to the Comptonization of the soft photons emitted by the innermost part of the accretion disk, while in the long timescales the optical variability is not related to X-rays (see more in Czerny et al. 1999). Therefore, we assumed that 80 day binning would be long enough to filter short variations and to analyze only longer ones. We find periodicities with very low false alarm probability in radial velocity curves of half widths measured at 25%, 50%, 75%, 90% of $H\beta$ line maximum, see Table 3. As could be seen the obtained periodicities show similar values. We also, searched for periodicity in radial velocity curves of the full widths at 25%, 50% and 75% of maximum intensity of the broad $H\beta$ emission line. The results are presented in Fig 5. We can see that there is a significant peak at about 3000 days, which is about a half of the value detected at half widths radial velocity curves (see Table 3). As argued below, these periodicities are far from being sinusoidal and cover a very small number of repeating periods (a little less than 3). We suspect that the standard LS analysis may not be reliable enough in such cases, and searched for a more robust method that is more suitable for the type of data discussed in this paper. The method is explained below and the numbers listed here that are based on the standard LS method should be regarded as "tentative periods". We note that the LS method is known to give spuriously high significance levels to low frequency periods for red noise variability (see Westman et al. 2011; Vaughan et al. 2016; Bon et al. 2016)

It is interesting to note red and blue side radial velocity curves at 25% and 50% are anti-correlated, while red and blue radial velocity curves at 90% show a positive correlation, as could be seen in Fig. 6. As we go toward the top of the line, the anti correlation switches to correlation, see Fig. 6. This indicates that the peak of the line is shifting together with the red side of the line, while at the base of the line radial velocity curves could be affected by two different kinematic components.

To analyze the $H\beta$ line shifts we also obtained single Gaussian fit of spectra and con-

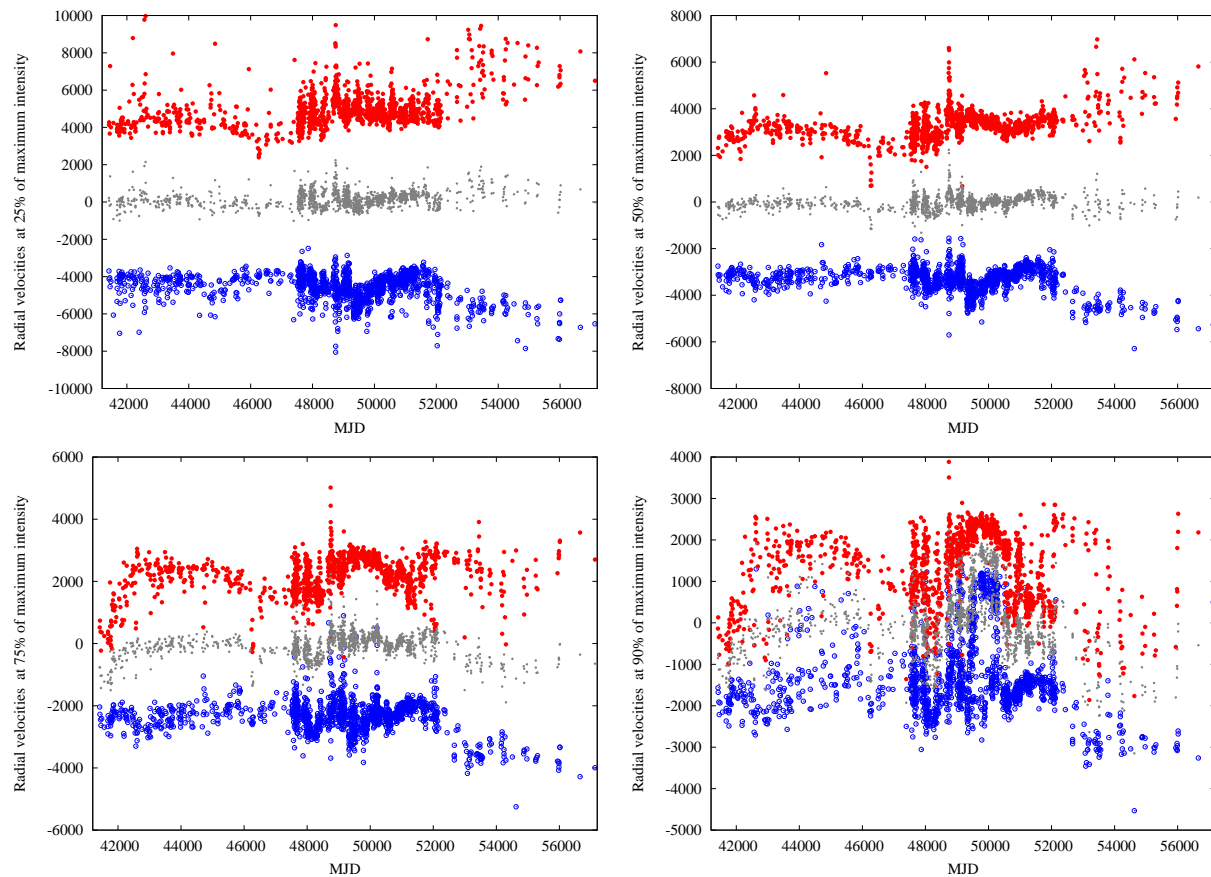


Fig. 3.— Radial velocities measured on the blue (open circles) and red (filled circles) sides of $H\beta_{BC}$ at fractional intensities of 25% (top left), 50% (top right), 75% (bottom left) and 90% (bottom right). Centroids (gray dots) are calculated as averaged value of blue and red side fractional intensity radial velocity measurements.

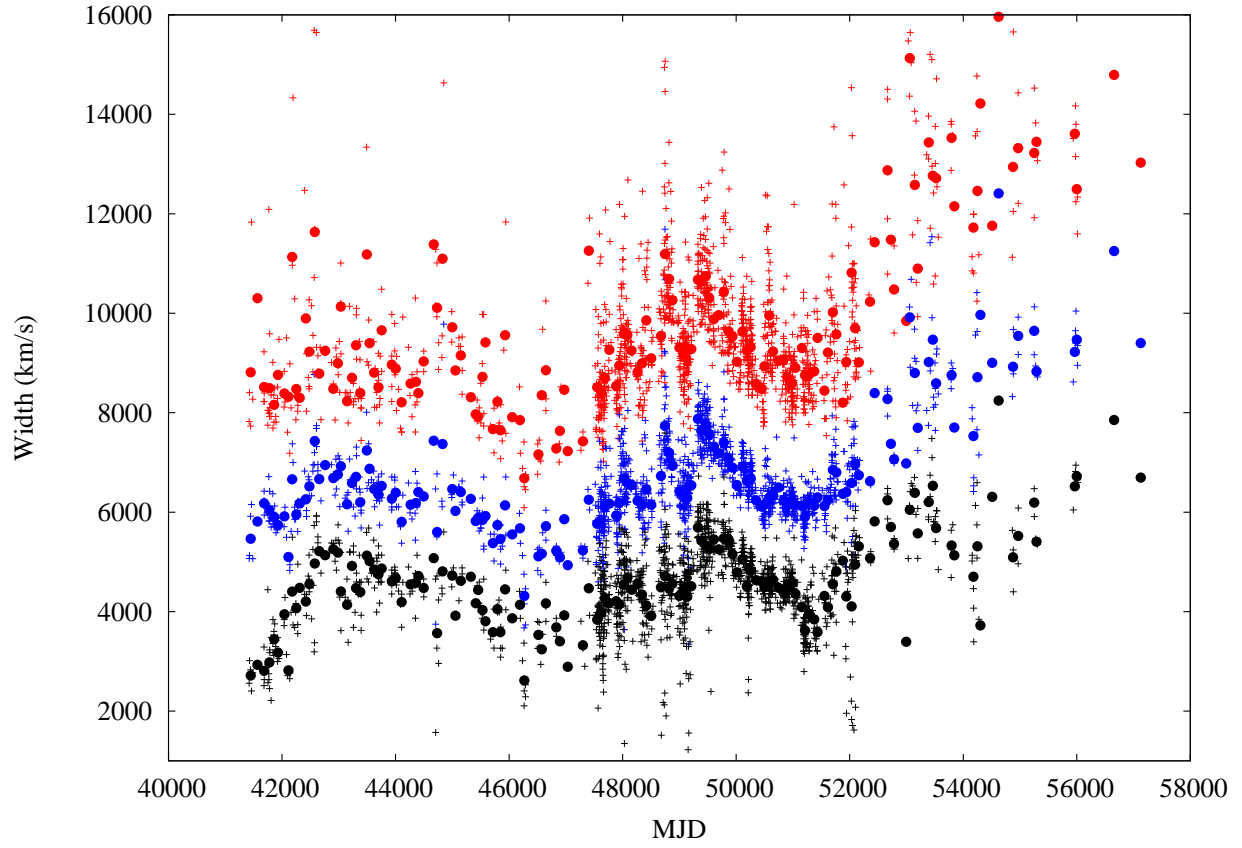


Fig. 4.— Curves of the full width at different heights of the broad H β line in \AA : 25% (red), 50% (blue), 75% (black). The observations are presented with crosses, while the binned averaged data are plotted with full circles.

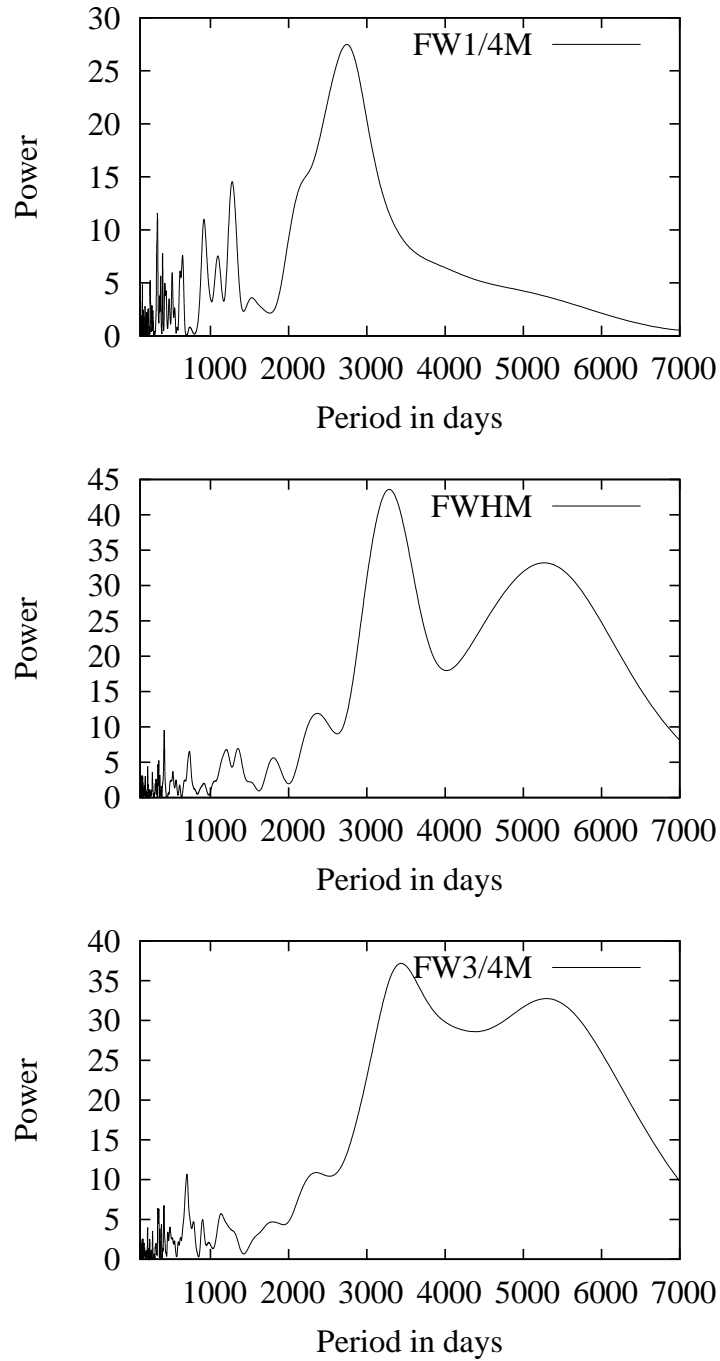


Fig. 5.— Lomb-Scargle periodograms of radial velocity curves of full widths at 25% (top panel), 50% (middle panel), 75% (bottom panel).

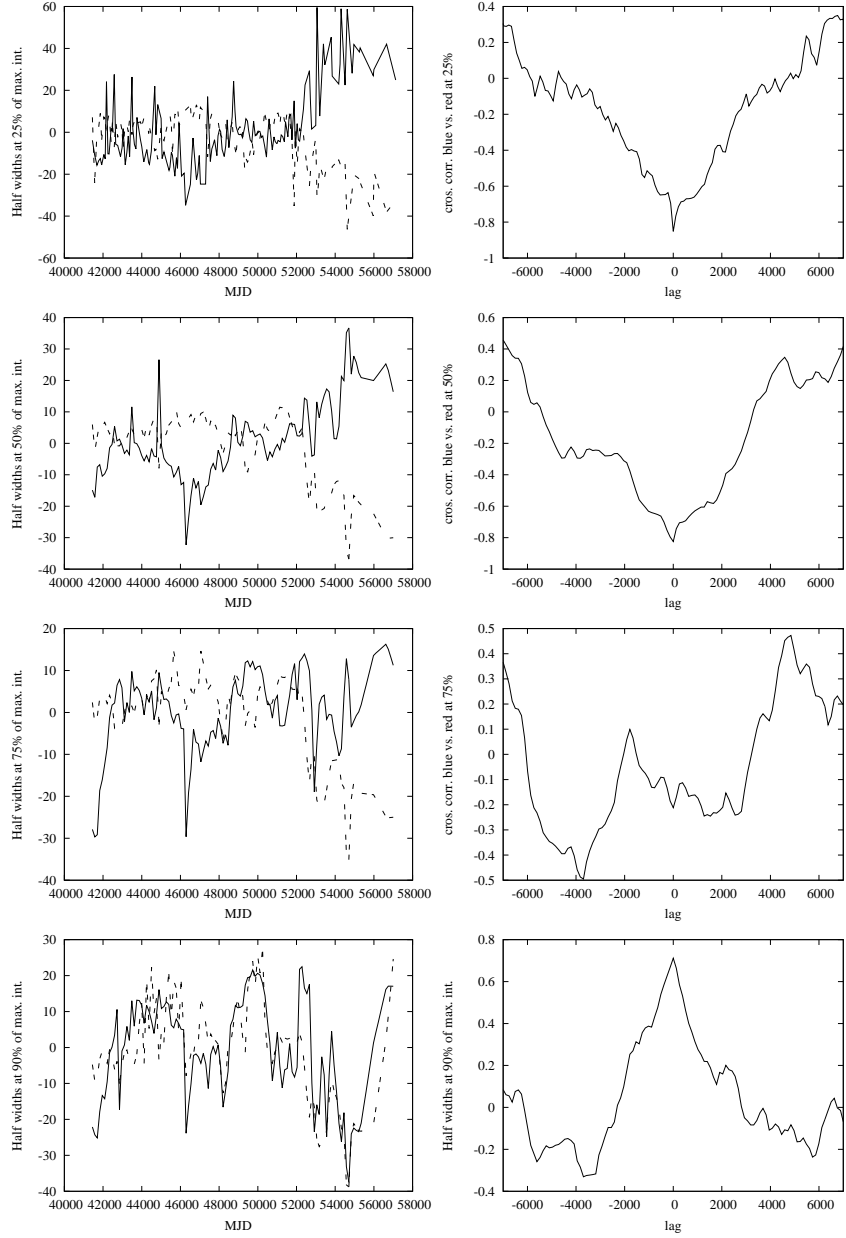


Fig. 6.— Left: Radial velocity curves measured as red side width (thick line) and blue side width (slashed line) of the broad $H\beta$ emission line, at 25%, 50%, 75% and 90% of the line maximum, rebinned to 80 days with mean value subtracted, over plotted to show shape similarity. Right: Cross-Correlation functions between corresponding pairs of curves. The cross correlation functions of red and blue side radial velocity curves at 25%, 50%, 75% broad $H\beta$ emission line are negative (anti correlated), while at 90% they are correlated. This indicates that the peak of the line measured at blue and red side on 90% is shifting as a single component, while at the base of the line radial velocity curves could be affected by two oppositely moving components.

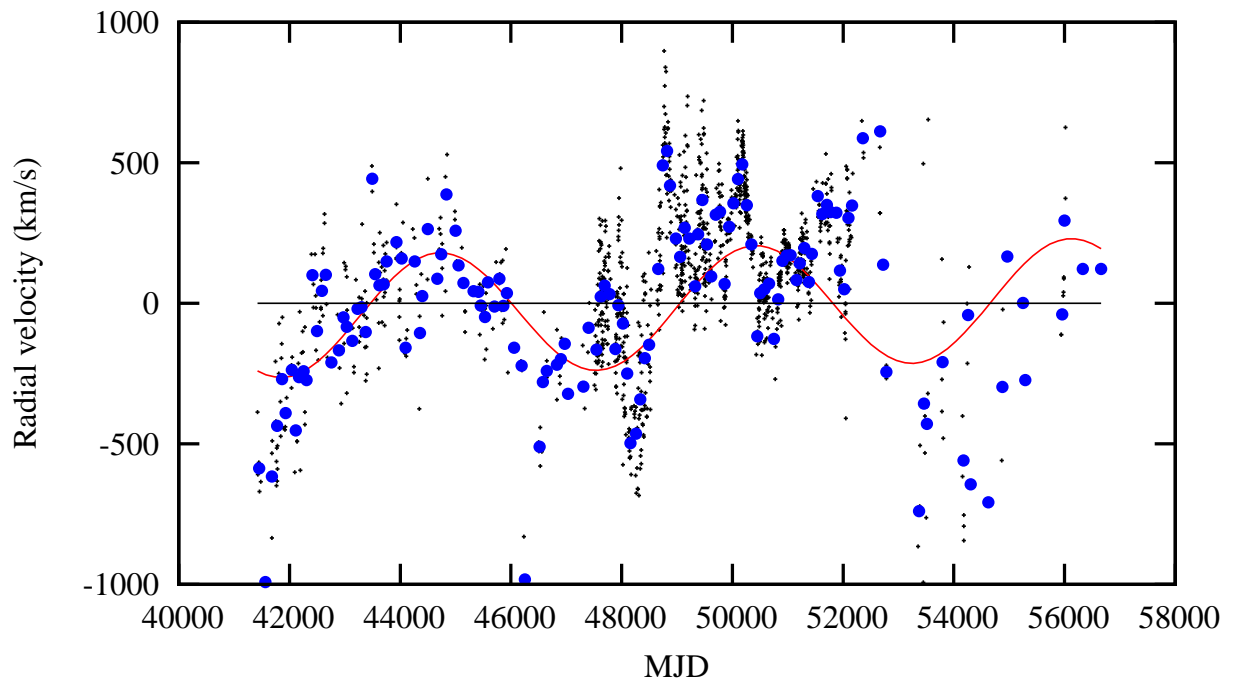


Fig. 7.— Radial velocity curves resulting from fitting a Gaussian to the broad $H\beta$ line of NGC 5548 as discussed in the text. The solid red line shows the best fit of a sine wave of period 5700 days.

structed a radial velocity curve from the obtained shifts. We fit a sine function, assuming the expected periodicity of 5700 days (see Fig. 7), just to lead an eye, and not to claim a simple sinusoidal periodicity, since there are obvious deviations from the sinusoidal curve in several epochs. One can see some similarity of this radial velocity curve and the one obtained from measurements of red half width at 75% of the line maximum (see Figs. 7 and 3), implying that the line shifts are mainly affected by variations on the red side of the line. Also, similarity of these curves could indicate the same periodicity.

4.3. A new method for finding periodicity in unevenly sampled data

As explained, our data are obtained from many different monitoring campaigns with very different sampling patterns. From the light curves one can see that the number of data is much higher in the second third of the observed interval, then compared with the first and third parts that contain less than few hundred observations each, while the second third contained above thousand spectra. Such distribution of the data introduces various biases in standard methods for periodicity analysis of unevenly sampled data based on sine function decomposition as Fourier and Lomb - Scargle. The Lomb-Scargle method is commonly used to detect periodicities in unevenly sampled time series. LS follows the approach of Fourier methods and fits a sinusoid to the data. However, in classic Fourier methods, uniform sampling gives rise to orthogonality properties of the trigonometric functions, which have profound statistical implications. Thus, the Fourier series terms can be shown to be statistically independent under very broad conditions. This is no longer the case in LS of unevenly sampled data. Nevertheless, it is a common practice to interpret the LS periodogram as a kind of Fourier series, relying on the assumption that the uneven sampling times are uniformly distributed. Sometimes it is possible to neglect this effect if many cycles are included in the analyzed time span. In our case it is clear that the sampling has an obvious nonuniform nature, where the middle part of the time series is sampled much more densely than the rest. Moreover, we focus our attention on long periods, meaning only 2-3 cycles in total. Thus, the simplifying assumptions allowing the use of LS are no longer valid, and we have to tailor a method to the specific problem, that will take into account the nature of the specific sampling pattern. As could be seen comparing Table 3 and Fig. 5 even though Lomb–Scargle analysis gives very high probability of periodicities, the values of obtained periods are dispersed. Periodicity result values span between 5500 and 6200 days. Obviously, very unevenly sampled data required a method that would be able to recognize repeating patterns, and not only sine functions (as in cases of Fourier or Lomb–Scargle analysis). For that purpose we proposed method tailored to this specific case, with the special conditions of very few cycles, and specific sampling characteristics.

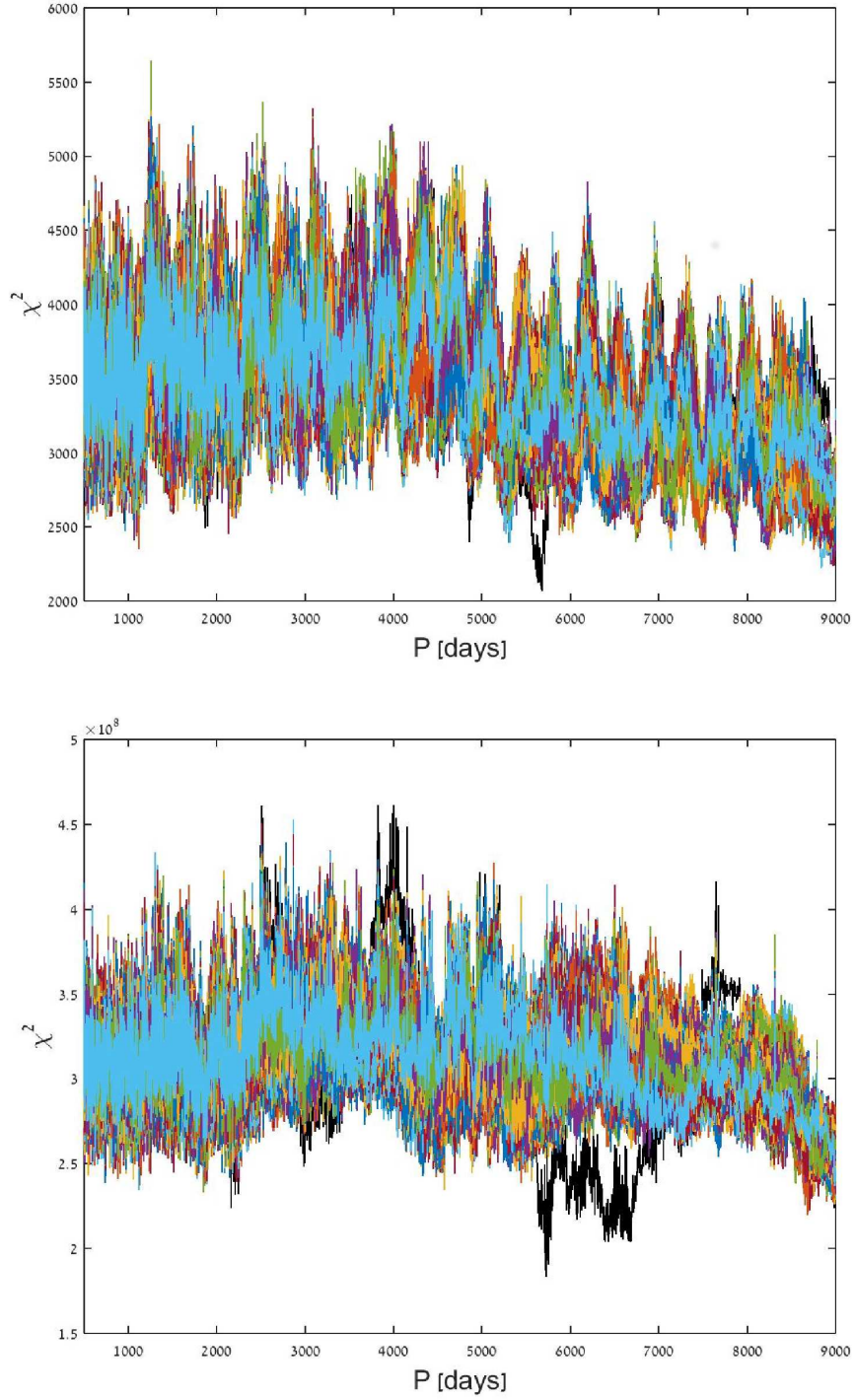


Fig. 8.— Periodogram of the 1000 permutations for continuum light curve at 5100Å (top) and radial velocity curve measured at 75% of the maximum line intensity at the red side of H β (bottom).

We started from the working assumption that the data between JD=47508 and JD=52175 are well sampled and of better quality, than the rest (see for example, Fig. 2). Those two problems prevent proper use of conventional period search techniques, since they usually have a hidden assumption of a homogeneous data quality and sampling, and many cycles. Our new method treat the 'best sampled' part as fixed, and tests only the noise and sparsely sampled parts on both ends, to see how well they fit the hypothesis of a period. We first linearly interpolate the 'best sampled' part. Then we produce a periodogram by trying many periods. For each trial period we 'fold' every point we test into the best sampled part, and calculate its deviation from the interpolation (similar to the phase dispersion minimization method, (see Stellingwerf 1978; Plavchan et al. 2008). We sum those squared deviations and obtain a significance score, similar to the χ^2 score for the periods. If there is a periodicity it should come up as a lower than usual value of this score.

We look for a minimum (that is basically a χ^2 , but without normalization by the errors), and found it at a period of 5676 days (see Fig. 8). The question remains how statistically significant is this minimum. To check it made the following test: We consider the central segment as reference that we do not change. and test whether the points in the first and third segments actually fit the central part after phase - folding. For this we carry out the following permutation test. In each iteration we randomly reshuffle the values of the points in the first and third segment (the measurements, not the sampling times). Thus we "ruin" their time dependency, but keep their "window function". We then calculate the periodogram again, and look for the minimum value. The idea is to check what is the fraction of random reshufflings that will produce a value lower than the value we got with the actual lightcurve. Only 2 out of 10000 values were lower. This means this results has a significance p-value of around 0.0002.

The Fig. 8 shows the actual periodogram in black, against the background of 1000 periodograms out of the 10000. One can see that the structure of the problem imposes some structure on the periodograms, but the result stays significant, since the 5676 period the χ^2 trough looks quite displaced from its randomly produced counterparts.

We repeated the analysis on the radial velocity curves shown in Fig. 3 and show the results in the bottom panel of Fig. 8. One can see that the periodicity looks very significant on the radial velocity curve measured at red side 75% of the line maximum , the lowest point (i.e. best fit), is at a period of 5725 days - essentially identical to the 5676 day period in the flux. As judged from the new method, none of the other radial velocity curves shown in Fig. 3 shows a statistically significant periodicity.

It is important to emphasize that real radial velocity periodicities may well be present in the H β profile but the noisy half width radial velocity curves do not allow us to detect

them unambiguously.

If we assume that the periodic component is sine-like, with periodicity of 5676 days, the variance (see eg. Nandra et al. 1997; Nikolajuk et al. 2004) of the data carried by the periodic component (with a secular trend) is about 19%. We consider both the variance in the data and the secular component under the assumption of long time scale (15.7 years) sinusoidal variations

5. Possible interpretations

The main results of our investigation are the detections of significant periodicities in the the luminosities of the 5100Å continuum and H β light curve, as well as in the radial velocity curve of the H β profile. The periods are very similar and consistent with $P \approx 5700$ days (≈ 15.6 years) - see Table 3. This value is practically identical to the period found in the supermassive binary black hole (SMBBH) candidate NGC 4151 (of 15.8 years, see Oknyanskij 1978; Bon et al. 2012) and similar to 11 year period of OJ287 (Valtonen & Ciprini 2012). It is about twice the periodicity found for the case of another recently found supermassive binary candidate, PG 1302-102 (Graham et al. 2015a). Our best measured periodicity is similar to the 14-year periodicity found recently by Li et al. (2016) for NGC 5548, but our result is based on a more robust analysis and more data. In this section we discuss, briefly, several possible physical scenarios that can give rise to the observed periodicity. We focus on the more secure results obtained with the new method of simulations presented in section §3. We consider these results as the most reliable and the ones obtained with the LS method more questionable. This does not exclude the possibility that some of the LS results, like the suggested periodicity of the FWHM velocity curve, are not part of the suggested scenario. In all our models we assume a BH mass based on the results of via multiple reverberation-mapping campaigns. We adopt $5.73_{-0.24}^{+0.25} \times 10^7 M_{\odot}$ as given in the BH mass data base of Bentz & Katz (2015) and our own estimate of the normalization factor $f \approx 3.75$ used in expression $M_{BH} = f \sigma_{rms}^2 r_{ct} / G$, with the velocity dispersion computed from the rms spectrum. This mass differs by only 30% from the mass given by Bentz et al. (2007) who assumed $f = 5.5$ and $6.3 \times 10^7 M_{\odot}$. A circular orbit around such a BH would have a period $P \approx 17.5 r_{15ld}^{\frac{3}{2}} \times M_{5.710^7}^{-\frac{1}{2}} \text{yr}$, where $r = 15\text{ld}$ is the radius in units of 15 ld. This reference radius was chosen since it is typical of the many annual means of the lags of H β . Since reverberation time delays vary within 6 ld and 27 ld (Bentz & Katz 2015) expected periods are between 8 and 36 years. Obviously the reverberation mapping results give a responsivity-weighted radius and the total line emission from from a wider range of radii.

The H β reverberation mapping distances can be compared with the reverberation mea-

measurements of the inner radius of the dust torus which range between 40 and 80 ld depending on observing season and on delay computation techniques (Koshida et al. 2014). Finally, since some of the models we discuss in this section involve a second BH, we refer to the $5.7 \times 10^7 M_{\odot}$ black hole as the “primary BH” in the system.

5.1. Geodetic precession, disk-self warping, hot spots and spiral arms

We can readily exclude two mechanisms that could give rise to a significant periodicity in a single black hole system, as discussed in Bon et al. (2012): geodetic precession, and disk-self warping induced by radiation pressure (Pringle 1996). The first of these occurs on time scales that are in general much longer than the observed periodicity (Begelman et al. 1980). As for the latter, Graham et al. (2015a) showed that warped disks around single black holes are not favored in an AGN context. In particular, the expected periodicity in such scenario is much longer than the period found for NGC 5548 (e.g., a black hole mass of $10^8 M_{\odot}$ gives a period between $10^{2.2-6.9}$ years, Pringle 1996; Graham et al. 2015b). Mechanisms that could produce orbital periodicity are re perturbation in a very large central disk that extend far beyond the inner accretion disk whose dimensions are known from recent reverberation mapping to be of order 2 ld (De Rosa et al. 2015; Edelson et al. 2015; Fausnaugh et al. 2016). A hot spot rotating at a distance of about 15 ld, which is not observed during a fraction of the orbit, can explain the periodic continuum variations. Emissivity perturbation by spiral arms in a large central disk can result in a double-peaked profile and emission line shape variability (see Chakrabarti & Wiita 1994; Lewis et al. 2010; Jovanović et al. 2010). Spiral arms can be triggered by a close passage of massive object such as massive star cluster or super massive black hole (see Lewis et al. 2010, , and references within) by gravitational instabilities (see e.g., Flohic & Eracleous 2008, and references therein), or by an object passing through the extended disk (Chakrabarti & Wiita 1993). Fragmented spiral arms can in principle account for emission line shape variation on relatively short time and radial velocity changes occurring on the dynamical timescale (Lewis et al. 2010; Jovanović et al. 2010). Such sub-structures in a non-uniform central disk could cause an excess emission moving across the line profile (Lewis et al. 2010; Jovanović et al. 2010; Goosmann et al. 2014). We do not consider such models as plausible explanations for NGC 5548 because of the huge central disk that is not observed in this source, the hot spot that, in order to explain the periodic variation should emit a sizable fraction of the luminosity of the small inner disk, and because the overall emission line spectrum of NGC5548 is very similar to the ones observed in thousands of AGN of similar luminosity and these scenarios cannot explain all the population properties.

5.2. Tidal disruption events

A tidal disruption event (TDE) when a star is disrupted by a black hole creates an appearance somewhat like an AGN for a limited duration. The tidal radius (the distance from the black hole at which a star is tidally disrupted) can be written as $r_t \approx 1.5 \times 10^{13} (M_{BH,7})^{\frac{1}{3}} (M_{\star,\odot})^\beta \text{cm}$ (Hills 1975; Komossa 2015), where M_{BH} is the mass of the black hole in units of $10^7 M_\odot$, and the mass of the star is in solar masses. The exponent β is $\approx 2/3$ or $1/6$ depending on whether the star is a main sequence star M_\star has mass $\lesssim 1M_\odot$, or belongs to the upper main sequence with $M > 2M_\odot$ (Torres et al. 2010). For the NGC 5548 black hole mass, and for a main sequence star the tidal radius is extremely small, a few gravitational radii. A main sequence star may therefore orbiting at 2-15 ld without suffering a TDE. In the absence of a pre-existing accretion disk, tidal disruption causes a luminous flare with a short rise, and a longer-lasting decline (e.g., Rees 1990), as observed in several cases (eg. Komossa & Bade 1999; Gezari et al. 2012, and references therein). A partially stripped star in an orbit around the SMBH can cause repeated accretion events each time its orbit passes near pericentre, and may thus produce a semi-periodic signal in the light curve (e.g., Hayasaki et al. 2015). However, in the case of NGC 5548, this is an unlikely explanation, if we were to interpret all its properties in the context of a TDE. For instance, its optical narrow emission lines imply the presence of a classical narrow-line region, and therefore a much longer-lived AGN. Similar arguments hold for the possibility of causing a semi-periodic light curve from a TDE in a binary SMBH system (Liu et al. 2009). Another possibility is that we may have a TDE in addition to the permanent accretion disk of a long-lived AGN, and the TDE contributes extra accretion during each pericentre passage. This would boost the accretion onto the BH in a periodic fashion but material must be added to the accretion flow very close to the event horizon since the viscous time of accreting through the disk is very long. Perhaps such material is added to the central part which increases, periodically, the X-ray emission from the disk corona which, in turn, illuminates the central disk thus boosting the optical light emitted from its surface. X-ray illumination is known to be very important in NGC5548 (Kaastra et al. 2014; Mehdipour et al. 2015, 2016), thus such possibilities cannot be excluded. A detailed discussion of such a scenario is beyond the scope of the present paper. We note, however, that TDEs are very rare events (Rees 1990; Magorrian & Tremaine 1999, one event per inactive galaxy every $10^4 - 10^5$ years; e.g.), even though rates can be higher in AGN (Karas & Šubr 2007), and in the presence of supermassive binary black holes (e.g. Ivanov et al. 2005; Chen et al. 2011). In any case, chances of seeing such an event in only one single nearby galaxy analyzed are very small, and we therefore consider this possibility as very unlikely. Similarly, Landt et al. (2015) concluded that a TDE is a very unlikely explanation in NGC 5548.

5.3. Binary black holes

There are several scenarios involving binary BH systems in AGNs. These can be divided into two broad groups. One is where only one of the BHs has an accretion disk and a BLR associated with it. The other is the case where both BHs are accreting through their own disks. For roughly equal BH mass (the only case considered here) the average separation of the two is of order 20 ld and hence there is only one dusty toroidal structure around the two. In general, such systems are thought to be the end result of a galaxy merger, where the two BHs from the two galaxies are at the final stage of merging (see Milosavljević & Merritt 2001; Merritt & Milosavljević 2005). Earlier studies of NGC5548 suggest some evidence for a merger 0.6-1.0 Gyr ago (more details in Tyson et al. 1998; Steenbrugge et al. 2005; Slavcheva-Mihova & Mihov 2011). Some simulations performed in order to characterize the SMBBH systems, show the formation of a circum binary disk, inside of which the two BHs are accreting matter forming mini accretion disks (e.g. Hayasaki et al. 2008; MacFadyen & Milosavljević 2008; Bogdanović et al. 2008; Bogdanović et al. 2009; Cuadra et al. 2009; Smailagić & Bon 2015). Further out, the circum-binary disk cools and may form a torus. Blending BLRs, have also been investigated (e.g., Shen & Loeb 2010; Popović 2012), or in case of a high-mass-ratio system, only one shifting BLR may be seen. A second black hole can give rise to a host of phenomena that can yield periodic signals (see Katz 1997; Sillanpaa et al. 1988; Bogdanović et al. 2008; Bon et al. 2012; Kun et al. 2014; Graham et al. 2015a,b). A detailed scenario of this type has been investigated in several papers by Bogdanović and collaborators (Bogdanović et al. 2008; Bogdanović et al. 2009). They simulated a high-mass-ratio system with nearly identical time interval and periodicity as found here. These involve disk disruption, the formation and destruction of spiral arms in the gas between the BHs, and more. Some features of this model are appealing, especially those corresponding to periodic changes in the velocity curve of part of the gas, including cases where only one side of the profile is affected. Unfortunately, there have been no attempts to use the results of the dynamical simulation to calculate the resulting emission line spectrum, line profile and time variations in the systems. While we are not in a position to look into this in detail, we note that the gas configuration in this model, and the gas properties, might be very different from what is known from many years of study of NGC 5548. Moreover, as noted earlier, the broad-line spectrum of this source is very similar to the spectra of thousands of other type-I AGN. We thus consider it less plausible that NGC 5548 contain such a binary BH system.

A binary BH system where only one of the BHs carries its own disk and BLR (although the outskirts of the BLR must be disturbed by the “naked” BH) is perhaps easier to explain. Obscuration in this scenario is very inefficient. However, we note that gravitational lensing of the luminous disk around the primary BH by the second BH can enhance the continuum

emission by a factor of order 1.11 over a period of a few hundred days, while the effects over BLR emission would be even smaller, by a factor of less than 1%. For example, if both BHs have a mass of $5 \times 10^7 M_{\odot}$ and their separation is 20 ld, the size of the Einstein ring is ≈ 0.48 ld. This size should be compared with the size of the disk at 5100\AA (≈ 2 ld). Such an enhancement is achromatic which gives the immediate prediction that other continuum wavelengths would show an identical change of amplitude during the passage. Such a scenario cannot explain the periodic $H\beta$ variations or its periodic light curve. Moreover, 15 ld is well inside the BLR so dynamical changes in the line-emitting gas must be considered too.

Using a radial-velocity test for supermassive BBH for broad, double-peaked emission lines (Liu et al. 2016) assuming equal mass components, the line peaks should be at about 2300 km s^{-1} . At some epochs very small moving peaks in emission lines are identified corresponding such velocities (see Shapovalova et al. 2004). However, it is very clear that the red and blue wings of $H\beta$ respond to the same continuum variability at roughly the same time, so the gas emitting them is approximately at the same distance from the primary accretion disk. Recently, Li et al. (2016) proposed a BBH scenario in NGC 5548, as a result of their two Gaussian decomposition model, fitted into 150 day averaged spectra. We tried to test these claims, using series of two Gaussian decomposition models with different types of constraints (e.g., a constant intensity ratio with a significant width difference of each Gaussian, forcing them to fit different parts of the line, narrower fits for the core, and wider for the wings). We found that such a configuration could result in Gaussian components that switch sides and cross from blue to red and opposite. Unfortunately, in all cases we tested (assuming constant initial parameters of component shifts), there were additional crossings in radial velocity curves, that ruined the expected periodicity. We also note that in our modeling with a single Gaussian fit to the spectra (Fig. 7), we obtained a radial velocity curve appearing somewhat similar to the one of 75% red half width (see Figs. 7 and 3). This could imply the possibility of the same periodicity and could eventually indicate the presence of high-mass-ratio system. According to such analysis, we again find BBH hypothesis to be unlikely, except for the case of high-mass-ratio system, which we can neither disprove nor support.

5.4. Obscuration by gas and dust inside and outside the BLR

This category includes several possibilities of obscuration of the central disk, and part of the BLR, by a moving object at a distance corresponding to a 15.7 yr period. We consider two different possibilities, one an object inside the BLR moving around the primary BH, and the other an object which is part of an outflowing wind moving around the polar axis of

the disk. Both scenarios correspond to a situation where the length of obscuration is a small fraction of the period, perhaps a year or even less. Such a situation is consistent with the new scheme presented in section 4 which confirm the periodicity but do not show whether it is sinusoidal in shape or whether it corresponds to only one short event of dimming or enhancing the radiation of the central source. A large dust-free cloud moving around the primary BH, inside the BLR, at a distance corresponding to a period of 15.7 yr, can cause periodic obscuration of the central continuum source. This explanation is appealing since the required distance, about 15 ld, is exactly in the middle of the range of the multi-year RM size of the H β line and coincidental agreement between the two distances is unlikely. There are various difficulties to this scenario. The obscuring material must be thick enough and large enough to occult a large fraction of the central accretion disk which is 2 ld in radius, (see e.g. Fausnaugh et al. 2016). This dimension is larger than the typical size of BLR clouds that are of order 0.1 ld across assuming the density and column density are $\approx 10^{10} \text{cm}^{-3}$ and $\approx 10^{14} \text{cm}^{-2}$, respectively (e.g. Netzer 2013). A dust-free cloud must be Compton thick to block the 5100Å continuum since the ionized column of such gas is only of order $10^{22-23} \text{cm}^{-2}$. Thus both the radial and lateral dimensions of such a cloud are orders of magnitude larger than those considered typical of the BLR (a collection of clumps adding up to the required dimensions is just as difficult to explain). Obscuration by a dusty gas cloud is easier to explain since a very small column density, corresponding to $A_V < 1$ is all that is required to absorb much of the radiation at 5100Å. However, 15 ld is well within the dust sublimation radius for this source and such grains will not survive in this environment. One can consider a very large dusty cloud in a spiraling elliptical orbit (e.g. Netzer & Marziani 2010) where, in this case, part of the dust is not sublimated because it is shielded from the central source radiation during a big part of the orbit. We did not explore this possibility in detail but consider it problematic because efficient shielding of the dust from the radiation at wavelengths longer than the Lyman or Balmer continuum edges is hard to explain. Explaining the observed periodic variations in L(H β), and the period in its velocity curve, is even more challenging. Obscuration by dusty gas spiraling along the polar axis, as part of a large scale disk wind, is an alternative explanation. Disk winds have been considered for years as a general scenario to explain both the BLR and the dusty torus structure around the BH (see e.g. Elvis 2000; Elitzur & Shlosman 2006; Elitzur 2008; Czerny & Hryniewicz 2011; Netzer 2013; Arav et al. 2015; Netzer 2015; Elitzur & Netzer 2016). This geometry, which is sketched in Fig. 9 allows a period of 15.7 years at a distance much larger than 15 ld from the BH since material is rotating around the polar axis of the system, with small opening angle of about 30 degrees (as suggested earlier for this object, see eg. Rokaki et al. 1993; Kaastra et al. 2014) or less. For example, a dusty cloud at a distance of 50 ld, well inside the dust sublimation radius, can obscure the central source every 15.7 yr for a few hundred days. The required column density is small, corresponding

to $A_V < 1$ mag, and the lateral dimension of order the disk size, ~ 2 ld (while we talk about “a cloud” this may well be a collection of clumps). Such a cloud can also obscure part of the BLR although this fraction is much smaller because of the much larger dimensions of the BLR. Obscuration by dusty material must result in a wavelength dependent reddening of the central continuum. In principle, the obscuration may last only a few hundred days every 15.7 years and the available spectroscopy is not good enough to exclude such short-term events of reddening. Another difficulty with spiraling out material is that the outward motion of the gas will result in a continuous change of radius and hence periodicity. Such a change may be small over the 43 years of observations considered here. All these details are, again, beyond the scope of the present work. The geometry of the torus considered here is very different from the simple tori considered in earlier studies (Netzer 2015, and references therein). This opens a range of possibilities that may be related to the periodicity discussed here, in particular the obscuration by line-of-sight dust. Large structures in the non-uniform torus wall, scattering by the torus dust, etc, all should be investigated in detail.

5.5. Periodic X-ray enhancement and reflection

The main difficulty in all previous scenario is the lack of explanation of the clear connection between the periodic continuum variations, the periodic $H\beta$ flux variations, and the periodic $H\beta$ velocity variations. A more logical explanation is a mechanism that causes a periodic enhancement of the ionizing continuum, which in turn causes a periodic $H\beta$ intensity variations (reverberation), which will cause time-dependent changes in the mean emissivity radius of the $H\beta$ line. In a virialized cloud system, an increase in the $H\beta$ emission region is correlated with smaller gas velocities which is in agreement with the observed line width variations. About 2/3 of the bolometric luminosity in NGC 5548 is due to far-UV and soft X-ray emission (Gaskell 2008). The X-ray source is probably illuminating the central disk causing much of the optical-UV continuum variations (see Fausnaugh et al. 2016; Uttley et al. 2003; Edelson et al. 2015). Accretion events close to the primary BH, that enhance the emitted X-ray flux in a periodic fashion, can trigger the entire chain of events from optical continuum variations, to $H\beta$ flux variations, to $H\beta$ velocity variations. As suggested above, a pericenter passage of a partially tidally disrupted star is perhaps one possibility for such an event. Also, an orbiting G2 like object (see Witzel et al. 2014) or some other stellar size object with an orbit in a collision with the disk are perhaps some possibilities that could lead to such events. The energetics of these kind of pericentric encounters depend very much on the consistency of the medium (the accretion disk or the torus) that is being crossed with their orbit. One can also imagine one or more gas clouds from the BLR in very eccentric orbit the origin of such events. However, the mass of a single BLR cloud is tiny which makes it very unstable

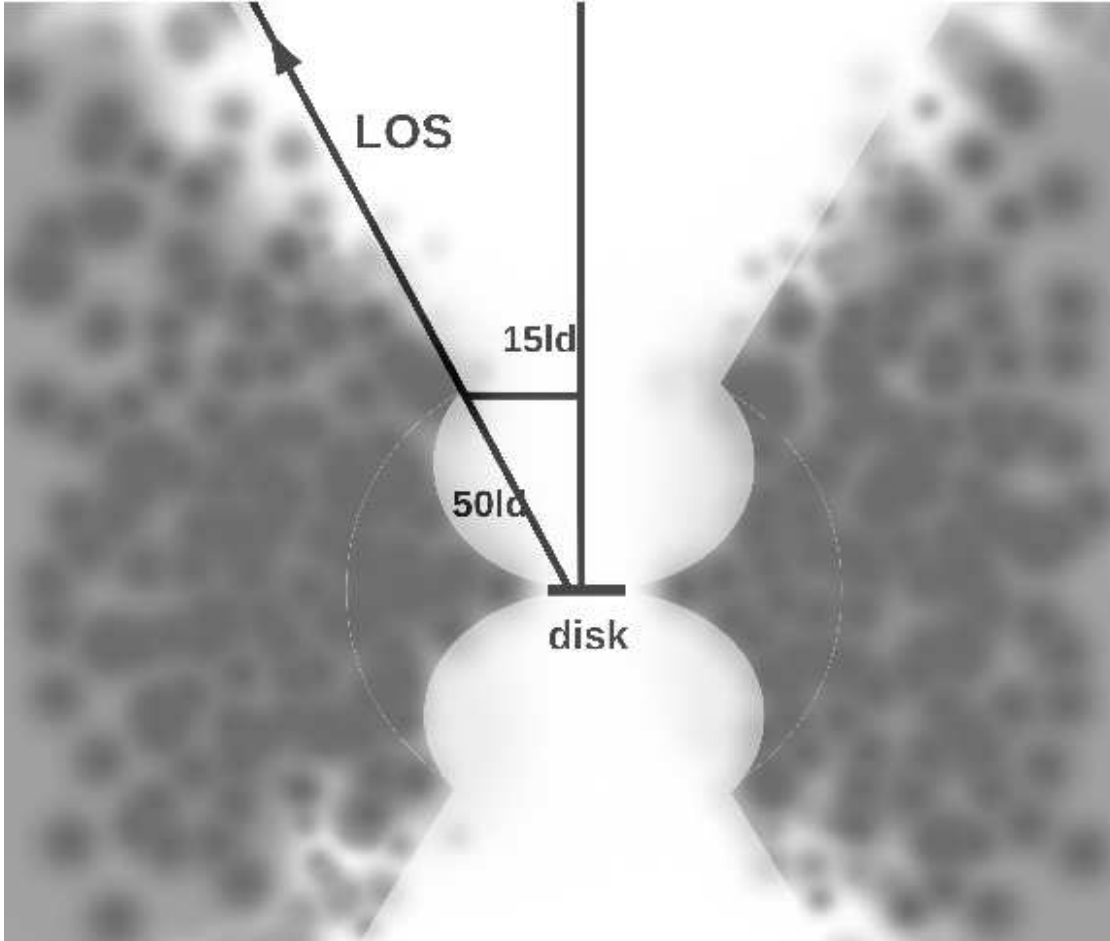


Fig. 9.— A representation of the disk obscuration, where partially obscured disk is seen through the inner edge of the torus cone (15ld from the axes and at the distance from the disk of about 50ld). Obscuration in such configurations are possible if the line of sight (LOS) is similar to the cone opening angle. In this case it would correspond to angles of about 30° , or less. The obscuration model assumed here has been inspired by various torus simulations obtained with SKIRT code (Stalevski et al. 2016).

against tidal forces and its mass supply to the BH is many orders of magnitude below what is required to produce a significant X-ray flare.

5.6. Orbiting body crossing the accretion disk

Periodic variations could be caused by an orbiting object perturbing the accretion disk while passing through it (eg. Syer et al. 1991; Chakrabarti & Wiita 1993; Armitage et al. 1996; Šubr & Karas 1999; Kieffer & Bogdanović 2016; Pihajoki 2016; Nguyen & Bogdanovic 2016). Such scenario was proposed for NGC 5548 in Shapovalova et al. (2004) and was connected to the appearing and shifting bumpy features in the red wing of $H\beta$. If we assume a stellar-mass object passing through the disk at a radius smaller than 15 ld, it could cause a perturbation in the disk, producing shocks (eg. Chakrabarti & Wiita 1993).

Such a collision could heat the disk (see e.g. Kieffer & Bogdanović 2016, raising the temperature above 10^7 K) producing periodic optical and X-ray emission. It is not our intention to attempt such calculations for NGC 5548, only to mention that the disk dimension, and the orbit eccentricity, are likely to be the limiting factors in such cases. The hot spots caused by impacts may not necessary need to live for the complete orbital time, but would be made periodically with each collision. Knowing that in our Galaxy there are a number of central stars (the “S0 stars”) that are on highly eccentric, randomly inclined orbits (Eckart & Genzel 1997; Ghez et al. 1998; Gillessen et al. 2009), and some of them show similar periodicities as here (e.g., for S0-2 the periodicity is 15.2 years, for S0-14 it is 38 years (eg. Zucker et al. 2006) (e.g., Zucker et al. 2006), and for S0-102 it is 11.5 years (see Meyer et al. 2012)), it is conceivable that one could find objects on inclined orbits that could cross the accretion disk of NGC 5548. In the case of a star passing through the part of the disk responsible for the optical emission, at about 2 ld radius, the eccentricity of the orbit would be about 0.7.

6. Conclusions

We have analyzed the 5100 Å continuum and the $H\beta$ light and radial velocity curves of NGC 5548 using about 1600 spectra spanning 43 years, including 12 years of new data. The main results of the study are as follows:

1. The continuum light curve shows a of periodicity of about 5700 days at a high confidence level. Similar periodicities are found in the light and radial velocity curves of the broad $H\beta$ emission line. The period has been detected through a standard periodogram analysis which we consider not very significant, as well as through a new method specif-

ically devised for the present data set that takes into account its heterogeneous quality and uneven sampling.

2. The detected periodicity is consistent with orbital motion inside the BLR of the source.
3. We examined various physical scenarios that can explain the observed periodicity. These include binary BHs, a TDE of a massive star, orbiting dust-free and dusty clouds around the central BH and the polar axis of the system (in a polar wind), and periodic enhancement of the inner part of the disk producing the X-ray emission. While none of these can explain all the observations, the preferred explanation is the one linking the enhanced continuum, the enhanced line emission and the lowering of the velocity through a single scenario related to the X-ray emission in this source. The enhanced X-ray emission could be triggered by an orbiting object periodically colliding with the accretion disk.

We would like to thank the International AGN Watch group for spectra available on their website, especially Bradley Peterson for with kind permission to use unpublished spectra observed at Asiago. Also, we would like to thank Tamara Bogdanović, Jack Sulentic and Mike Eraclous for all comments and suggestions. This research is part of the projects 176003 "Gravitation and the large scale structure of the Universe" and 176001 "Astrophysical spectroscopy of extragalactic objects" supported by the Ministry of Education and Science of the Republic of Serbia. This work was supported by: CONACyT research grant 151494 (Mexico), INTAS (grant N96-0328), RFBR (grants N97-02-17625, N00-02-16272, N03-02-17123, 06-02-16843, N09-02-01136, 12-02-00857a, 12-02-01237a, N15-02-02101) and MS acknowledges support by FONDECYT through grant No. 3140518.

Table 1:: Log of the new observations 2003-2015 from SAO, INOAE and Asiago. Columns in order are: number of the observation; date of the observation (DD.MM.YYYY); Julian date; a code assigned to the observatory (N); the aperture used; the spectral region covered and the seeing.

No	Date	JD-2400000	Observatory	Aperture	Sp. domain	Seeing
1	26.01.2003	52665.924	GHO	2.5x6.0	5700-7360	3.5
2	27.01.2003	52666.926	GHO	2.5x6.0	3800-7090	1.5
3	28.01.2003	52667.901	GHO	2.5x6.0	3800-7090	2.5
4	27.03.2003	52725.893	GHO	2.5x6.0	5700-7360	2.3
5	12.04.2003	52741.582	SAO	4.0x19.8	5590-7300	2.0
6	11.05.2003	52771.272	SAO	2.0x6.0	5738-8097	1.2
7	23.05.2003	52782.728	GHO	2.5x6.0	3700-7170	3.6
8	23.06.2003	52813.778	GHO	2.5x6.0	5600-7300	2.7
9	22.12.2003	52995.604	SAO	4.0x20.25	3742-6950	3.5
10	27.01.2004	53031.969	GHO	2.5x6.0	3800-7090	2.3
11	13.02.2004	53048.536	SAO	4.0x19.8	5640-7300	6.0
12	18.02.2004	53054.015	GHO	2.5x6.0	3800-7090	4.0
13	02.03.2004	53066.566	SAO	2.0x6.0	5800-8120	2.0
Observatory codes:						
SAO - Special Astrophysical Observatory of the Russian Academy of Science (Russia)						
GHO - INOAE Guillermo Haro Observatory (Mexico)						
ASG - Asiago Astrophysical Observatory (Italy)						
Continued on next page						

Table 1 – continued from previous page

No	Date	JD-2400000	Observatory	Aperture	Sp. domain	Seeing
14	18.03.2004	53082.826	GHO	2.5x6.0	5700-7360	2.3
15	19.03.2004	53083.862	GHO	2.5x6.0	3800-7090	2.3
16	12.04.2004	53107.523	SAO	4.0x12.15	3740-7400	2.0
17	12.04.2004	53107.894	GHO	2.5x6.0	3800-7090	3.5
18	15.05.2004	53140.504	SAO	4.0x20.25	3740-7400	1.5
19	19.05.2004	53144.756	GHO	2.5x6.0	3800-7090	2.3
20	21.05.2004	53146.703	GHO	2.5x6.0	5700-7360	2.7
21	11.06.2004	53167.751	GHO	2.5x6.0	3800-7090	1.8
22	13.06.2004	53169.727	GHO	2.5x6.0	5700-7360	1.8
23	14.06.2004	53171.406	SAO	4.0x20.25	3740-7400	2.0
24	11.07.2004	53198.356	SAO	4.0x20.25	3740-7400	4.0
25	12.07.2004	53199.331	SAO	4.0x20.25	3740-7400	4.0
26	14.12.2004	53354.021	GHO	2.5x6.0	3800-7090	3.6
27	16.12.2004	53355.995	GHO	2.5x6.0	5700-7360	2.3
28	16.01.2005	53386.960	GHO	2.5x6.0	3800-7090	2.3
29	18.01.2005	53388.935	GHO	2.5x6.0	5700-7360	2.3
30	19.01.2005	53389.929	GHO	2.5x6.0	3800-7090	4.1
31	14.02.2005	53415.861	GHO	2.5x6.0	3800-7090	3.6
32	16.02.2005	53417.569	SAO	4.0x09.45	3740-7400	4.0
33	17.03.2005	53446.808	GHO	2.5x6.0	5700-7360	2.7
34	18.03.2005	53447.797	GHO	2.5x6.0	3800-7090	3.1
35	22.03.2005	53451.563	SAO	4.0x09.45	3740-7400	6.7
36	16.04.2005	53476.823	GHO	2.5x6.0	5700-7360	2.3
37	16.04.2005	53477.460	SAO	4.0x09.45	3740-7400	5.5
38	17.04.2005	53477.785	GHO	2.5x6.0	3800-7090	1.8
39	17.04.2005	53478.437	SAO	4.0x09.45	3740-7400	6.5
40	12.05.2005	53502.783	GHO	2.5x6.0	3800-7090	3.6
41	14.05.2005	53504.760	GHO	2.5x6.0	5700-7360	2.3
42	16.05.2005	53507.487	SAO	4.0x09.45	3740-7400	2.5
43	18.05.2005	53508.515	SAO	4.0x09.45	3740-7400	2.5
44	18.05.2005	53509.483	SAO	4.0x09.45	3740-7400	2.5
45	09.06.2005	53530.753	GHO	2.5x6.0	3800-7090	1.8
46	11.06.2005	53532.706	GHO	2.5x6.0	5700-7360	3.6
47	16.06.2005	53538.428	SAO	4.0x09.45	3740-7400	2.5
48	08.07.2005	53560.391	SAO	4.0x09.45	3740-7400	4.0
49	23.01.2006	53758.951	GHO	2.5x6.0	5700-7360	1.8
50	20.02.2006	53786.962	GHO	2.5x6.0	3800-7090	2.7
51	21.02.2006	53787.539	SAO	4.0x09.45	3740-7400	2.0
52	22.02.2006	53788.567	SAO	4.0x09.45	3740-7400	2.0
53	22.03.2006	53816.542	SAO	4.0x09.45	3740-7400	4.0
54	18.04.2006	53843.803	GHO	2.5x6.0	3800-7090	2.3
55	21.04.2006	53846.780	GHO	2.5x6.0	5700-7360	2.6
56	21.02.2007	54152.926	GHO	2.5x6.0	3550-7090	1.8
57	25.02.2007	54156.565	SAO	4.0x09.45	3740-7400	4.0
58	26.02.2007	54157.604	SAO	4.0x09.45	3740-7400	4.0
59	23.03.2007	54182.522	SAO	4.0x09.45	3740-7400	2.5
60	23.03.2007	54183.467	SAO	4.0x09.45	3740-7400	4.0
61	25.03.2007	54184.901	GHO	2.5x6.0	3550-7100	2.7
62	26.04.2007	54216.521	SAO	4.0x09.45	3740-7400	4.0
63	21.05.2007	54241.756	GHO	2.5x6.0	3550-7090	1.8
64	22.05.2007	54243.430	SAO	4.0x09.45	3740-7400	2.0
65	23.05.2007	54244.399	SAO	4.0x09.45	3740-7400	2.0
66	24.05.2007	54245.406	SAO	4.0x09.45	3740-7400	2.0
67	23.06.2007	54275.395	SAO	4.0x09.45	3740-7400	3.0
68	21.07.2007	54303.331	SAO	4.0x09.45	3740-7400	2.5
69	14.02.2008	54510.605	SAO	4.0x09.45	3740-7400	4.0
70	06.06.2008	54624.450	SAO	4.0x09.45	3740-7400	2.5
71	04.02.2009	54866.564	SAO	4.0x09.45	3740-7400	4.0
72	19.02.2009	54881.596	SAO	4.0x09.45	3740-7400	5.7
73	20.02.2009	54882.563	SAO	4.0x09.45	3740-7400	2.5
74	16.05.2009	54968.419	SAO	4.0x09.45	3740-7400	2.5
75	17.05.2009	54969.410	SAO	4.0x09.45	3740-7400	2.5
76	23.02.2010	55250.556	SAO	4.0x09.45	3740-7400	5.5
77	24.02.2010	55251.574	SAO	4.0x09.45	3740-7400	3.5
78	20.03.2010	55275.510	SAO	4.0x09.45	3740-7400	2.6
79	19.04.2010	55306.462	SAO	4.0x09.45	3740-7400	2.5
80	28.03.2012	56014.519	SAO	4.0x09.45	3640-7900	7.5
81	29.03.2012	56016.497	SAO	4.0x09.45	3640-7900	4
82	12.01.2012	55939.686	ASG	5.0x6.0	3275-7950	4
83	20.02.2012	55978.603	ASG	5.0x6.0	3275-7950	4
84	28.02.2012	55986.473	ASG	5.0x6.0	3275-7950	4

Observatory codes:

SAO - Special Astrophysical Observatory of the Russian Academy of Science (Russia)
 GHO - INOAE Guillermo Haro Observatory (Mexico)
 ASG - Asiago Astrophysical Observatory (Italy)

Continued on next page

Table 1 – continued from previous page

No	Date	JD-2400000	Observatory	Aperture	Sp. domain	Seeing
85	30.12.2013	56657.595	ASG	5.0x6.0	3250-7925	4
86	15.04.2015	57128.311	ASG	5.0x6.0	3700-7920	4

Table 2: Spectral parameters obtained from the best fits. Table lists: Julian Date (N1); H β flux; Continuum flux measured at 5100 Å in units of $10^{15} \text{ erg/s/cm}^2$ and broad H β emission line in units of $10^{13} \text{ erg/s/cm}^2/\text{Å}$; and wavelengths measured at blue and red side of 25%, 50%, 75% and 90% of maximum intensity of broad H β emission line in units of kms^{-1} . Here we present only example of the table (with beginning and the end part). The complete table in electronic version is appended.

JD-2400000	Flux H β	Err.	Fl. 5100	Err.	B25%	R25%	B50%	R50%	B75%	R75%	B90%	R90%
41420.546	7.64	0.14	5.02	0.08	-3695.2	4127.0	-2750.7	2317.6	-2040.4	518.9	-1565.9	-137.8
41426.531	8.38	0.16	4.86	0.09	-4131.3	4272.3	-3116.2	2012.3	-2277.5	737.1	-1677.0	131.7
41446.471	6.10	0.02	4.33	0.01	-4065.1	3665.6	-3169.5	2749.3	-2451.0	379.8	-1911.0	-345.5
41460.463	6.44	0.18	4.44	0.13	-4542.0	7289.4	-3349.8	2805.7	-2632.2	-227.5	-2212.7	-770.2
41484.456	8.85	0.15	6.10	0.05	-4265.2	4006.7	-3131.6	1932.5	-2413.4	355.8	-1933.6	-308.7
41566.266	13.35	0.42	11.18	0.02	-6064.2	4237.7	-3640.7	2173.0	-2689.5	242.6	-2153.1	-418.1
41681.662	14.71	0.73	11.96	0.40	-5332.9	3892.3	-3795.3	2435.8	-2904.6	384.4	-2368.8	-516.2
41682.658	14.33	0.05	12.77	0.00	-4086.0	4141.3	-3136.8	2986.7	-2482.4	29.4	-2065.2	-630.5
41684.66	12.46	0.09	13.43	0.05	-4269.1	3953.2	-3379.8	3041.9	-2666.5	144.1	-2130.3	-516.0
41686.668	16.26	0.05	10.07	0.01	-4633.0	3761.8	-3151.2	2790.5	-2318.1	315.5	-2318.1	-285.1
41749.513	9.35	0.57	12.49	0.42	-3722.4	4029.1	-3009.7	2996.1	-2474.1	1966.6	-2116.5	-981.2
41750.508	14.38	0.30	12.66	0.16	-3984.5	4063.5	-3094.3	2909.2	-2380.2	553.5	-1843.5	-227.6
41752.432	13.77	0.36	11.65	0.18	-4884.4	3564.5	-3225.6	2714.8	-2452.2	120.2	-1915.6	-480.0
41766.534	13.59	0.62	12.13	0.35	-4249.6	3791.9	-3360.2	2759.7	-2646.7	104.4	-2170.0	-555.8
41767.426	15.15	0.12	12.51	0.02	-7037.7	5051.1	-3853.8	2860.7	-2963.2	-35.4	-2487.2	-994.6
41768.511	13.48	0.65	11.62	0.36	-3899.8	4092.1	-3068.5	2755.4	-2413.8	219.8	-1936.7	-500.7
41779.529	13.50	0.03	11.11	0.01	-4098.9	3824.2	-3149.6	2670.8	-2376.1	557.6	-1839.4	-103.5
41780.537	12.69	0.07	11.11	0.04	-3956.6	4033.6	-3185.0	2818.4	-2530.5	-78.2	-2113.2	-678.2
41782.509	13.31	0.12	14.10	0.02	-5435.3	4151.3	-3483.1	2936.1	-2532.0	700.8	-1876.3	-20.7
41783.516	16.87	0.79	13.76	0.39	-4335.7	3765.0	-3268.3	2854.0	-2435.3	739.1	-1779.2	77.5
41806.418	15.41	0.27	14.75	0.12	-3959.0	4396.8	-3068.5	2876.7	-2413.7	580.8	-1936.6	-380.7
41807.428	17.41	0.40	12.57	0.06	-4097.1	3825.9	-3029.0	2672.5	-2374.4	-161.8	-1957.0	-641.6
41809.462	15.14	0.45	11.40	0.22	-3885.5	4289.2	-2935.3	2951.6	-2220.6	1257.9	-1743.2	-66.3
41838.434	14.94	0.10	6.41	0.03	-4491.2	4521.0	-3126.8	3242.9	-2174.0	1185.0	-1517.2	462.1
41839.372	9.53	0.26	5.92	0.11	-3991.5	4182.8	-3160.3	2784.7	-2445.9	1393.0	-1968.8	248.2
41840.404	10.38	0.04	8.38	0.01	-3763.1	3928.0	-2871.9	2895.1	-2097.5	1081.0	-1560.1	178.0
41856.327	15.67	0.01	9.31	0.01	-3996.9	4360.2	-2808.7	2961.2	-1974.2	1146.2	-1376.7	423.2
41857.348	11.90	0.02	9.26	0.01	-3889.8	3919.8	-2820.6	2886.9	-1986.3	1615.9	-1388.9	590.9
41870.318	17.19	0.03	8.19	0.01	-3971.4	4523.7	-2952.6	3172.7	-2171.2	1583.9	-1629.0	185.4
41887.302	11.19	0.28	6.24	0.10	-4137.1	3788.7	-3128.1	2816.8	-2234.9	1063.1	-1578.2	340.5
41894.285	11.04	0.31	7.74	0.18	-3920.9	3890.3	-2911.0	2675.3	-2196.0	1223.7	-1718.4	79.4
41919.257	12.06	0.45	8.41	0.25	-4378.5	3906.8	-3072.9	2570.6	-2298.8	697.6	-1761.6	-204.4
41922.267	10.42	0.28	8.09	0.16	-4781.0	3736.0	-3299.0	2582.3	-2287.1	1191.6	-1570.7	528.7
41945.235	8.51	0.01	7.66	0.01	-5291.4	4183.3	-3040.0	2664.1	-2206.2	851.1	-1669.0	8.7
42036.641	6.26	0.07	6.39	0.02	-3876.2	4239.6	-2925.7	2780.7	-2270.5	1449.5	-1793.1	-176.2
42037.653	7.89	0.48	4.33	0.22	-4496.3	4332.9	-3310.3	2631.0	-2417.6	1421.3	-1761.3	517.1
42050.664	5.34	0.81	4.86	0.63	-4033.3	4183.3	-3078.3	3021.8	-2360.0	1925.6	-1820.1	46.9
42077.624	10.99	0.20	5.90	0.03	-4115.0	5388.6	-2861.2	2633.8	-1962.3	1174.8	-1361.6	447.9
42097.615	7.29	0.24	5.11	0.16	-3933.7	3674.0	-2858.7	2270.9	-2139.8	571.4	-1659.6	-93.6
42136.548	7.41	0.09	6.47	0.03	-3744.3	3440.8	-2668.5	2160.3	-1889.1	764.0	-1408.5	219.4
42137.547	8.66	0.28	6.78	0.04	-5006.7	3978.1	-3099.7	1843.3	-2141.6	630.1	-1514.3	85.8
42158.568	5.62	0.12	5.17	0.09	-3996.3	4100.3	-2921.3	2695.0	-2202.6	1782.0	-1722.4	387.4
42182.533	8.69	0.44	4.51	0.20	-4682.0	6283.4	-3549.6	3825.6	-2892.1	2604.0	-2472.9	1448.2
42194.422	6.18	0.04	7.68	0.01	-5540.0	8792.6	-3934.5	3063.1	-2979.1	752.7	-2380.3	-456.2
42221.351	7.36	0.23	6.30	0.17	-4053.8	4286.1	-3098.7	3002.0	-2380.4	2027.2	-1780.4	1176.9
42223.371	8.68	0.21	7.28	0.15	-4495.0	5795.6	-3123.2	2732.3	-2165.3	1515.6	-1504.8	727.3
42239.341	9.85	0.10	8.57	0.07	-4121.0	4218.1	-2926.8	2934.1	-2147.9	1837.8	-1607.5	261.4
42244.368	9.01	0.06	5.92	0.01	-3752.2	4106.6	-2975.6	3006.1	-2316.9	1848.8	-1896.9	-150.7
42276.289	8.06	0.13	5.94	0.07	-4370.8	3959.9	-3237.5	2799.1	-2399.7	1339.2	-1799.8	248.9
42277.277	7.16	0.02	7.41	0.01	-4236.5	3792.4	-3222.2	2388.5	-2324.3	1233.7	-1724.2	385.6
42278.279	7.37	0.08	6.95	0.01	-4362.3	3785.6	-3228.9	2991.3	-2450.9	2503.6	-1911.1	2077.4
42311.217	8.04	0.11	6.13	0.06	-4033.5	4266.7	-3195.8	2979.5	-2535.9	1941.4	-1994.9	300.0
42396.633	8.84	0.53	5.66	0.32	-6985.3	5484.8	-3364.5	3461.8	-2167.6	2181.4	-1447.1	1270.2
42429.616	5.86	0.08	5.95	0.07	-3645.0	4386.8	-2809.6	3104.3	-2151.6	2191.5	-1732.1	-168.8
42430.606	8.98	0.63	6.37	0.34	-3966.6	5221.8	-3072.3	2959.2	-2055.5	1864.5	-975.1	1137.0
42462.544	5.10	0.43	5.08	0.37	-4251.6	4456.0	-3236.8	3476.0	-2338.4	2377.2	-1617.7	1282.4
42476.521	4.72	0.02	2.94	0.01	-4130.1	4397.1	-3294.2	3356.1	-2635.8	2501.5	-2156.0	1770.9
42477.595	6.48	0.22	3.93	0.14	-3927.2	4553.5	-3101.7	3223.8	-2392.3	2260.5	-1859.1	1480.0
42478.601	10.82	0.38	3.93	0.14	-4661.1	5609.4	-3351.7	3222.1	-2455.5	1944.4	-1736.7	1035.0
42520.432	6.86	0.76	4.30	0.40	-4511.0	5640.6	-3260.7	3070.5	-2244.7	1611.5	-1525.5	763.7
42544.348	5.35	0.07	3.60	0.05	-4429.1	4390.7	-3475.1	3350.4	-2877.3	2374.5	-2158.4	1644.6
42545.356	5.99	0.04	6.00	0.01	-4664.0	4890.5	-3531.1	3419.5	-2573.7	1955.6	-1853.6	801.7
42566.413	4.63	0.33	3.82	0.11	-5917.3	9773.9	-4194.0	4575.2	-3298.7	2435.0	-2640.4	-53.0
42567.398	5.87	0.08	3.23	0.06	-4914.3	5803.4	-3423.6	3531.2	-2705.4	487.5	-2165.6	-540.3

Note: (1) Julian dates of IAW watch data in the form “*.1” are used to artificially make a difference between two different spectra under the same MJD on IAW watch web site (as for example 48325.0 and 48325.1)

(2) File names differs according to the observatory/monitoring campaign:

PTG* : Crimean Astrophysical Observatory data

n* : AGN watch data

5* : SAO/GHO data

A* : Asiago data

Continued on next page

Table 2 – continued from previous page

JD-2400000	Flux Hb	Err.	Fl. 5100	Err.	B25%	R25%	B50%	R50%	B75%	R75%	B90%	R90%
42573.433	6.34	0.30	5.95	0.23	-5330.2	6358.8	-3542.9	3653.8	-2705.2	669.5	-2225.5	-540.1
42605.343	9.33	0.28	10.22	0.06	-5679.6	9965.0	-3656.1	4026.0	-2878.7	3047.3	-2399.4	2559.2
42606.321	7.09	0.05	9.34	0.04	-4793.0	6853.0	-3779.9	3960.3	-3122.6	2798.7	-2703.5	2006.5
42607.339	10.50	0.07	8.34	0.04	-4476.4	4839.9	-3581.7	3736.0	-2863.9	2941.2	-2264.4	2392.2
42631.296	10.74	1.34	9.85	0.92	-4140.1	5003.1	-3184.4	3776.0	-2525.6	2859.0	-2105.6	2188.2
42632.285	9.85	0.95	10.52	0.74	-4292.3	4536.5	-3337.4	3495.1	-2619.2	2884.2	1301.5	2518.2
42671.226	11.05	0.07	6.68	0.03	-4635.3	4673.6	-3442.6	3203.8	-2664.8	2532.5	-2185.1	1923.5
42685.216	8.32	0.19	6.33	0.06	-3816.6	4044.6	-3099.6	3127.0	-2440.8	2334.0	-2020.7	1360.8
42758.63	9.05	0.09	6.03	0.05	-4728.3	4517.4	-3655.3	3292.5	-2758.2	2377.1	-2098.5	1586.0
42870.59	5.33	0.03	5.19	0.01	-4479.3	4530.1	-3465.0	3488.4	-2687.0	2694.3	-2147.2	-401.2
42902.438	8.28	0.20	9.32	0.15	-4254.1	4325.0	-3478.8	3285.0	-2821.3	2553.0	-2342.1	-839.8
42934.37	7.20	0.15	7.22	0.00	-4138.8	3714.5	-3362.7	2980.9	-2764.3	2249.1	-2344.7	-901.7
42949.358	8.99	0.18	5.84	0.10	-4936.2	4365.2	-3863.9	3201.9	-3027.2	2408.6	-2428.1	1799.7
42956.419	7.72	0.13	8.04	0.09	-4819.4	4301.7	-3328.4	3138.7	-2610.0	2223.7	-2130.1	-504.9
42987.302	8.01	0.07	7.65	0.04	-4479.1	4467.1	-3524.7	3609.3	-2807.0	2937.1	-2327.5	2510.1
42989.321	8.30	0.13	6.77	0.09	-4410.9	4353.0	-3575.9	3128.9	-2978.0	2457.7	-2438.9	2153.1
43009.28	5.30	0.10	4.83	0.02	-4673.5	4758.2	-3719.7	3348.9	-2822.8	2552.2	186.7	2007.0
43016.28	8.60	0.14	7.23	0.03	-3941.7	4468.0	-2806.0	3304.6	-2086.5	2206.4	-1545.7	22.0
43034.214	8.37	0.11	8.68	0.08	-5385.2	4819.2	-3957.1	2982.3	-3001.3	2189.7	-2342.3	1642.3
43036.23	10.76	0.13	8.29	0.06	-5220.7	5789.7	-3612.7	3335.1	-2356.0	2054.3	-1214.4	1385.5
43038.223	9.66	0.08	6.75	0.05	-4726.0	4458.3	-3473.8	3417.1	-2636.1	981.1	-2036.2	-169.0
43112.636	8.40	0.01	4.94	0.00	-4154.3	4248.5	-3378.4	2902.8	-2420.6	1867.0	-1978.1	1198.8
43142.626	6.76	0.30	3.27	0.15	-4298.9	4100.6	-3284.3	3060.7	-2446.0	2206.9	-1665.5	1598.5
43163.65	5.47	0.59	4.54	0.42	-4638.4	3689.8	-3744.3	2651.3	-2188.2	2042.1	-1407.1	766.7
43164.631	8.35	0.25	4.40	0.12	-4041.9	3753.3	-3086.1	2531.4	-1886.9	1496.7	-1165.0	829.0
43190.601	6.55	0.02	5.81	0.01	-5478.8	4662.1	-3752.7	3314.5	-2676.3	2521.0	-1956.4	1304.3
43200.378	6.56	0.07	5.73	0.03	-4109.0	4295.6	-3273.2	3377.3	-2614.7	2583.6	-2135.0	1852.8
43256.491	8.15	0.26	7.61	0.18	-4069.8	4091.3	-3054.3	3051.4	-2095.3	1589.2	-1313.9	860.8
43257.489	7.31	0.08	7.84	0.06	-4112.4	4476.2	-3276.5	3251.6	-2618.1	2580.2	-2138.4	1971.1
43258.479	8.63	0.07	6.51	0.04	-4110.9	4109.9	-3275.0	3314.3	-2616.6	2703.7	-2076.8	2277.0
43285.372	10.98	0.14	7.05	0.06	-4032.2	4251.4	-3016.7	2905.7	-2177.8	1809.1	-1216.1	1080.3
43308.416	13.52	0.25	9.74	0.13	-5127.2	4841.6	-3817.1	3493.2	-2141.3	2394.4	-998.7	1603.3
43310.384	10.72	0.12	9.18	0.05	-4893.9	5205.9	-3403.5	3733.4	-2145.8	2450.8	-1244.1	1538.0
43311.408	9.72	0.20	8.91	0.12	-4200.1	4877.9	-3244.8	3223.5	-2526.3	2247.4	-1968.3	1699.7
43346.287	11.45	0.07	9.61	0.03	-4121.2	4160.9	-3105.9	3059.6	-2267.1	2084.1	-1606.4	1293.7
43362.306	13.71	0.18	7.68	0.07	-4169.3	4295.0	-3273.8	3193.3	-2495.5	2095.6	-1895.4	759.4
43363.281	12.16	0.97	8.57	0.49	-4588.8	4844.8	-3455.7	3251.8	-2737.8	2397.5	-2258.2	1849.6
43374.288	10.31	1.57	8.74	0.99	-4735.6	4327.9	-3602.6	2798.2	-2705.1	1884.1	-2045.3	1215.5
43391.239	12.96	0.24	10.30	0.13	-4354.5	3737.2	-3280.2	2759.5	-2322.0	2028.3	-1607.7	1481.1
43393.248	8.96	0.21	9.11	0.14	-4085.6	4014.2	-3070.1	2913.4	-2291.2	1330.4	-1750.7	57.9
43394.235	13.42	0.11	9.28	0.05	-3532.2	3908.0	-2814.4	2868.6	-2094.9	1832.9	-1554.1	800.6
43395.233	7.86	0.26	6.91	0.18	-4032.1	4253.2	-3016.4	3151.6	-2297.3	2297.4	-1756.9	838.8
43489.641	10.90	0.09	7.63	0.05	-5377.6	7961.9	-3423.1	4586.7	-2649.6	2943.3	-2112.9	2336.9
43497.607	9.18	0.43	8.51	0.31	-3921.0	5104.8	-2964.7	3510.2	-2185.5	2472.1	-1644.8	1498.3
43522.603	12.37	0.11	6.85	0.05	-4157.9	4797.3	-3142.8	3449.1	-2244.2	2350.5	-1583.6	1377.3
43525.618	9.89	0.06	11.55	0.03	-4647.0	5216.9	-3693.1	3682.9	-2915.7	2766.2	-2256.3	2156.6
43574.53	10.66	0.88	11.39	0.60	-4383.6	4996.1	-3309.4	3341.0	-2471.1	2303.6	-1870.9	1391.1
43611.5	13.04	0.14	9.75	0.03	-3989.4	4786.8	-3153.2	3438.7	-2434.6	2340.1	-1954.5	881.5
43612.477	14.98	0.05	10.02	0.02	-4427.6	4397.6	-3413.4	2990.0	-2635.4	2136.4	-2155.6	-289.2
43614.507	9.44	2.04	6.94	1.25	-4839.0	4588.9	-3646.8	3180.1	-2989.1	2447.7	-2569.7	1960.5
43630.379	7.82	0.08	8.91	0.06	-3744.7	4363.3	-2907.8	3200.3	-2008.5	2468.0	-382.9	1920.0
43639.417	14.11	0.03	11.77	0.02	-4312.5	4577.7	-3297.8	3108.2	-2459.6	2315.1	-1799.3	1706.5
43667.432	11.08	0.03	10.56	0.01	-3788.8	4319.2	-2772.3	3461.8	-1992.6	1997.6	-1391.4	661.6
43668.419	15.06	0.11	8.28	0.01	-3919.8	4490.0	-3143.2	3326.5	-2484.5	2593.9	-1944.5	2106.6
43672.384	11.29	0.36	10.45	0.22	-4360.8	4220.9	-3465.8	3119.5	-2688.0	2326.4	-1848.1	1717.8
43696.359	14.38	0.36	9.00	0.16	-4361.1	4834.3	-3406.4	3302.5	-2628.4	2508.9	-2088.6	1960.8
43697.393	12.44	0.12	7.71	0.05	-4052.2	4599.6	-2976.8	3313.4	-2137.7	2458.9	-1356.5	1910.9
43699.383	11.42	0.32	8.65	0.16	-4195.8	4573.4	-3240.7	3348.6	-2582.3	2738.0	-2042.5	2372.3
43717.313	10.39	0.04	5.71	0.02	-4106.2	4053.3	-3210.5	3013.5	-2432.1	2342.6	-1891.9	1734.0
43718.307	12.59	0.03	5.65	0.01	-4006.3	3788.9	-2990.6	2750.0	-2091.4	2079.7	-164.2	1653.9
43726.292	12.76	0.50	5.70	0.16	-3985.5	4299.9	-3089.5	3259.3	-2370.7	2465.9	-1890.5	1857.1
43728.283	9.82	0.07	5.83	0.03	-4166.2	4973.3	-3091.3	3257.4	-2192.6	2403.1	-1471.6	1794.4
43754.259	8.47	0.03	5.99	0.02	-4464.8	6019.1	-3450.7	3317.9	-2672.9	2463.4	-2133.2	1915.4
43755.254	7.24	0.02	5.41	0.01	-4164.1	4668.3	-3029.3	3259.6	-2130.4	2466.2	-1288.9	1979.1
43931.565	6.62	0.13	7.66	0.12	-4166.7	4972.8	-3031.9	3195.9	-2133.0	2585.6	883.2	2220.0
43932.519	9.06	1.79	5.98	1.08	-3953.7	4270.4	-2938.0	3107.9	-1978.8	2375.9	-172.0	1949.7
43933.553	10.57	0.11	8.30	0.06	-4170.4	4355.1	-3095.5	3008.9	-2256.7	2277.1	-1355.5	1851.0
43934.578	9.15	0.28	8.05	0.19	-4795.6	5183.3	-3424.4	3283.0	-2406.9	2428.7	-1446.0	1880.8

Note: (1) Julian dates of IAW watch data in the form “*.1” are used to artificially make a difference between two different spectra under the same MJD on IAW watch web site (as for example 48325.0 and 48325.1)

(2) File names differs according to the observatory/monitoring campaign:

PTG* : Crimean Astrophysical Observatory data

n* : AGN watch data

5* : SAO/GHO data

A* : Asiago data

Continued on next page

Table 2 – continued from previous page

JD-2400000	Flux Hb	Err.	Fl. 5100	Err.	B25%	R25%	B50%	R50%	B75%	R75%	B90%	R90%
43984.367	8.95	0.60	9.70	0.45	-4835.9	4958.6	-3644.0	3059.5	-2686.9	2144.8	-1125.1	1597.4
43986.462	9.37	0.16	8.75	0.10	-4828.5	4413.4	-3517.1	3128.0	-2559.7	2334.9	-1719.4	1848.0
43987.468	9.77	0.08	9.68	0.06	-4446.4	4377.0	-3312.8	3030.8	-2354.8	2238.1	-308.8	1751.3
43988.482	9.44	0.06	8.39	0.01	-4462.5	4361.0	-3388.6	3075.8	-2430.8	2343.9	-1349.6	1856.9
43989.451	10.24	0.70	11.19	0.52	-4481.1	4281.1	-3287.7	3057.2	-2449.5	2325.3	-1789.2	1899.1
44015.381	10.11	0.33	8.54	0.21	-3795.1	4250.0	-2958.4	3148.5	-2119.3	2416.4	291.2	1929.3
44018.431	10.07	0.15	9.42	0.10	-4416.4	4715.8	-3222.7	3184.6	-2204.3	2391.4	-157.1	1843.5
44052.367	10.47	0.57	9.36	0.37	-3966.3	4503.1	-2950.6	3156.3	-1991.4	2424.2	-63.8	1937.1
44085.348	13.48	0.91	9.66	0.49	-4011.7	3678.4	-3001.7	2706.3	-2167.3	1979.3	-1151.0	1495.6
44106.273	16.26	1.84	14.34	0.97	-4053.3	3556.8	-2918.1	2457.8	-2018.8	1666.5	-1237.2	1059.3
44107.268	12.75	1.61	10.82	0.93	-3986.1	3625.5	-3090.1	2709.2	-2311.3	2039.0	-1650.8	1613.3
44127.242	6.98	0.07	7.86	0.05	-4639.8	5283.6	-3387.3	2955.0	-2549.4	2040.7	-1889.4	1493.5
44225.632	8.93	0.12	7.31	0.07	-4462.0	4852.5	-3328.4	3259.6	-2430.3	2466.2	98.6	1979.1
44254.646	10.25	0.20	9.94	0.14	-4016.9	4328.1	-2881.7	3104.3	-1922.3	2433.2	-175.6	1885.3
44289.582	10.78	0.04	11.09	0.02	-3923.0	3996.3	-2966.9	2895.7	-2247.8	2286.0	343.2	1860.0
44290.607	10.20	0.13	10.93	0.09	-4352.7	4413.0	-3218.6	2944.3	-2260.3	2151.8	-1178.4	1604.3
44342.469	11.31	0.56	10.87	0.37	-4231.9	3924.3	-3276.8	2701.9	-2558.4	1970.9	-2078.6	1423.7
44348.444	9.31	0.43	7.74	0.26	-6078.1	4226.2	-3938.2	2880.5	-2682.7	2088.1	-1602.4	1601.6
44349.43	9.09	0.29	8.51	0.19	-3989.1	3622.5	-2913.5	2523.3	-2014.2	1853.5	-1292.8	1306.6
44377.389	11.98	0.69	11.38	0.45	-4476.7	4345.0	-3462.9	3121.1	-2685.2	2450.1	-2085.6	1963.0
44378.425	10.64	0.27	11.51	0.19	-4277.6	3938.2	-3083.5	3020.9	-2184.7	2411.0	-1283.3	1923.9
44400.381	6.59	0.74	6.40	0.64	-4433.9	3960.6	-3300.3	3104.4	-2222.3	2494.3	126.7	2068.0
44494.241	5.59	0.09	6.01	0.09	-4412.0	4413.3	-3278.2	3005.7	-2260.0	2395.7	876.2	2091.2
44497.231	8.83	0.34	5.73	0.19	-4951.8	4286.4	-2983.2	3368.1	-1843.9	2452.5	-1122.0	993.3
44672.516	10.71	0.51	8.99	0.32	-5122.5	6262.5	-3633.3	3803.9	-2676.3	2399.1	-2016.5	1608.0
44705.496	9.00	0.23	8.70	0.17	-5091.9	5061.2	-3304.0	3161.8	-2286.0	2368.7	-1384.9	1881.8
44706.507	6.92	0.20	7.96	0.18	-6063.2	5223.5	-1827.9	1920.4	-1045.9	524.5	-684.2	161.3
44728.409	8.66	0.17	6.59	0.10	-4450.1	5479.3	-2598.2	2905.1	-1457.5	1808.5	-734.8	1201.0
44729.461	8.82	0.61	6.55	0.34	-5190.1	5822.6	-3462.3	3306.3	-2204.8	2512.8	750.2	2086.4
44757.441	10.75	0.35	9.61	0.23	-4936.0	3934.5	-2608.2	2956.2	-1828.2	2407.3	-1467.5	2041.9
44759.412	14.13	0.23	13.65	0.14	-5405.8	4001.2	-2842.3	2717.6	-1642.4	1317.9	-1040.6	650.8
44815.338	13.33	0.44	12.60	0.26	-5136.8	3972.1	-3289.3	2932.7	-2271.3	2201.1	-1550.6	1653.6
44819.298	12.25	0.24	11.80	0.15	-4845.2	4701.4	-2816.4	3292.8	-1796.8	2560.4	-954.6	2073.1
44849.246	8.63	0.12	7.78	0.07	-6147.4	8485.9	-4253.0	5526.6	-2883.8	2717.2	-1987.5	2170.6
44988.593	12.95	0.18	8.65	0.09	-4259.6	5162.0	-2957.1	3338.7	-2006.2	2491.6	-1291.1	1345.8
44989.567	9.93	0.21	9.23	0.09	-4192.8	5839.9	-3068.2	3285.1	-2177.3	2619.5	-1283.7	2196.7
45018.567	11.30	0.23	7.84	0.07	-4773.8	4931.8	-3525.6	3221.3	-2511.3	2369.6	-1493.5	1823.3
45054.539	13.47	0.87	6.79	0.35	-4721.4	4129.5	-3115.2	2909.9	-1919.9	1998.4	-539.3	1392.2
45114.399	11.43	0.10	10.32	0.01	-4901.3	4433.2	-3296.1	3212.4	-2281.0	2360.7	-1502.4	1693.2
45115.421	9.92	0.08	8.10	0.01	-5274.1	4232.5	-3492.2	3012.3	-2059.0	2161.2	-799.1	1554.6
45144.393	10.70	0.30	8.60	0.15	-4951.2	4381.4	-3465.6	2978.1	-2331.5	2309.3	-1493.0	1945.1
45171.312	11.93	0.02	7.71	0.00	-4719.2	4804.6	-3470.8	3155.6	-2575.8	2304.1	-1857.8	1758.0
45172.331	10.93	0.65	12.01	0.46	-4379.6	3993.0	-3189.3	2956.4	-2293.4	2287.5	-1754.6	1802.0
45173.319	12.10	0.54	8.72	0.30	-4728.1	4122.8	-3420.0	2781.5	-2465.1	2295.2	-1687.0	1991.7
45326.651	12.76	0.07	8.20	0.03	-4358.8	3952.7	-3228.1	3038.1	-2272.6	2429.8	552.1	2065.5
45411.546	13.29	1.50	13.52	0.95	-4181.3	3785.8	-3151.5	2669.9	-2118.0	2051.8	-224.3	1619.9
45436.517	11.22	0.08	8.92	0.05	-4129.4	3700.3	-3117.1	2786.4	-2280.8	2178.6	-1262.3	1753.9
45437.538	9.36	0.06	8.87	0.02	-4190.1	4065.3	-2999.0	3028.6	-2162.4	2359.6	-1503.5	1934.7
45471.479	9.41	0.15	8.16	0.09	-3730.2	3765.1	-2773.6	2848.4	-1994.0	2177.9	-1272.7	1691.3
45473.467	11.22	0.09	9.97	0.06	-4152.1	3944.5	-3017.3	2966.2	-2178.4	2417.3	-1517.6	2051.9
45501.403	11.00	0.01	11.24	0.00	-4051.4	4539.0	-2856.3	2825.6	-2016.9	2094.2	-1415.8	1607.7
45503.493	13.55	0.75	9.19	0.37	-3992.3	3802.9	-2916.7	2764.0	-1957.4	2032.8	-1115.4	1424.8
45528.379	10.65	0.21	7.47	0.12	-5064.6	3924.7	-3395.9	2580.4	-2198.2	1667.2	-1356.9	1059.9
45529.326	10.17	0.22	10.56	0.16	-4860.5	5116.3	-3190.8	3094.3	-1992.3	1997.1	-1210.7	1207.1
45552.289	14.46	0.65	9.32	0.28	-4871.7	5105.1	-3500.9	3205.3	-2363.6	2290.2	-1522.8	1864.2
45553.326	9.50	0.20	10.73	0.14	-4042.2	3690.2	-2787.3	2468.8	-2067.8	1920.8	706.5	1677.6
45554.278	9.40	1.31	8.80	0.93	-3942.3	4038.2	-2686.9	2632.4	-1666.6	1962.3	-1064.9	1050.9
45584.237	13.31	2.18	10.21	1.23	-5186.6	4227.9	-3040.3	2882.2	-1961.2	1846.5	-1059.0	1178.2
45674.629	9.96	0.78	7.58	0.49	-4170.2	3559.2	-2975.6	2582.0	-1535.7	1912.1	-330.5	1425.8
45732.6	10.73	0.15	8.59	0.08	-3612.2	3580.1	-2475.4	2542.1	-1334.2	1933.1	-128.3	1507.5
45734.623	12.44	0.45	7.09	0.11	-4384.5	3705.6	-2951.5	2606.1	-1992.4	2057.9	-1331.2	1571.4
45793.505	12.05	0.23	7.56	0.11	-4171.5	4108.9	-3036.7	2763.7	-2017.7	2093.4	-90.1	1667.6
45794.515	12.17	1.42	8.79	0.80	-3957.2	4205.5	-2821.8	2860.1	-1862.3	2128.7	-296.4	1642.1
45821.699	11.70	1.59	7.54	0.79	-3539.3	4205.6	-2701.9	3043.3	-1922.2	2311.5	-1321.0	1763.8
45825.385	8.58	0.13	6.37	0.08	-3973.2	3822.1	-2957.5	2783.1	-2058.3	1930.2	-975.8	1383.2
45850.368	12.18	0.43	12.22	0.23	-4010.8	3662.0	-2815.5	2440.6	-1434.9	1649.4	-651.7	1102.8
45851.367	16.15	1.22	12.28	0.60	-3446.9	3627.4	-2429.4	2528.2	-1528.6	1736.7	-806.0	1190.1
45852.356	11.02	0.07	8.97	0.04	-4050.1	4111.0	-2855.0	2887.9	-1595.0	2095.5	-510.8	1548.1

Note: (1) Julian dates of IAW watch data in the form “*.1” are used to artificially make a difference between two different spectra under the same MJD on IAW watch web site (as for example 48325.0 and 48325.1)

(2) File names differs according to the observatory/monitoring campaign:

PTG* : Crimean Astrophysical Observatory data

n* : AGN watch data

5* : SAO/GHO data

A* : Asiago data

Continued on next page

Table 2 – continued from previous page

JD-2400000	Flux Hb	Err.	Fl. 5100	Err.	B25%	R25%	B50%	R50%	B75%	R75%	B90%	R90%
45880.344	12.68	0.22	7.44	0.01	-3796.6	3636.0	-2780.3	2536.8	-1520.0	1745.3	-616.5	1259.3
45907.319	7.52	0.13	4.99	0.03	-4292.9	4965.7	-3098.8	3066.7	-2260.1	2212.9	-1479.1	1665.3
45941.272	8.82	0.22	4.59	0.11	-4706.1	7127.8	-3453.9	3253.5	-2496.3	2338.3	-1836.2	1608.2
45942.252	11.22	0.43	7.96	0.22	-4132.7	3452.9	-3060.8	2479.0	-2164.5	1871.9	-1205.6	1447.6
46054.618	9.66	0.74	9.27	0.51	-4292.8	3616.9	-3158.5	2395.7	-2079.9	1787.0	-213.1	1361.6
46182.493	8.96	1.25	11.17	1.04	-4374.5	4144.2	-3300.4	2677.1	-2462.3	1946.1	-1802.2	1520.6
46198.477	12.20	1.70	8.69	0.93	-3929.6	3255.5	-2973.6	2401.2	-2134.5	1731.7	-1353.2	1245.7
46234.389	13.58	0.61	10.61	0.32	-3992.0	2886.3	-3215.6	1911.4	-2557.1	454.8	-2137.2	-512.3
46262.333	10.00	0.02	8.49	0.01	-4035.5	3375.3	-3141.5	1611.5	-2603.8	763.6	-2244.9	219.9
46263.33	12.59	0.06	7.36	0.02	-3698.2	2393.9	-2980.9	692.5	-2381.8	-275.4	-1961.7	-697.8
46265.371	10.09	0.20	4.51	0.09	-3994.7	2517.7	-3218.3	936.9	-2559.7	-152.6	-2139.9	-695.9
46288.316	10.05	0.22	6.71	0.13	-3974.2	2782.1	-3197.8	1260.7	-2539.3	-11.3	-2119.4	-675.4
46289.306	8.04	0.44	7.47	0.31	-3860.6	2593.4	-3024.1	709.2	-2365.1	-77.5	-1945.0	-560.5
46502.527	9.24	0.77	7.02	0.51	-3686.0	3077.1	-2968.7	2284.2	-2309.6	1493.5	-1829.4	341.4
46503.518	13.22	1.29	9.35	0.64	-3856.1	3513.9	-2839.9	1988.9	-2120.6	1138.2	-1640.0	410.9
46528.404	7.46	0.35	6.80	0.23	-3772.5	3291.3	-2943.1	2142.6	-2230.3	1058.4	-1754.2	97.9
46529.461	13.40	0.33	7.70	0.15	-3839.5	3611.0	-2948.0	2336.2	-2411.9	1368.5	-2053.9	343.7
46558.503	10.34	0.28	3.96	0.11	-3704.1	3323.7	-2752.8	1989.6	-2096.9	842.2	-1559.3	119.7
46591.344	6.80	0.08	5.24	0.05	-4898.9	4777.9	-3000.4	2586.9	-1927.0	1618.2	-1329.1	1255.8
46647.323	6.60	0.32	5.92	0.24	-4223.5	6022.1	-3148.8	2527.4	-2310.2	1796.7	-1709.8	219.8
46648.302	6.28	0.13	5.62	0.11	-3897.5	4144.3	-2821.7	2616.2	-2102.3	1703.0	-1561.7	974.5
46649.29	7.78	0.52	5.21	0.33	-4235.2	4043.5	-3280.1	2759.6	-2501.8	2089.3	-1961.7	1602.7
46830.646	8.00	0.06	6.14	0.04	-3693.9	3619.3	-2797.0	2520.1	-2077.4	1789.5	-1596.8	1303.4
46831.641	8.62	0.96	6.79	0.67	-3858.1	3389.7	-2901.8	2230.4	-2002.5	1500.5	-1281.1	954.3
46883.621	5.99	0.14	5.35	0.06	-3752.5	3253.5	-2736.0	2277.4	-1896.3	1486.6	-1295.0	819.1
46884.467	8.27	0.44	8.75	0.31	-3694.4	3680.0	-2917.2	2154.1	-2017.9	1424.3	-935.2	878.2
46914.442	7.74	0.24	8.88	0.21	-4356.3	4164.2	-2863.1	2331.0	-1903.6	1479.3	-1121.7	933.0
46972.342	8.98	0.27	9.60	0.20	-4240.7	4221.8	-3166.0	2693.1	-2267.4	1658.0	-1606.8	868.7
47033.25	11.34	0.65	7.44	0.30	-3846.8	3380.5	-2893.2	2042.4	-1577.0	1315.0	-736.4	770.6
47265.465	7.76	0.20	8.25	0.17	-3982.0	3262.8	-2966.3	2347.6	-2067.1	1739.0	-924.4	1253.0
47299.464	9.87	0.36	8.58	0.21	-3917.8	3695.3	-2722.3	2352.1	-1762.3	1500.4	-1040.4	954.1
47333.376	9.83	0.07	5.80	0.01	-4240.2	3182.0	-3285.1	2023.4	-1606.2	1294.0	-763.2	808.7
47390.28	9.54	0.16	8.77	0.08	-6310.3	4292.2	-3694.8	2763.1	-2857.8	2153.6	-2498.3	-1357.1
47417.244	7.18	0.08	6.35	0.06	-4295.4	7617.3	-3041.4	3003.2	-2202.5	1723.7	-1601.8	691.9
47517	7.84	0.03	8.05	0.00	-4472.6	4469.8	-3177.7	3382.6	-1995.6	2780.2	-689.8	2419.4
47524	8.15	0.19	8.88	0.10	-4527.7	3781.7	-3354.7	2460.6	-2295.1	1622.9	-1586.5	906.7
47528	4.68	0.22	7.12	0.15	-5301.2	4774.1	-3360.4	2780.0	-2237.2	1697.8	-1466.2	918.7
47533	6.14	0.23	6.64	0.15	-3600.7	4091.8	-2853.9	2980.8	-2173.4	1666.7	-1627.8	358.3
47534	7.88	0.08	8.44	0.06	-3700.9	3925.2	-2632.9	2357.2	-1829.3	1203.4	-1292.4	526.8
47535	9.37	0.05	9.00	0.02	-3959.1	3704.1	-2909.7	2037.0	-1856.6	1206.8	-1034.9	733.5
47539	5.81	0.09	7.84	0.09	-3961.6	4621.3	-3032.9	2482.1	-2101.4	1536.2	-1283.8	828.7
47543	7.17	0.40	8.22	0.32	-3697.8	4201.8	-2747.2	2743.7	-1998.1	1982.7	-1452.2	1430.5
47560	7.03	0.22	7.21	0.16	-3886.8	5103.3	-2953.1	2779.4	-2284.4	1827.6	-1815.4	-336.5
47561	12.42	0.71	11.23	0.35	-4226.5	4076.1	-3054.4	2756.1	-2231.2	1561.1	-1523.8	608.5
47567	6.89	0.22	7.37	0.06	-4689.7	4609.8	-3772.6	3129.3	-3115.9	1789.6	-2589.4	-606.9
47568	10.50	0.03	9.28	0.02	-4235.9	3269.6	-2797.8	1802.2	-1232.1	827.9	-567.2	463.3
47570	7.42	0.39	6.64	0.26	-4438.9	3700.3	-3145.7	2084.0	-1774.5	1279.1	-760.1	768.0
47571	6.90	0.24	7.09	0.13	-4512.7	5418.9	-3338.2	2871.8	-2421.5	1672.6	-1370.3	1008.5
47572	9.26	0.05	7.38	0.03	-4379.2	3487.8	-3324.5	2409.0	-2531.1	1602.3	-1602.7	1065.8
47573	8.07	1.44	6.82	0.98	-3956.0	4284.2	-3006.3	3103.0	-2326.0	2202.9	-1848.9	-1.5
47573	8.30	0.04	6.71	0.02	-4242.8	4337.8	-3090.3	3017.7	-2205.8	1910.4	-1592.0	807.2
47574	9.47	1.02	7.87	0.52	-4224.9	5345.3	-3122.0	2955.4	-2138.2	1954.7	-1151.1	1331.0
47582	5.32	0.20	5.99	0.12	-3949.8	3906.8	-2890.5	2583.0	-1945.7	1623.9	-998.0	1026.0
47587	5.28	0.35	6.10	0.29	-4134.9	3878.2	-3119.5	2683.3	-2355.7	1803.1	-1845.3	-52.4
47589	6.15	0.11	7.29	0.08	-4304.6	4027.3	-3238.7	2693.1	-2288.0	1786.8	-1334.2	1123.9
47590	6.63	0.07	7.71	0.02	-4129.0	3814.2	-2974.0	2632.8	-2046.8	1456.1	-1349.5	752.2
47591	5.11	0.12	6.90	0.12	-3724.6	4675.3	-2795.5	2841.0	-1930.1	1894.2	681.3	1624.2
47592.1	9.75	0.28	9.04	0.18	-3726.4	3926.0	-2780.5	2596.8	-1475.0	1633.8	-760.4	1033.5
47592	5.55	0.63	7.37	0.61	-4573.1	3775.1	-3276.6	2568.2	-2330.1	1366.1	-1499.5	647.1
47593.1	5.80	0.45	6.67	0.40	-3445.8	4484.7	-2515.8	2922.4	-1649.6	2043.0	291.7	1637.9
47593.2	6.63	0.07	8.01	0.05	-3600.1	5012.0	-2869.7	2835.8	-2204.1	1888.6	-1603.7	1416.1
47593	5.35	0.30	6.15	0.27	-6000.7	5594.7	-3606.5	3820.3	-2680.4	2685.1	-1937.5	1930.6
47598	4.94	0.81	7.96	0.76	-4104.9	4064.1	-2998.9	2593.0	-2111.3	1466.2	-1443.7	680.0
47599.1	9.86	0.50	5.66	0.25	-4944.7	3726.1	-4082.1	2297.5	-3350.4	1551.8	-2750.3	1078.3
47599	5.03	0.29	7.70	0.31	-3529.3	5285.7	-2799.0	3651.4	-2200.1	2905.2	-1666.8	2431.3
47600	6.77	0.06	8.92	0.02	-5559.3	5444.5	-2024.0	3694.2	-439.2	2889.8	489.2	2221.0
47606	6.19	0.08	8.54	0.07	-4157.8	3787.7	-2827.9	2551.6	-1857.0	1566.3	-1248.6	829.4
47615	6.31	0.36	7.57	0.30	-4107.5	4041.6	-2922.9	2829.3	-2090.9	1862.9	-1375.9	899.6

Note: (1) Julian dates of IAW watch data in the form “*.1” are used to artificially make a difference between two different spectra under the same MJD on IAW watch web site (as for example 48325.0 and 48325.1)

(2) File names differs according to the observatory/monitoring campaign:

PTG* : Crimean Astrophysical Observatory data

n* : AGN watch data

5* : SAO/GHO data

A* : Asiago data

Continued on next page

Table 2 – continued from previous page

JD-2400000	Flux Hb	Err.	Fl. 5100	Err.	B25%	R25%	B50%	R50%	B75%	R75%	B90%	R90%
47616.1	10.70	0.44	6.81	0.19	-5173.1	5959.4	-3386.1	3504.0	-2308.7	2162.0	-1708.4	1189.7
47616	8.83	0.02	6.49	0.01	-3229.3	5580.0	-2285.7	4128.3	-1542.2	3095.6	-1000.3	1655.7
47617	6.60	0.56	9.18	0.50	-4727.6	5067.7	-3535.6	3474.0	-2578.5	2253.7	-1978.7	1159.7
47618.1	4.35	0.22	7.38	0.22	-4503.8	4915.9	-3445.5	2863.8	-2619.8	1783.0	-1673.3	1064.7
47618	9.90	0.12	9.59	0.04	-3779.7	4532.0	-2813.7	3401.0	-2052.6	2625.9	-1567.2	1852.8
47620.1	7.21	0.14	7.64	0.10	-3211.2	4681.4	-2313.7	3692.2	-1621.5	2917.3	-1136.0	2144.3
47620	5.89	0.22	8.97	0.20	-3558.2	4550.6	-2798.6	3560.2	-2106.4	2573.2	-1551.5	1378.9
47621	5.73	0.24	8.61	0.24	-4381.1	3774.8	-3277.0	2418.8	-2279.7	1293.4	-1613.0	508.2
47622	8.57	0.11	7.42	0.06	-3229.8	4395.0	-2482.8	3353.3	-1802.1	2384.2	-1324.6	936.4
47623	5.95	0.08	8.64	0.06	-4520.3	4199.2	-3527.1	2728.2	-2752.3	1714.1	-1864.4	1039.9
47624	7.57	0.36	9.10	0.30	-3713.7	4816.5	-2954.4	3542.7	-2331.8	2696.4	-1846.6	2063.3
47626	7.19	0.52	9.57	0.35	-3634.4	4750.0	-2465.9	3264.7	-1703.5	1997.4	-1217.3	1015.3
47627	6.54	0.43	10.00	0.43	-3888.4	4406.5	-2952.0	2848.6	-2130.2	1893.9	-1541.8	1417.7
47627	6.97	0.11	9.99	0.10	-3523.3	4445.6	-2556.0	3032.2	-1655.0	2117.0	-960.1	1485.0
47629	9.33	0.64	12.58	0.57	-3512.8	4814.9	-2821.8	3046.2	-1990.6	2130.5	377.4	1708.8
47642	10.39	0.08	10.78	0.05	-4055.8	4612.1	-3049.0	3064.2	-2375.9	2378.8	-1954.4	1865.8
47643	9.07	0.61	9.34	0.40	-4235.3	4082.0	-3268.8	2597.4	-2541.7	1734.8	-1934.6	1120.1
47644.1	8.75	0.14	10.75	0.06	-3788.5	5013.2	-2974.3	3412.6	-2294.0	2442.4	-1816.9	30.5
47644	8.28	0.79	9.83	0.62	-3737.9	5067.8	-2787.3	2842.2	-1970.0	1942.6	-1013.8	1459.4
47649	8.95	0.09	9.06	0.06	-3792.0	3676.6	-2934.6	2362.8	-1809.7	1490.2	-813.6	954.4
47650.1	6.91	0.24	6.73	0.13	-3698.2	3648.0	-2760.4	2212.1	-1584.0	1258.6	-757.7	782.9
47652	12.98	4.28	12.44	2.51	-3335.4	4296.4	-2519.7	2629.8	-1428.5	1523.8	-607.5	972.3
47652	14.18	5.08	12.53	2.93	-4258.3	4198.2	-3234.9	2912.8	-2473.4	1901.8	-1876.0	1196.1
47653.1	14.20	0.15	9.76	0.06	-4172.9	4310.1	-3110.8	2738.9	-2282.1	1655.9	-1451.1	936.0
47653	13.57	0.12	10.13	0.00	-4152.5	3941.9	-3061.6	2690.1	-2199.2	1712.6	-1534.1	939.6
47654.1	8.55	0.58	9.21	0.40	-3684.3	3702.3	-2741.4	2258.4	-1677.0	1419.3	-846.5	821.4
47654.3	6.43	0.60	7.77	0.46	-3654.1	3616.1	-2710.6	2292.0	-1645.6	1452.4	-695.8	973.7
47654	8.21	0.13	9.20	0.05	-4211.8	4029.0	-3149.7	2579.4	-2083.9	1617.0	-1133.2	1016.9
47655	8.52	0.15	7.57	0.10	-3471.5	4983.5	-2657.0	3523.0	-1976.6	2760.8	-1431.2	2345.9
47656.1	10.05	0.21	10.46	0.14	-3870.7	4793.4	-2852.4	2777.1	-1898.7	1739.4	-1147.2	1049.6
47656	11.14	0.12	9.54	0.06	-4110.9	4058.1	-3226.4	2587.0	-2561.4	1572.7	-1783.6	898.4
47657.1	8.62	0.60	8.55	0.40	-3657.3	3601.4	-2715.3	2159.6	-1296.7	1321.6	-584.9	843.9
47657	8.37	0.09	8.87	0.06	-3715.6	3673.8	-2785.2	2181.3	-1384.1	1336.6	-647.6	830.9
47663.1	7.68	0.17	6.55	0.00	-4139.8	4224.7	-3062.0	2753.1	-2341.3	1837.0	-1618.8	1106.2
47663.2	7.04	0.25	5.58	0.16	-4063.8	4678.7	-2984.9	3203.8	-2263.4	2102.4	-1540.2	1370.3
47663.3	8.12	0.29	4.62	0.14	-4712.8	5100.9	-3458.7	2892.2	-2739.8	1976.6	-2019.0	1246.2
47663.4	5.94	0.09	5.17	0.07	-4522.8	4937.1	-3242.1	3058.6	-2323.8	2123.6	-1771.5	1191.6
47663	7.46	0.03	5.65	0.02	-2649.1	4375.6	-1588.1	3053.4	-167.6	2215.0	426.3	1736.9
47664	10.01	0.27	9.21	0.08	-4491.9	3436.3	-3862.3	1778.5	-2778.8	678.5	-2235.6	-52.8
47665.1	9.67	0.63	8.92	0.39	-4223.5	4169.3	-3228.7	2697.6	-2563.7	1795.6	-2119.5	1458.0
47665	7.24	0.05	6.97	0.01	-4296.4	4397.4	-3052.0	2867.3	-2177.8	1851.5	-1426.4	1091.8
47666	12.54	0.54	9.61	0.30	-3721.7	3697.4	-2833.2	2252.4	-1776.6	1348.7	-849.1	847.8
47668	11.84	1.23	9.27	0.63	-4402.8	3650.0	-3152.6	2371.1	-2161.8	1331.9	-1466.4	629.9
47673	6.80	0.35	7.05	0.26	-4080.5	3801.6	-3052.6	2479.1	-2021.1	1566.9	-1019.4	960.3
47674	10.15	0.73	7.75	0.39	-3715.9	4810.7	-2969.3	3141.4	-2288.9	2241.1	-1743.4	1826.4
47678	10.27	0.05	8.44	0.03	-3922.2	4607.4	-2886.5	2698.7	-1916.6	1713.8	-1152.3	1152.4
47678.1	5.91	0.09	7.08	0.03	-4222.7	3780.6	-3143.9	2554.2	-2181.6	1576.7	-1337.1	967.3
47679	6.88	0.71	7.61	0.56	-3504.5	4750.3	-2813.7	3194.0	-2259.9	2559.7	-1774.5	2137.5
47680.1	6.13	0.33	6.57	0.26	-3654.5	4595.2	-2839.7	2927.1	-2159.0	2027.3	-1681.5	1612.9
47681.1	6.60	0.59	7.14	0.47	-3789.1	4805.3	-3042.7	3205.4	-2430.5	2374.0	-1953.5	1959.2
47682.1	6.36	0.45	6.74	0.35	-5438.7	4734.6	-3877.8	2837.1	-2880.2	1723.5	-2260.9	517.8
47683	7.63	0.38	7.24	0.26	-3587.9	4663.6	-2841.0	3064.4	-2160.3	2164.3	-1682.8	1680.7
47684	6.42	0.28	7.16	0.23	-4148.1	4785.0	-3130.9	3462.7	-2314.6	2353.7	-1769.2	1524.6
47685	5.90	0.34	5.62	0.21	-3671.3	4996.8	-2924.5	3465.2	-2243.9	2563.9	-1834.9	1941.4
47686	6.34	0.18	6.50	0.13	-3684.0	4426.3	-2801.2	3036.2	-2052.1	2067.0	-1437.8	1445.5
47687	8.56	0.37	10.40	0.25	-3452.8	4663.0	-2637.5	3063.9	-1819.9	2094.6	-794.7	1611.1
47700	12.90	1.90	11.14	0.86	-4664.1	3998.9	-3553.1	2746.0	-2884.5	1611.4	-2438.0	819.7
47701	7.78	0.72	9.48	0.44	-5648.5	6427.2	-3702.0	3612.7	-2723.9	2414.4	-1939.1	229.8
47705	5.99	0.21	6.07	0.15	-4403.4	5670.7	-2845.4	3668.7	-2063.4	2473.7	-1279.2	1878.0
47707	5.40	0.40	7.10	0.36	-4033.6	4624.6	-2947.9	3303.0	-1994.7	2125.3	-1312.0	1227.8
47708	6.73	0.48	7.44	0.40	-3611.3	4919.2	-3000.3	3665.8	-2456.1	2833.1	-2047.3	2348.4
47709	6.85	0.33	7.33	0.25	-4174.7	5175.0	-3157.7	3781.7	-2273.5	2671.7	-1591.5	1910.8
47710	4.36	0.15	5.31	0.09	-4551.7	5275.9	-3468.0	3812.5	-2584.6	2840.7	-1903.3	2286.9
47710	7.71	0.48	7.36	0.37	-3643.1	4536.9	-2760.3	3354.6	-2011.2	2107.8	-1397.0	1003.9
47715	6.86	0.33	7.24	0.25	-3974.9	4362.0	-2798.0	3216.9	-1853.2	1716.8	-1201.9	880.0
47736	8.44	0.78	6.14	0.49	-3922.4	4739.8	-3040.2	3486.9	-2291.7	2654.6	-1677.8	1962.7
47742	7.05	0.46	4.21	0.24	-4175.5	4274.7	-3162.1	2931.0	-2384.8	1653.9	-1845.5	624.0
47746	8.55	5.39	5.41	2.12	-4024.6	4475.8	-3104.7	2709.4	-2182.0	1654.5	-1256.5	1070.1

Note: (1) Julian dates of IAW watch data in the form “*.1” are used to artificially make a difference between two different spectra under the same MJD on IAW watch web site (as for example 48325.0 and 48325.1)

(2) File names differs according to the observatory/monitoring campaign:

PTG* : Crimean Astrophysical Observatory data

n* : AGN watch data

5* : SAO/GHO data

A* : Asiago data

Continued on next page

Table 2 – continued from previous page

JD-2400000	Flux Hb	Err.	Fl. 5100	Err.	B25%	R25%	B50%	R50%	B75%	R75%	B90%	R90%
47748	6.70	0.69	4.24	0.34	-4492.9	4840.4	-3048.0	2802.7	-2322.9	1697.0	-1596.0	962.1
47749	6.00	0.26	5.19	0.19	-3814.5	5030.3	-2907.7	2707.9	-2111.9	1668.5	-857.1	1092.7
47757	5.62	0.19	4.74	0.00	-3469.9	5318.1	-2369.2	3328.2	-1589.8	2404.1	-1003.9	1877.2
47758	4.47	0.03	4.12	0.01	-4228.4	4826.1	-3156.2	3176.0	-2439.3	1898.8	-1720.7	989.9
47766	10.05	0.13	8.01	0.01	-5143.5	4834.4	-3712.7	2445.9	-2994.7	1349.9	-2275.0	439.6
47777	5.53	0.17	5.87	0.08	-5301.1	6140.9	-3943.2	3339.0	-2774.3	1749.4	-1796.7	760.2
47797	8.31	0.04	7.78	0.02	-4342.4	5069.9	-3126.6	3593.8	-2239.2	2463.3	-1571.9	1561.9
47809	7.82	0.05	7.34	0.03	-4085.6	4768.0	-3090.1	3066.8	-2202.4	1937.9	-1312.0	1150.2
47861	5.29	0.04	6.08	0.04	-2490.9	5757.9	-1621.8	4200.9	-750.1	3204.1	14.7	2541.4
47868	11.90	1.47	9.46	0.77	-5374.7	3444.8	-4383.0	1750.1	-3609.4	962.5	-3055.6	289.0
47884	7.52	0.25	7.86	0.19	-5178.9	4492.8	-3454.1	2839.5	-2298.5	1781.4	-1370.9	960.9
47891	8.98	0.06	6.93	0.03	-4108.5	4072.5	-3171.4	2753.3	-2466.6	2036.1	-1878.0	1439.8
47895	5.83	0.11	5.10	0.07	-4253.3	4044.6	-3199.3	2366.6	-2376.9	1531.0	-1316.1	935.7
47896	6.49	0.51	5.92	0.37	-3805.8	4251.9	-2921.2	2668.1	-2033.9	1654.4	-921.0	1092.6
47897	5.33	0.28	5.62	0.22	-3665.4	4787.9	-2987.0	2842.6	-2307.0	1943.6	-1625.5	1391.7
47899	6.65	0.02	6.50	0.01	-4122.8	4456.1	-3309.8	2997.6	-2698.7	2029.2	-2222.4	1201.6
47900	7.54	0.06	6.05	0.04	-3966.1	3758.5	-3040.4	2339.1	-2228.0	1514.3	-1180.2	926.4
47901	7.99	0.07	6.59	0.04	-4383.1	3702.5	-3224.8	2280.6	-2294.8	1454.2	-1011.4	865.3
47907	7.06	0.32	5.15	0.19	-4402.5	4039.7	-3128.0	2379.4	-2197.7	1552.7	-1264.5	963.6
47912.1	7.50	0.04	7.14	0.02	-4025.5	4276.7	-3139.0	2914.7	-2361.1	2236.1	-1915.7	1558.9
47912	4.12	0.16	3.96	0.12	-3876.4	4782.0	-2994.6	2351.8	-2042.0	1523.1	-1154.7	971.9
47912	4.62	0.15	4.06	0.10	-4322.1	4045.0	-3259.4	2593.9	-2311.6	1750.7	-1122.5	1029.9
47915	5.49	0.18	5.49	0.13	-4440.6	5072.7	-3267.8	2666.1	-2483.4	1469.9	-1893.8	873.5
47917.63	5.74	0.06	4.89	0.05	-3865.6	4116.5	-3088.9	2101.0	-1950.0	1128.6	-1228.5	522.5
47918	6.09	0.56	5.35	0.46	-4453.2	3881.2	-3293.3	2574.7	-2362.2	1391.9	-1661.9	566.7
47919	4.81	0.20	4.34	0.15	-3728.8	4581.2	-2847.0	3053.1	-2098.8	2015.7	-1553.5	1050.6
47921	3.49	0.44	3.83	0.37	-3435.6	4048.6	-2552.7	2315.5	-1735.5	1418.2	-1121.1	798.6
47922	3.51	0.22	4.08	0.19	-3604.3	4431.1	-2722.0	2834.4	-1973.5	1452.9	-1359.6	558.2
47927	3.61	0.19	3.94	0.18	-3797.2	5277.7	-3051.4	3191.0	-2507.8	2153.1	-2099.5	-802.7
47929	6.60	0.01	4.52	0.00	-3595.3	5274.4	-2917.0	2980.4	-2305.3	2081.5	-1828.6	1805.4
47940	2.98	0.12	3.97	0.12	-4846.6	4303.9	-3340.9	2404.0	-2293.9	1222.6	-1593.9	516.0
47941	3.23	0.28	4.27	0.32	-4064.7	4583.9	-2980.2	3125.1	-1959.9	1949.3	503.1	1535.4
47944.595	8.26	0.06	4.88	0.00	-5708.0	6480.6	-3869.5	4088.6	-2975.8	2686.7	-2378.4	1533.5
47945	3.58	0.30	4.52	0.26	-3945.6	5125.2	-3064.4	3524.9	-2316.7	2624.1	-1771.7	2140.2
47946.1	4.37	0.38	5.02	0.37	-3648.5	4804.8	-2766.3	3414.0	-1949.6	2029.6	-1335.6	995.4
47946	2.76	0.37	3.65	0.38	-3830.2	4269.2	-2676.8	3019.5	-1109.1	2189.2	-150.8	1637.0
47947	3.66	0.37	4.90	0.44	-4362.4	5779.4	-3260.0	4218.6	-2292.1	2736.1	-1668.1	1541.3
47949	4.40	0.05	4.54	0.04	-3595.0	5500.7	-2766.9	3871.4	-2075.0	2883.8	-1381.5	2461.6
47951	4.47	0.20	5.18	0.22	-4342.0	4435.3	-3186.5	2777.3	-2258.8	1480.9	-1677.6	658.9
47955	2.61	0.06	3.81	0.06	-4423.2	5645.1	-3321.1	4155.7	-2353.4	2884.8	-1452.0	1970.3
47957	3.79	0.15	4.39	0.14	-4168.8	4466.9	-2902.6	3237.4	-1765.1	2148.7	-1026.7	1402.5
47958	4.15	0.16	4.92	0.17	-4707.6	4522.4	-3439.4	2984.0	-2513.6	1570.7	-1701.2	749.4
47967	2.83	0.31	3.90	0.40	-4604.1	5288.3	-3686.9	3636.5	-2882.0	2110.6	-2305.8	475.9
47968	2.33	0.23	3.60	0.24	-3935.4	4719.1	-2986.1	3189.9	-2169.9	1737.5	-1556.4	773.0
47969	1.81	0.26	2.52	0.26	-4454.7	4855.8	-3456.6	3283.9	-2655.8	1923.6	-2053.7	299.4
47970	2.17	0.21	3.70	0.29	-4343.1	5275.2	-3259.4	3673.9	-2239.8	2150.0	-1558.1	1115.3
47971.1	2.21	0.23	3.15	0.26	-4788.5	4593.7	-3399.8	2575.4	-2470.4	1276.5	-1304.5	688.0
47971	3.35	0.34	3.75	0.30	-3738.8	4360.6	-2653.3	2903.2	-1836.6	1659.5	-1154.3	901.9
47973	2.87	0.13	3.64	0.16	-4021.4	5049.4	-3072.3	3379.7	-2392.5	2340.8	-1915.7	1857.2
47974	3.38	0.30	3.42	0.25	-4575.9	5175.4	-3425.1	3713.3	-2474.0	2465.6	-1724.6	1498.7
47975	2.34	0.21	3.68	0.18	-5373.0	5211.1	-3512.7	3296.0	-2176.7	1935.4	-1640.6	-228.8
47980	2.59	0.18	4.06	0.13	-4497.5	6022.5	-3414.5	4139.2	-2667.7	2544.0	-2055.3	1508.2
47982	2.13	0.11	3.65	0.16	-5718.9	4770.0	-4093.2	2976.4	-2809.6	1549.1	-1989.9	483.0
47982	3.81	0.12	4.46	0.11	-4229.4	6117.6	-3364.0	4265.7	-2496.1	2833.1	-348.8	2085.4
47990	3.42	0.12	5.43	0.11	-4503.4	5218.4	-3705.3	3917.6	-2838.1	2826.4	-894.6	2010.7
47994	5.01	0.01	5.24	0.00	-4784.4	4915.2	-3618.3	3356.4	-2564.8	1924.7	-1860.4	855.3
47999	2.81	0.19	4.15	0.21	-5774.4	5300.3	-3918.1	3267.0	-2752.0	1721.2	-1933.0	773.9
48002	4.35	0.24	4.61	0.20	-4116.2	4861.9	-3117.0	3494.6	-2181.4	2201.4	-1511.3	1184.3
48005.1	7.08	0.04	4.41	0.02	-3850.8	4732.0	-2901.7	3411.6	-1131.0	2649.7	994.1	2235.0
48005	2.40	0.24	4.70	0.29	-4604.4	6283.7	-3673.2	3541.6	-2805.8	2383.7	-1198.0	1636.9
48007.1	3.26	0.39	4.16	0.33	-5329.9	5751.3	-3938.0	3002.0	-2773.0	1814.3	-1954.8	867.6
48007	6.22	0.07	5.81	0.02	-6272.4	5028.3	-4492.8	2886.3	-3001.6	1517.3	-2103.3	608.0
48008	3.29	0.46	4.30	0.47	-4482.5	6107.5	-3602.9	4015.1	-2924.5	2697.4	-2516.7	1937.1
48009	3.03	0.27	4.57	0.29	-3970.0	5700.7	-2970.1	3236.7	-1832.9	1808.6	-489.3	1198.6
48011	4.01	0.08	6.57	0.10	-4294.8	5294.2	-3363.0	3720.2	-2495.1	2698.0	-1892.7	2290.2
48013	5.13	0.09	6.38	0.08	-4661.6	5309.1	-3668.3	3718.6	-2893.4	2136.5	-2227.7	674.7
48020	5.14	0.09	6.23	0.01	-5042.0	4570.4	-3770.4	2907.3	-2842.2	1725.0	-2260.5	77.5
48022	3.89	0.05	5.75	0.05	-5366.2	4318.1	-4085.2	2881.2	-3150.1	1808.0	-2681.4	1094.7

Note: (1) Julian dates of IAW watch data in the form “*.1” are used to artificially make a difference between two different spectra under the same MJD on IAW watch web site (as for example 48325.0 and 48325.1)

(2) File names differs according to the observatory/monitoring campaign:

PTG* : Crimean Astrophysical Observatory data

n* : AGN watch data

5* : SAO/GHO data

A* : Asiago data

Continued on next page

Table 2 – continued from previous page

JD-2400000	Flux Hb	Err.	Fl. 5100	Err.	B25%	R25%	B50%	R50%	B75%	R75%	B90%	R90%
48028	5.18	0.10	6.59	0.09	-4613.2	4335.3	-3450.9	2785.6	-2868.1	1362.2	-2401.0	-525.3
48030	5.52	0.67	5.68	0.51	-4544.1	3954.7	-3494.9	2164.2	-2324.7	1094.9	-796.6	620.9
48031	4.28	0.18	6.42	0.19	-4133.6	4228.5	-2131.9	1505.5	-588.0	761.0	-318.7	490.7
48032	3.17	0.49	4.68	0.55	-3976.2	4391.5	-3176.6	3366.8	-2575.5	2481.6	-2107.1	1531.1
48034.388	10.41	0.08	6.35	0.02	-4954.3	6993.8	-3583.7	4099.9	-2506.6	2328.0	-1545.9	1597.9
48034	4.16	0.32	5.54	0.32	-4250.8	4881.4	-3370.4	3629.1	-2895.3	2658.7	-2623.4	1760.4
48035.316	9.73	0.01	6.03	0.00	-4490.9	4944.4	-3357.5	2923.6	-2579.5	1948.7	-2039.8	1219.6
48036	3.95	0.30	5.76	0.33	-4082.5	4760.6	-3283.3	2712.4	-2615.5	2236.5	-2013.3	2032.7
48037.1	3.84	0.23	5.69	0.24	-4653.5	5022.5	-3723.2	3348.3	-3023.5	1564.7	-2439.2	-208.3
48037	5.54	0.28	7.61	0.28	-4025.6	5330.8	-3156.6	3203.5	-2486.4	2111.4	-1949.2	-331.5
48039	4.78	0.09	5.32	0.07	-4287.5	4789.2	-3283.5	3006.9	-2412.1	1983.4	-1336.1	1643.0
48040	3.56	0.18	6.35	0.15	-4437.5	4760.2	-3489.7	3438.8	-2742.8	2261.4	-1311.8	1433.1
48041	4.48	0.37	6.06	0.13	-3944.9	3944.0	-3199.2	2972.5	-2587.8	2349.6	-2179.4	-745.8
48042	4.21	0.20	6.08	0.08	-4193.7	5193.7	-3328.2	3415.4	-2660.6	2394.2	-1991.6	1783.1
48043	5.35	0.77	7.03	0.85	-3788.7	5567.7	-2974.8	3339.9	-2294.8	646.8	-1817.9	-177.0
48044	4.50	0.03	6.16	0.03	-4074.6	4152.6	-3075.2	2584.2	-2005.4	2108.5	1227.1	1837.0
48056	5.34	0.08	5.32	0.05	-4480.3	4226.9	-3525.3	2880.2	-2807.0	1782.8	-2207.1	810.7
48059	4.23	0.35	5.34	0.34	-4850.0	4434.7	-3635.9	2735.3	-2638.9	1382.7	-1972.4	484.3
48060	4.84	0.14	5.53	0.12	-3897.3	4951.8	-3097.5	3174.7	-2362.4	2154.2	-1893.7	1746.9
48061.1	3.66	0.44	4.42	0.39	-4920.4	4389.6	-3727.6	2553.2	-2889.8	1700.0	-2289.9	-241.1
48061	5.70	0.06	5.77	0.03	-4309.0	5488.1	-3443.6	3571.3	-2776.2	2549.4	-2241.2	2005.8
48063.345	9.16	0.12	7.95	0.08	-4480.1	5818.9	-3226.8	3058.3	-2328.5	2143.6	-1667.9	1596.1
48064.349	7.41	0.06	10.78	0.05	-3863.5	5900.9	-2607.8	2285.8	-1467.1	1373.5	-804.7	827.5
48064	4.44	1.53	5.44	1.30	-4287.3	4684.8	-3422.1	3386.6	-2621.2	2297.7	-1550.0	1483.5
48067	4.70	1.08	5.65	1.01	-4587.2	4924.6	-3722.8	3420.6	-2989.4	2603.3	-2454.9	1788.2
48068	4.62	0.06	4.90	0.01	-4944.3	4172.4	-3775.9	2374.6	-2955.3	1539.2	-2485.4	-598.2
48068	5.32	0.02	5.25	0.01	-4136.2	4568.0	-3403.8	3065.6	-2736.4	2317.3	-2335.2	1706.3
48077	4.68	0.15	5.04	0.13	-4154.9	4839.9	-3342.2	3379.8	-2731.1	2272.0	-2323.0	-616.7
48089.1	3.97	0.01	4.06	0.00	-4902.5	4719.5	-3578.4	3132.0	-2581.4	1890.5	-1914.9	541.9
48089	3.68	0.02	4.23	0.01	-4898.2	3923.5	-3721.2	2475.3	-2894.5	1393.6	-2302.6	435.3
48090	5.62	0.02	5.08	0.00	-4880.6	4807.9	-3438.1	2771.3	-2351.7	1666.1	-1625.2	565.0
48091	3.06	0.38	4.88	0.46	-5503.8	4353.0	-3863.9	2667.6	-2686.9	1589.0	-1860.3	633.5
48092.33	11.95	0.14	14.11	0.10	-5229.4	7449.1	-3800.5	4244.5	-2844.1	2654.8	-2124.7	2045.6
48093.316	12.27	0.06	14.29	0.04	-4181.5	5388.4	-2927.1	3425.5	-2147.9	2448.8	-1607.2	1718.2
48097	3.50	0.16	3.99	0.04	-4997.4	4440.1	-3833.9	2886.2	-2899.8	1696.3	-2197.3	511.1
48097	4.22	0.11	5.86	0.12	-4223.8	5217.3	-3306.1	3667.9	-2583.1	2193.2	-1990.2	526.2
48102	4.18	0.20	5.36	0.20	-4900.5	4874.6	-3704.3	3370.9	-2837.4	2485.8	-2168.8	2078.2
48128	5.08	0.08	5.86	0.07	-4857.8	4767.8	-3754.4	3292.9	-2868.6	2163.2	-2202.6	813.1
48132	4.86	0.04	4.36	0.03	-4713.3	4278.0	-3662.6	2840.3	-2842.8	1766.5	-2138.3	103.7
48143	4.51	0.05	5.32	0.04	-5092.6	4340.7	-3971.7	2843.5	-3072.0	1925.8	-2395.3	326.5
48148	4.30	0.06	5.35	0.06	-5056.8	4265.9	-3892.7	2592.5	-3075.1	1759.3	-2489.7	-254.7
48149	4.89	0.09	5.81	0.01	-4790.8	4148.8	-3746.1	2719.5	-2930.9	1533.5	-2464.1	-119.0
48151	4.45	0.02	5.50	0.02	-4993.0	4422.9	-3832.1	2634.8	-2900.1	1330.2	-2316.2	267.0
48160	4.30	0.26	6.77	0.32	-4750.3	4451.2	-3703.0	2778.8	-3002.7	1708.5	-2417.8	997.1
48179	5.17	0.05	7.97	0.03	-4296.3	4903.6	-3365.6	3231.5	-2782.5	622.4	-2315.2	-673.7
48225	6.15	0.50	7.07	0.43	-4477.5	4284.1	-3542.6	2965.5	-2722.2	1771.6	-2252.3	-10.3
48231	6.07	0.07	7.71	0.06	-4593.1	4350.0	-3710.7	2652.8	-2936.5	1526.6	-2160.3	852.8
48236	5.59	0.13	8.03	0.12	-4760.1	4183.2	-3714.9	2753.3	-2899.4	1803.7	-2315.6	267.1
48243	5.72	0.08	7.82	0.07	-4598.5	4131.1	-3550.3	2817.3	-2732.5	1627.9	-2147.0	679.7
48252	6.69	0.07	7.75	0.05	-5013.8	4604.6	-3800.7	2791.6	-3026.2	2001.9	-2471.7	-690.3
48267	6.49	0.11	8.77	0.06	-4777.4	3888.3	-3621.0	2702.5	-3041.1	1757.2	-2576.3	814.9
48275	6.96	0.04	7.74	0.01	-4625.1	3327.0	-3700.5	2262.3	-3005.2	1319.1	-2424.5	-675.5
48280.1	8.05	0.64	9.41	0.51	-4579.5	3567.8	-3529.3	2373.3	-2827.2	1658.8	-2358.1	-356.4
48280	6.15	0.06	8.35	0.01	-4619.6	4058.0	-3461.6	2633.7	-2648.3	1805.9	-2066.0	-77.6
48287	6.41	0.05	7.67	0.02	-4730.4	6372.0	-3627.5	2625.6	-2852.9	1949.3	-2298.5	-628.9
48294	5.79	0.04	8.27	0.01	-4563.0	3568.7	-3514.8	2376.4	-2814.0	1426.0	-2345.8	-230.0
48298	5.08	0.23	6.62	0.07	-4606.5	3540.8	-3673.2	2346.2	-2971.3	1631.7	-2385.1	-619.6
48302	5.85	0.51	7.53	0.48	-3828.2	4671.7	-3155.8	3030.9	-2738.8	1985.5	-2449.7	-1516.3
48310	6.28	0.08	8.77	0.00	-3980.7	4777.9	-3276.5	2809.4	-2634.9	2025.6	-2185.0	1699.6
48311	8.10	0.05	10.14	0.04	-4631.7	3635.3	-3698.4	2440.3	-3113.6	1487.7	-2762.2	-53.9
48323.1	5.96	0.59	10.01	0.68	-4317.4	3820.7	-3501.8	2389.5	-2684.0	1557.7	-2215.7	-217.0
48323	6.37	0.10	9.21	0.06	-6069.1	5325.1	-3869.0	2717.8	-2984.3	1703.7	-2097.0	1029.4
48324	7.09	0.19	8.27	0.03	-3828.3	5364.4	-3219.9	3195.3	-2674.4	2116.6	-2288.8	1692.7
48325.1	7.78	0.30	8.55	0.23	-4251.7	5056.8	-3196.0	2956.0	-2361.6	1032.1	-1814.8	123.3
48325	7.90	0.72	9.02	0.52	-4325.4	5018.1	-3333.5	2883.9	-2499.2	1871.3	-1920.1	115.4
48329	6.34	0.42	8.03	0.32	-4830.4	4454.3	-3726.9	2642.0	-2952.0	1852.5	-2397.3	-615.3
48330	6.59	0.46	9.63	0.46	-4207.7	4774.5	-3119.6	3166.0	-2252.7	1957.0	-1641.1	720.4
48338	7.02	0.02	8.38	0.01	-4070.5	4851.7	-3334.4	2784.2	-2724.9	1837.3	-2275.0	-727.4

Note: (1) Julian dates of IAW watch data in the form “*.1” are used to artificially make a difference between two different spectra under the same MJD on IAW watch web site (as for example 48325.0 and 48325.1)

(2) File names differs according to the observatory/monitoring campaign:

PTG* : Crimean Astrophysical Observatory data

n* : AGN watch data

5* : SAO/GHO data

A* : Asiago data

Continued on next page

Table 2 – continued from previous page

JD-2400000	Flux Hb	Err.	Fl. 5100	Err.	B25%	R25%	B50%	R50%	B75%	R75%	B90%	R90%
48344	5.92	0.08	7.26	0.07	-3954.8	3475.7	-3138.2	2046.1	-2319.4	1215.3	-792.9	741.6
48351	6.24	0.16	6.87	0.12	-9359.0	3094.7	-8056.2	-690.1	-6934.8	-2596.4	-6122.3	-3544.9
48352	7.06	0.09	6.98	0.05	-4500.4	3545.8	-3447.8	2229.5	-2626.6	1394.9	-2038.6	-149.1
48353	5.21	0.18	5.89	0.15	-4321.0	3585.9	-3387.9	2154.4	-2568.9	1203.7	-1630.2	729.5
48354	4.68	0.31	6.22	0.26	-4147.6	4998.8	-3261.8	2778.2	-2571.1	1607.1	-2109.7	-489.3
48355	5.42	0.47	6.31	0.41	-4324.6	5389.9	-3439.5	3133.0	-2716.3	2027.5	-2156.3	1660.0
48356	4.38	0.22	6.23	0.19	-4130.6	5117.0	-3330.8	2557.7	-2657.2	1872.3	-2175.2	1513.9
48360	4.02	0.17	6.19	0.16	-3815.1	4566.9	-3224.1	3068.8	-2756.7	2116.4	-2413.5	-1224.8
48361	5.86	0.38	5.50	0.27	-3720.4	4324.3	-2998.0	3180.9	-2372.6	2443.4	-1944.0	1908.2
48362	4.98	0.39	5.83	0.35	-3959.1	5023.4	-3105.7	2568.3	-2381.8	1698.6	-1755.1	1231.4
48365	5.13	0.05	7.65	0.04	-3940.2	5314.4	-3139.8	3571.8	-2497.9	1252.8	-2015.5	-304.9
48378	5.51	0.05	7.67	0.01	-4305.8	3844.7	-3255.2	2530.5	-2435.5	1816.0	-1848.6	37.2
48384	5.87	0.41	8.10	0.42	-4476.1	3778.4	-3427.5	2228.1	-2492.3	1041.1	-1789.0	212.9
48386	5.52	0.06	8.30	0.05	-4545.1	5572.7	-3485.6	4072.3	-2588.6	2748.6	-1855.8	1734.3
48390.469	9.17	0.13	10.04	0.09	-4755.9	6097.5	-3093.2	2678.8	-1840.1	1588.0	-761.7	1044.1
48393	5.44	0.06	7.01	0.05	-4795.6	4187.1	-3629.0	2750.8	-2575.1	1440.2	-1870.4	490.6
48394	5.05	0.38	7.16	0.41	-4926.9	4163.9	-3645.0	2490.5	-2709.3	1538.3	-2122.9	-2.5
48395	6.39	0.38	7.37	0.25	-4254.4	5408.4	-3422.1	4072.4	-2654.3	2946.5	-1817.5	2164.2
48400	5.32	0.10	6.63	0.09	-4819.5	5958.4	-3673.8	4168.8	-2819.8	2624.0	-2194.2	1187.1
48414	4.59	0.10	7.19	0.10	-4750.4	3853.5	-3703.0	2541.1	-2768.8	1471.6	-2183.4	51.5
48415	4.32	0.38	7.19	0.48	-4811.3	4270.4	-3530.8	2717.7	-2478.9	1291.5	-1892.9	462.7
48421	4.86	0.06	8.64	0.03	-4307.8	5521.2	-3273.7	3960.9	-2478.5	2443.6	-1854.6	1039.1
48425.381	12.19	0.70	13.01	0.45	-4391.7	6538.4	-2786.3	3844.7	-1830.9	2264.2	-1232.2	1295.6
48426.348	10.96	0.27	11.13	0.19	-4466.9	6640.9	-3041.3	3460.0	-1907.7	2003.1	-709.8	1458.6
48427	8.25	0.11	6.99	0.07	-4364.9	4072.0	-2955.5	2509.4	-2012.2	1312.9	-1421.2	597.2
48428	6.79	0.15	8.48	0.14	-5452.6	5223.3	-3586.2	2953.2	-2221.3	1737.8	-1365.0	872.7
48431	5.21	0.04	8.84	0.05	-5687.5	5580.0	-3369.8	3067.1	-2081.2	1631.6	-1280.7	823.3
48448.327	11.04	0.05	11.24	0.00	-4173.3	7254.2	-2678.5	3009.6	-1537.5	1547.1	-754.2	939.8
48449.324	9.76	0.06	7.51	0.03	-4346.2	5775.0	-3092.1	3014.1	-2313.1	1612.6	-1832.8	399.2
48455	6.14	0.15	7.46	0.11	-4674.5	4291.1	-3510.0	2857.6	-2458.2	1430.9	-1754.8	483.4
48456	5.66	0.15	6.64	0.11	-4715.4	4396.4	-3547.7	2838.5	-2610.2	1288.6	-2022.7	220.3
48460	4.86	0.10	5.91	0.07	-4587.4	3919.1	-3303.4	2484.5	-2248.7	1294.2	-1543.5	463.8
48477	4.54	0.47	6.73	0.51	-4732.5	3890.6	-3565.8	2575.3	-2512.0	1384.5	-1807.3	435.2
48512	5.24	0.06	8.14	0.04	-4834.6	4815.9	-3616.6	3250.9	-2623.3	1693.9	-2133.7	608.7
48513	6.82	0.04	8.15	0.02	-4436.9	4516.5	-3274.0	2966.0	-2340.5	1541.7	-1755.5	596.0
48514	5.35	0.07	8.15	0.03	-4791.0	4644.2	-3161.2	2852.4	-2108.7	1545.1	-1405.0	716.2
48516	6.94	0.03	8.09	0.02	-4498.0	4472.4	-3333.0	2561.6	-2397.6	1610.6	-1811.5	189.8
48534	4.89	0.07	6.09	0.06	-4970.4	4544.0	-3347.4	2759.2	-2532.6	1575.1	-1949.3	631.2
48636	6.31	0.25	9.06	0.24	-4318.0	4313.2	-3384.2	2996.6	-2564.7	2042.7	-1625.4	1448.0
48644	6.48	0.46	8.63	0.41	-4603.2	5486.5	-3433.7	3921.3	-2494.8	2722.8	-1788.6	1648.2
48651	5.64	0.10	7.45	0.07	-4624.7	5394.5	-3579.6	3959.7	-2647.5	2650.4	-1946.5	1583.3
48662	6.34	0.49	7.22	0.43	-4260.0	5171.6	-3330.2	3737.9	-2514.1	2310.9	-1812.8	1126.9
48670	6.18	0.37	7.41	0.33	-4026.7	5992.6	-3135.8	3807.4	-2345.5	2440.8	-1484.1	1986.6
48676	6.66	0.03	5.72	0.02	-4614.9	5275.4	-3583.1	3859.3	-2778.1	2449.7	-2086.3	1280.1
48677	4.13	0.01	3.65	0.01	-4196.2	5176.0	-3025.9	2775.6	-1733.3	1701.5	-671.5	1106.5
48679	4.18	0.16	5.86	0.17	-5601.3	4842.5	-3670.7	2724.6	-2506.3	1671.1	-1857.4	97.7
48681	4.69	0.20	5.91	0.14	-3498.5	5240.4	-2751.6	2945.2	667.2	2183.9	1011.3	1838.6
48682	3.95	0.68	5.14	0.65	-4003.6	5376.0	-3150.6	3938.1	-2466.3	2785.7	-1952.1	1950.3
48687	3.67	0.04	4.23	0.01	-3874.7	5586.1	-3264.5	3531.2	-2721.1	2526.2	-2380.9	2145.9
48689	4.12	0.32	4.83	0.34	-3793.3	5041.2	-2979.2	3406.1	-2060.8	1952.3	780.6	1572.7
48691	4.28	0.11	4.58	0.10	-3930.2	5214.2	-2980.7	3821.2	-2164.4	2573.0	-1516.6	1536.8
48692	5.10	0.12	3.96	0.09	-4550.7	4733.4	-3275.1	3304.6	-2227.4	2000.7	-1526.8	938.1
48693	3.77	0.46	4.31	0.44	-5059.7	5297.6	-3489.5	3680.8	-2503.8	2473.8	-1713.0	1271.6
48699	4.65	0.81	5.00	0.69	-3474.1	6141.9	-2681.5	3524.0	-1990.7	2293.7	-1263.5	1732.9
48707	3.19	0.19	4.46	0.07	-4304.5	5943.9	-3144.2	3319.3	-2445.9	2015.4	-1745.9	1424.6
48713	3.20	0.06	4.07	0.07	-3130.2	5675.4	-2425.8	3064.8	-471.5	1699.7	-31.8	1189.4
48718	3.02	0.16	3.93	0.22	-5020.4	5771.3	-3736.4	3965.7	-2681.7	2409.4	-2094.2	861.1
48720	2.30	0.08	3.53	0.11	-4535.3	5545.6	-3352.8	4084.6	-2284.6	2751.6	-1331.8	1906.4
48726	1.75	0.05	3.54	0.08	-4904.4	5866.8	-3290.1	3965.7	-2131.7	2194.1	-1434.4	1018.8
48733	1.91	0.05	3.82	0.07	-4700.1	6056.2	-3420.2	4376.2	-2369.0	2943.6	-1548.7	1992.3
48733	2.35	0.05	2.83	0.04	-5002.6	5865.5	-3490.6	4305.9	-2088.1	2873.2	-1149.4	1921.9
48734	2.62	0.06	2.48	0.05	-6056.0	6484.8	-2304.3	3074.1	-968.7	1158.2	-522.2	597.0
48736	2.54	0.02	3.67	0.03	-6431.6	8513.4	-3693.1	5538.7	-2254.2	2470.6	-1291.1	1982.6
48737	1.32	0.28	3.39	0.24	-5103.9	6298.5	-3434.4	4642.9	-1991.1	3201.7	-980.0	2176.4
48742.1	1.83	0.21	3.84	0.36	-4381.2	5573.8	-3096.3	4131.4	-1923.3	2815.2	-1099.5	1980.5
48742	1.55	0.15	4.30	0.35	-3301.1	6501.0	-2664.2	4776.3	-2160.4	201.8	-1790.4	-508.8
48743	0.65	0.15	2.34	0.42	-4328.7	5554.5	-2902.6	4087.8	-1708.9	2870.9	-750.5	1900.9
48743	1.74	0.14	3.63	0.17	-2943.6	5660.9	-1700.5	4421.5	-621.2	3324.0	156.9	2537.7

Note: (1) Julian dates of IAW watch data in the form “*.1” are used to artificially make a difference between two different spectra under the same MJD on IAW watch web site (as for example 48325.0 and 48325.1)

(2) File names differs according to the observatory/monitoring campaign:

PTG* : Crimean Astrophysical Observatory data

n* : AGN watch data

5* : SAO/GHO data

A* : Asiago data

Continued on next page

Table 2 – continued from previous page

JD-2400000	Flux Hb	Err.	Fl. 5100	Err.	B25%	R25%	B50%	R50%	B75%	R75%	B90%	R90%
48744.1	1.53	0.12	3.91	0.22	-3968.9	8445.4	-2125.7	6605.9	-541.5	5018.3	575.8	3884.4
48744	1.99	0.11	4.42	0.24	-4617.4	5608.4	-3313.6	4143.6	-2123.3	2807.0	-1167.7	1838.6
48745	1.49	0.12	4.17	0.32	-4332.7	5556.6	-2905.7	4088.9	-1711.4	2871.3	-752.4	1900.7
48745	1.68	0.10	3.88	0.19	-3064.6	7265.0	-1552.7	5743.0	-270.1	4434.6	678.6	3508.3
48746.1	3.61	0.02	3.76	0.01	-5761.7	7251.3	-3889.7	5308.8	-2339.1	3718.3	-1115.1	2474.4
48746	2.11	0.01	3.38	0.01	-4484.0	5523.9	-3295.8	4056.3	-2222.4	2838.6	-1264.9	1868.0
48747	4.42	0.13	4.82	0.04	-8054.5	8332.4	-5700.5	5988.9	-3684.6	3907.2	-2253.3	2324.9
48748	5.53	0.00	3.89	0.00	-7735.4	6723.3	-4780.5	3729.6	-2245.4	1598.3	-1345.4	765.1
48750.1	1.83	0.22	4.50	0.46	-5222.6	6249.0	-3593.9	4566.1	-2073.4	3131.0	-1133.8	2059.1
48750	2.09	0.09	4.17	0.12	-5581.5	9486.1	-4158.2	6515.2	-3127.8	2519.1	-2394.3	1942.9
48765.1	2.43	0.12	3.73	0.15	-3711.7	6223.8	-2263.0	4769.1	-1015.5	3497.6	-111.3	2617.6
48765	1.86	0.14	3.63	0.22	-3384.1	7318.7	-2041.6	5209.7	356.1	2260.9	865.2	1715.5
48766	2.48	0.27	3.69	0.35	-5644.5	6461.9	-3881.6	4637.4	-2330.4	3163.0	-1328.9	2033.7
48769	2.30	0.71	3.53	0.85	-4304.2	7225.6	-2982.8	5356.8	-2145.2	3606.2	-1585.6	1724.0
48771	2.25	0.22	3.77	0.14	-4135.0	5782.7	-3022.0	4279.4	-2359.2	2961.3	-1974.8	1932.1
48777	2.55	0.11	3.90	0.15	-4656.1	5705.2	-3350.7	4237.9	-2158.9	2899.0	-1202.1	1929.0
48778.1	2.84	0.02	4.27	0.00	-4137.2	6041.6	-3204.0	4581.6	-2372.0	3340.7	-1676.9	2386.9
48778	2.32	0.13	4.48	0.17	-5144.0	5460.6	-3600.9	3870.3	-2288.9	2531.1	-1331.1	1560.9
48779	3.01	1.47	6.32	2.30	-5037.8	6248.4	-3246.0	4276.4	-2045.4	2683.5	-1322.8	2195.0
48780.1	2.74	0.26	4.20	0.07	-5115.0	5358.0	-3608.0	3924.5	-2210.0	2497.7	-1274.4	1550.2
48780	2.89	0.09	5.33	0.07	-3716.1	6613.5	-2496.6	4640.7	-1061.6	2929.3	1439.8	2467.5
48783	3.34	0.10	4.70	0.10	-4295.5	6811.5	-2322.2	4564.3	-1208.6	2263.0	-615.3	1277.1
48789	3.78	0.08	5.48	0.08	-5299.7	6243.9	-3092.8	3967.6	-1315.4	2384.2	-534.5	1595.6
48796	2.91	0.04	4.02	0.04	-4625.7	5720.2	-3119.7	4288.3	-1722.7	2981.6	-787.7	2034.9
48798	2.92	0.13	3.95	0.14	-5189.2	5362.7	-3671.0	3798.2	-2380.2	2480.6	-1437.9	1526.0
48801	5.44	0.29	3.60	0.13	-5161.0	5136.2	-3616.8	3546.3	-2175.6	2303.0	-1062.2	1739.5
48804.1	3.14	0.17	4.20	0.20	-5074.5	5332.0	-3676.6	3771.8	-2506.6	2458.0	-1684.9	1506.0
48804	2.85	0.06	4.25	0.06	-4847.4	6083.5	-3596.0	4233.9	-2611.4	2949.4	-1589.4	2395.5
48805	4.25	1.30	4.19	0.99	-4810.2	5339.7	-3381.2	3868.5	-2065.1	2526.3	-1104.4	1675.2
48810.1	2.00	0.10	3.17	0.12	-4378.1	5494.3	-2973.1	4049.3	-1729.9	2816.2	-819.5	1996.9
48812	3.97	0.55	2.86	0.40	-4721.2	5135.6	-3285.4	3659.0	-2065.0	2415.2	-1174.4	1626.3
48816	4.00	0.17	3.04	0.11	-6783.5	5838.4	-3706.4	3247.8	-2443.5	1960.8	-1059.7	1144.6
48817	2.64	0.09	4.91	0.11	-6933.7	6503.9	-4088.4	3791.5	-2368.0	2268.9	-1446.3	1335.8
48825	2.41	0.08	4.72	0.06	-4702.7	5394.0	-3661.9	3964.7	-2617.5	2660.4	-1802.6	1597.4
48830	2.82	0.17	4.41	0.10	-4608.7	5391.5	-3217.0	3959.4	-1935.6	2652.6	-1117.2	1705.7
48831	2.79	0.06	4.17	0.04	-5044.5	6048.5	-3320.1	4269.7	-1585.6	2736.3	-307.2	1913.9
48831	2.95	0.19	5.05	0.16	-4851.8	5258.3	-3445.1	3810.2	-2149.7	2488.9	-1204.0	1651.0
48833	2.91	0.14	4.57	0.18	-4670.7	5542.8	-2655.7	3472.2	-1344.6	2139.9	-626.9	1415.6
48834.1	3.01	0.19	5.00	0.25	-4683.5	5261.0	-3266.1	3802.8	-1960.8	2713.7	-1007.8	1989.8
48835	3.45	0.17	4.48	0.21	-4683.3	5308.3	-3259.2	3843.1	-1947.8	2748.8	-990.4	2021.5
48836	3.32	0.12	4.88	0.04	-4867.4	5730.9	-3206.2	3897.8	-1655.3	2439.3	-216.5	1833.6
48837	3.85	0.15	4.53	0.14	-5054.6	5462.3	-3506.4	3500.4	-2070.1	2280.6	-385.7	1672.6
48848	3.45	0.09	5.81	0.06	-5604.1	6845.6	-3288.1	3769.6	-1622.8	2299.6	-730.7	1511.0
48858.1	4.48	1.82	4.39	1.66	-4615.6	5201.5	-3216.0	3762.2	-1927.3	2687.2	-986.5	1972.7
48858.21	4.33	0.09	5.34	0.01	-5975.5	5249.9	-3613.0	3368.1	-2099.8	2156.6	-905.4	1388.2
48861	6.60	0.24	4.86	0.14	-4727.2	4767.5	-3185.4	3427.3	-1874.5	2456.4	-797.6	1730.2
48862.1	4.65	0.28	5.40	0.25	-5537.3	5471.6	-3344.6	3687.6	-1834.9	2504.1	-785.2	1678.4
48862	5.66	0.04	5.81	0.03	-6298.0	5554.9	-3349.0	3364.8	-1803.8	2154.8	-729.4	1431.1
48867	5.26	0.09	5.19	0.07	-4504.4	4941.7	-3088.7	3608.5	-1903.7	2642.6	-952.3	1799.9
48869	4.09	0.09	6.26	0.07	-5871.3	5422.8	-3447.4	3491.9	-2005.6	2361.7	-780.3	1573.2
48876	4.41	0.08	6.27	0.06	-4872.1	5029.3	-3477.6	3594.7	-2310.5	2642.1	-1373.4	2048.2
48883	5.48	0.02	6.07	0.01	-4906.1	4922.7	-3521.7	3498.7	-2246.9	2435.2	-1316.3	1728.2
48886	4.17	0.17	5.10	0.15	-5312.3	5022.6	-3459.7	3592.2	-2295.8	2642.3	-1361.5	1931.9
48889	4.44	0.07	6.26	0.04	-5101.1	4968.5	-3446.3	3719.5	-1893.3	2701.5	-667.5	2024.7
48898.1	4.27	0.11	5.12	0.09	-5244.1	4567.3	-3728.5	3248.4	-2440.0	2292.8	-1499.4	1697.1
48898	4.67	0.06	5.40	0.01	-4826.4	4994.5	-3426.3	3554.6	-2137.1	2598.5	-1196.0	2121.6
48954	5.52	0.06	8.20	0.05	-4893.6	4955.8	-3348.3	3593.6	-2017.2	2688.8	-791.8	2124.7
48967	7.26	0.13	8.64	0.10	-4541.7	4852.4	-3035.1	3305.8	-1871.0	2476.2	1.2	2003.2
48973	6.19	0.12	9.85	0.12	-5083.1	4709.4	-3337.0	3154.4	-1580.5	2082.5	-757.3	1370.1
48981	7.47	0.08	8.80	0.06	-4649.3	5297.9	-3599.3	3856.6	-2662.8	2899.5	-1958.4	2302.8
48982	6.66	0.61	10.12	0.62	-5094.7	4718.4	-3344.9	3279.7	-1937.7	2324.3	-877.8	1609.8
48992.1	8.53	0.04	10.04	0.03	-3921.3	4997.0	-2615.5	3692.0	-1506.0	2597.4	-696.6	1779.0
49004	8.08	0.33	10.62	0.26	-4901.1	4499.8	-3277.2	2833.3	-1644.3	1885.1	-707.2	1175.9
49008	6.86	0.05	8.71	0.04	-4583.9	5268.3	-3259.4	3226.6	-2262.1	2211.0	77.9	1648.2
49010.1	8.96	0.04	8.15	0.02	-3893.2	5202.4	-2866.6	3266.4	-1770.0	2353.6	402.1	1881.4
49010	7.12	0.18	8.42	0.05	-4291.2	4572.8	-3241.3	2898.2	-2422.2	2183.4	167.1	1707.7
49011	7.28	0.50	8.82	0.36	-4251.9	4362.9	-3188.5	2789.1	-1764.7	1824.7	-811.7	1223.4
49012.1	5.69	0.04	7.74	0.02	-5289.9	5336.1	-3637.1	3406.8	-2640.9	2390.4	-1974.9	1939.7

Note: (1) Julian dates of IAW watch data in the form “*.1” are used to artificially make a difference between two different spectra under the same MJD on IAW watch web site (as for example 48325.0 and 48325.1)

(2) File names differs according to the observatory/monitoring campaign:

PTG* : Crimean Astrophysical Observatory data

n* : AGN watch data

5* : SAO/GHO data

A* : Asiago data

Continued on next page

Table 2 – continued from previous page

JD-2400000	Flux Hb	Err.	Fl. 5100	Err.	B25%	R25%	B50%	R50%	B75%	R75%	B90%	R90%
49012	6.71	0.05	8.84	0.02	-3488.6	4528.4	-2593.7	2968.7	-1596.0	2259.3	308.7	1821.0
49013.1	5.60	0.78	6.75	0.73	-4642.6	4407.5	-3366.4	2979.1	-2434.8	2148.9	-1617.2	1675.6
49013	7.32	0.04	7.99	0.03	-3723.8	5408.3	-3020.9	3518.5	-2316.2	2663.3	756.6	2151.4
49014.1	6.76	0.05	7.70	0.03	-3755.6	5168.8	-3086.2	3725.7	-2482.5	2835.9	-1742.9	2289.5
49014	6.11	0.49	7.15	0.41	-4395.6	5131.0	-3124.9	3037.2	-431.9	2115.0	448.6	1706.0
49017	6.77	0.04	7.18	0.01	-4361.3	4362.5	-3299.4	2790.3	-2352.4	2067.4	-1521.2	1586.4
49020	7.25	0.00	7.85	0.00	-4717.8	4562.4	-3283.2	3089.8	-2285.9	2299.9	-1396.6	1736.8
49029	7.36	0.08	8.40	0.07	-4877.7	4313.9	-3365.3	3000.5	-2313.7	2048.9	-1023.4	1455.6
49032	6.64	0.10	7.33	0.06	-4883.8	4300.2	-3489.2	2868.8	-2438.8	2037.0	-1619.4	1562.7
49034	4.80	1.44	6.34	1.43	-4691.0	4592.7	-3366.5	3006.6	-2369.2	2216.6	-811.2	1653.6
49036	6.26	0.23	7.44	0.12	-4171.1	4334.4	-3224.7	2879.9	-2394.2	2155.2	-1561.3	1552.6
49045.1	5.38	0.15	6.40	0.09	-4291.7	5296.9	-3173.5	3312.9	-2051.0	2343.1	344.1	1824.8
49045	6.65	1.22	7.61	0.98	-4174.6	6257.9	-3219.4	4219.4	-2535.1	2542.7	-2089.5	1742.5
49048	6.69	0.01	7.75	0.01	-3756.2	4858.4	-2885.7	3553.8	-2046.2	2937.8	1403.3	2562.0
49056	8.75	0.03	7.74	0.01	-4938.4	4351.5	-3313.1	3040.7	-2380.3	2090.8	-1444.5	1617.0
49061	6.43	0.72	6.73	0.48	-4930.6	5317.1	-3421.5	3168.1	-2255.4	2099.2	-1553.5	1388.8
49062	9.37	0.02	7.70	0.01	-4244.3	5266.1	-2742.8	3130.4	-1543.0	2224.7	1044.4	1911.8
49064	7.27	0.50	7.46	0.38	-4881.1	4642.9	-3256.5	2856.4	-2090.6	1789.4	-1037.4	1080.2
49065	4.97	0.65	6.16	0.21	-4303.9	5026.6	-3022.0	2875.1	-2086.2	2042.5	-205.9	1567.7
49066	5.92	0.69	6.19	0.48	-4279.6	5412.6	-2855.9	3983.9	-1630.0	2769.6	-775.8	1905.3
49067	5.63	0.38	7.42	0.03	-4127.1	4638.5	-2955.8	3270.7	-1485.0	2572.4	916.5	2174.2
49070.1	6.41	0.03	6.46	0.02	-4414.6	5078.2	-3016.3	3675.1	-1840.5	2477.5	-988.4	1615.5
49070	6.89	0.84	7.03	0.65	-4474.9	4917.4	-3369.8	3414.8	-2489.3	2483.6	-1835.3	1886.5
49071.1	6.27	0.42	6.82	0.34	-3702.6	4074.4	-2594.6	2542.7	-1416.8	2011.7	952.6	1746.6
49071	4.72	0.51	5.32	0.26	-4333.7	4029.6	-3153.2	2941.2	-2205.4	2217.8	-1492.5	1616.2
49074	6.52	0.11	6.38	0.06	-4076.3	4590.0	-2774.3	3322.3	-1597.6	2491.2	-679.2	1927.3
49075	5.80	0.53	6.36	0.29	-4725.9	4891.1	-3555.2	3446.8	-2497.7	2487.8	-1790.5	2009.4
49077	5.80	0.03	5.85	0.02	-3539.9	4807.8	-2366.2	2940.1	-1155.0	2209.4	786.5	1877.9
49078.1	5.90	0.04	5.79	0.02	-4248.4	4802.6	-2930.2	3150.2	-2048.0	2402.1	-1458.5	1954.1
49078	5.35	0.23	5.05	0.15	-4226.5	4239.0	-3048.6	2911.7	-2102.9	2070.1	-1273.0	1590.2
49079	6.02	0.12	6.11	0.08	-4133.8	4292.4	-3078.7	2971.4	-2255.5	2253.2	-1548.1	1775.4
49080	5.29	0.79	4.62	0.53	-4898.6	4321.5	-3615.5	3123.5	-2561.5	2407.0	-1856.7	1930.2
49083	6.33	0.39	4.50	0.20	-4390.7	4501.5	-3073.7	3150.8	-2045.2	2253.7	-1308.4	1657.1
49085	6.48	0.01	5.66	0.01	-4328.0	5020.3	-3157.0	3067.4	-2128.5	2170.2	-1244.2	1573.6
49088	5.72	0.26	5.89	0.21	-4520.8	4465.0	-3236.8	3028.2	-2299.5	2193.2	-1594.6	1598.2
49089	5.64	0.08	5.56	0.06	-4332.2	4282.4	-3150.5	3071.0	-2320.4	2346.5	-1726.2	1864.5
49090.1	5.97	0.47	5.68	0.39	-4187.8	4562.9	-3137.2	3126.5	-2317.4	2410.8	-1730.4	1934.6
49090.2	6.59	0.59	5.26	0.02	-4493.0	4534.3	-3582.9	3132.9	-2735.3	2501.1	976.7	2135.8
49090	5.12	0.10	6.35	0.08	-4346.9	4120.4	-3168.7	2913.3	-2222.9	2071.2	-1511.4	1591.0
49091.1	7.05	0.27	5.42	0.15	-3633.8	4582.0	-2753.8	3113.8	-2034.7	1619.6	-1510.7	528.5
49091	5.00	0.44	5.68	0.43	-4435.3	4746.0	-2998.4	3271.6	-1999.5	2255.1	-550.8	1579.3
49092.1	4.13	1.20	4.03	0.96	-3914.0	5263.2	-2741.4	3092.3	-1662.3	2128.7	46.0	1664.6
49092	5.64	0.25	6.27	0.16	-4878.6	5084.7	-3111.8	3269.0	-2224.4	2365.3	-1557.1	1801.8
49094.1	5.26	0.17	6.21	0.16	-4701.7	5725.0	-3376.6	4132.1	-2378.8	2886.5	-1600.5	2096.4
49094	4.85	0.36	6.43	0.30	-4730.1	4675.1	-3293.8	3200.2	-2517.5	2296.1	-1461.7	1845.0
49096	4.51	0.53	5.96	0.30	-4284.2	5315.3	-3341.3	3777.4	-2591.3	2878.3	-2003.0	2379.9
49098.1	7.41	0.02	5.84	0.01	-3508.5	5241.0	-2498.0	3104.6	-1713.4	2274.1	-959.5	1876.2
49098	5.17	0.19	5.96	0.16	-4015.2	5358.1	-2908.4	3320.1	-2124.6	2389.2	-1535.4	1924.8
49099	5.64	0.04	7.04	0.03	-5692.1	4636.7	-3569.6	2890.4	-2431.3	1876.3	-1717.6	1154.1
49101	5.64	0.19	8.34	0.17	-4577.6	4786.7	-3191.6	3008.6	-2380.0	2182.3	-1799.0	1593.5
49102	5.92	0.60	6.30	0.45	-4577.7	5505.9	-2920.6	3235.7	-1588.1	1881.7	-137.9	1431.8
49103	7.38	0.01	6.06	0.01	-4057.0	5580.4	-2559.2	3241.8	-1643.8	2477.3	-889.8	2079.2
49106	8.50	0.05	6.39	0.01	-5758.3	4667.1	-3759.5	2757.8	-2755.0	2026.6	-2035.4	1297.2
49107.1	7.36	0.01	6.55	0.01	-4363.0	5120.2	-3193.9	3079.9	-2255.3	2005.3	-1195.8	1528.9
49107.2	7.44	0.46	5.92	0.26	-5110.8	5072.6	-3013.1	3257.0	-1903.0	2240.4	-1123.5	1564.6
49107	6.59	0.35	7.91	0.30	-6183.2	5248.2	-3616.8	3190.4	-2325.3	2020.8	-1461.1	1146.5
49114.1	4.24	0.17	5.47	0.08	-4133.0	4663.3	-2841.7	3219.3	-1899.0	2260.5	-1190.1	1782.2
49114	6.24	0.15	7.34	0.13	-5237.6	5101.2	-3693.9	3670.3	-2453.2	2246.0	-1519.2	1300.3
49120.1	7.45	0.36	6.72	0.24	-4190.8	4978.3	-2986.6	3641.7	-1941.1	2477.0	-1121.7	1647.8
49120	6.40	0.66	6.81	0.53	-2864.2	6462.8	-1569.9	3224.1	-704.0	2054.8	-125.3	1471.9
49121	6.86	0.31	6.39	0.21	-4617.3	4198.5	-3166.0	3008.1	-2145.8	2118.2	-1561.2	1378.7
49122	6.57	0.07	8.04	0.06	-4372.4	4592.6	-2775.5	3401.5	-1900.8	2511.3	-1170.0	2067.2
49125	5.91	0.46	6.48	0.33	-4504.8	4406.7	-3331.9	3083.0	-2390.2	2363.4	-1681.9	1884.7
49126	5.34	0.19	6.51	0.11	-4209.8	4773.3	-3139.2	3194.6	-2266.6	2271.9	-1660.9	1828.6
49127	7.20	0.63	7.48	0.52	-3723.5	4455.2	-2386.7	3121.0	-1076.7	2223.7	767.1	1892.0
49128.1	6.10	0.42	5.78	0.27	-4360.1	4496.2	-3077.5	3180.9	-2023.9	2346.8	-1201.9	1752.4
49128	7.94	0.04	7.87	0.02	-4091.2	5328.4	-2959.9	3252.4	-1582.8	2307.1	807.7	1922.8
49129	7.60	0.04	7.41	0.03	-4134.3	4506.9	-2862.3	3237.6	-1786.9	2280.6	-1011.6	1735.0

Note: (1) Julian dates of IAW watch data in the form “*.1” are used to artificially make a difference between two different spectra under the same MJD on IAW watch web site (as for example 48325.0 and 48325.1)

(2) File names differs according to the observatory/monitoring campaign:

PTG* : Crimean Astrophysical Observatory data

n* : AGN watch data

5* : SAO/GHO data

A* : Asiago data

Continued on next page

Table 2 – continued from previous page

JD-2400000	Flux Hb	Err.	Fl. 5100	Err.	B25%	R25%	B50%	R50%	B75%	R75%	B90%	R90%
49130	6.34	0.04	6.41	0.03	-4921.6	4592.1	-3278.4	3266.0	-2335.4	2425.1	-1862.7	1945.7
49131.1	7.22	0.25	6.66	0.19	-3943.4	5139.7	-2504.1	3776.7	-1392.1	2871.4	-387.8	2194.2
49131	5.45	0.31	7.75	0.29	-4748.3	4219.5	-3568.1	2766.5	-2501.8	1922.2	-1788.8	1440.8
49132.1	7.09	0.10	7.46	0.08	-4769.9	4638.4	-3469.3	3120.4	-2400.9	2334.0	-1567.2	1911.5
49132	8.32	0.09	9.38	0.03	-4381.5	4517.6	-3210.2	3195.8	-2152.0	2357.7	-1090.0	1879.7
49135.1	6.81	0.25	6.39	0.19	-4555.3	4563.0	-3152.5	3243.3	-2213.5	2406.5	-1507.4	1810.2
49135	6.94	0.14	6.64	0.10	-4240.7	4817.2	-3182.2	3368.8	-2238.2	2527.1	-1528.2	2167.0
49140	6.97	0.03	6.98	0.02	-4215.9	4906.7	-3190.1	3446.0	-2360.3	2735.2	-1594.8	2296.0
49141	6.90	0.21	7.18	0.15	-4714.7	4595.0	-3419.2	3143.9	-2355.1	2300.5	-1524.8	1819.7
49142	6.38	0.15	7.39	0.13	-4284.2	4689.1	-3103.2	3235.2	-2155.0	2390.4	-1203.8	1908.7
49149	6.01	0.16	6.35	0.12	-4415.7	4717.1	-3479.7	3275.4	-2658.3	2557.2	-2070.2	2198.7
49150	5.33	0.13	5.30	0.09	-4273.9	4495.9	-3103.7	3176.0	-2164.2	2339.1	-1457.7	1861.9
49151	5.05	0.25	4.87	0.16	-4399.5	5399.1	-3033.2	3960.6	-1955.2	2827.9	-1070.3	2064.1
49153.3	4.48	0.30	5.24	0.26	-4707.4	6423.2	-2657.8	4077.2	-2004.2	2844.4	-1644.0	2213.3
49153.3	5.92	0.41	5.13	0.20	-3954.4	4318.3	-3010.2	2652.1	895.9	2120.8	1226.5	1888.7
49155	5.91	0.36	5.72	0.26	-3266.5	4656.2	-2418.3	3554.4	-1698.6	2955.1	-1042.9	2556.2
49156.1	5.26	0.20	5.16	0.03	-4744.8	4792.3	-3700.1	3360.2	-2768.3	2646.7	-2067.5	2171.9
49156.2	5.80	0.31	6.06	0.21	-3591.8	5225.7	-2679.2	3454.8	-1796.5	2456.9	636.1	1992.4
49156	6.68	0.16	6.81	0.12	-4579.3	4600.1	-3387.5	3009.9	-2430.6	2278.8	-1831.0	1913.9
49157.1	8.04	0.08	5.63	0.05	-4325.9	5514.2	-2920.7	3794.5	-2047.4	2699.0	-1475.1	1301.2
49157	8.03	0.73	7.09	0.45	-4424.4	4582.0	-3239.1	3244.1	-2287.5	2395.7	-1452.3	1912.0
49158.1	6.04	0.11	6.17	0.08	-4253.4	4692.2	-3149.8	3353.9	-2411.7	2533.2	-1806.4	2123.7
49158	4.72	0.24	4.86	0.18	-4973.6	4562.4	-3305.7	3094.3	-2228.5	2241.2	-1508.2	1390.4
49159.1	5.72	0.05	5.60	0.02	-3355.2	5166.4	-2311.4	2763.9	-968.5	2332.2	1404.3	2099.9
49159	5.47	0.18	5.81	0.06	-4655.4	4574.2	-3235.7	3238.2	-2285.4	2391.1	-1570.6	1908.1
49160	4.32	0.35	5.24	0.36	-4495.7	4485.1	-3195.3	3151.0	-2245.9	2425.8	-1531.9	1943.3
49163	5.99	1.27	5.08	0.88	-3774.7	4498.8	-2736.2	3195.3	-140.8	2511.4	706.8	2101.9
49164	2.89	0.07	3.28	0.07	-4371.9	5995.1	-2397.1	4560.1	-1229.2	3607.3	-409.0	2894.6
49166	7.93	0.04	5.98	0.02	-4984.9	3838.1	-2664.9	681.2	-1998.6	-438.3	-1665.0	-773.4
49169	5.76	0.19	6.35	0.15	-5653.4	5415.9	-3339.4	3599.1	-2231.2	2581.9	-1452.9	1905.7
49176	5.92	0.14	6.84	0.12	-4479.9	4723.4	-3082.3	3289.0	-2029.8	2455.5	-1326.0	1861.5
49182	6.17	0.23	6.52	0.17	-4447.2	4630.8	-3167.1	3317.1	-2115.6	2365.2	-1295.2	1890.4
49183	7.92	0.05	7.25	0.03	-4344.4	4726.7	-2907.0	3478.6	-1907.7	2574.2	-905.1	2010.3
49187	5.60	0.27	6.56	0.25	-5172.5	4698.5	-3317.3	3387.2	-2151.9	2437.2	-1721.6	1844.9
49188	6.03	0.21	7.41	0.07	-4047.5	4973.1	-2607.6	3427.9	-992.0	2402.2	1141.9	2095.1
49189	5.03	0.05	6.99	0.05	-3706.5	4877.5	-2768.5	3675.3	-1793.9	2956.3	741.5	2477.9
49190	6.97	0.22	7.28	0.16	-3302.0	4385.4	-1829.4	3060.7	-526.1	2204.5	180.8	1706.2
49191	7.65	0.16	8.17	0.11	-4533.6	4723.9	-3261.6	3417.6	-2100.6	2353.1	-1168.4	1881.2
49196	6.59	0.27	6.37	0.18	-3806.3	4742.4	-2499.2	3609.0	-1321.2	2719.0	-476.9	2036.2
49197	7.32	0.09	7.49	0.06	-4231.3	4843.1	-3015.0	3481.3	-1905.0	2464.0	-1014.0	2013.0
49205	6.56	0.14	7.43	0.11	-4955.6	4582.8	-3445.1	3269.6	-2394.9	2436.8	-1575.4	1962.0
49211	6.70	0.09	8.46	0.08	-4696.9	4592.0	-3304.4	3281.3	-2372.4	2450.2	-1671.5	1976.2
49212	7.25	0.38	7.36	0.27	-4623.9	4827.7	-3575.4	3390.9	-2640.2	2556.0	-1819.6	2198.8
49240.1	6.63	2.13	6.89	1.48	-5486.1	4870.5	-3746.0	3437.1	-2580.2	2485.2	-1878.5	1773.3
49240	7.37	0.07	6.66	0.00	-4922.0	4927.5	-3487.3	3452.0	-2267.8	2547.5	-1377.8	1983.6
49242	5.99	1.52	6.52	1.08	-4815.1	4924.3	-3490.5	3448.8	-2382.1	2431.4	-1603.8	1867.8
49243	5.27	0.14	5.81	0.10	-4998.8	4738.9	-3562.1	3264.0	-2564.7	2359.9	-1786.6	1796.2
49255	5.44	0.21	6.37	0.17	-5011.3	4610.8	-3576.5	3249.5	-2579.2	2345.4	-1801.1	1669.1
49309.1	7.03	0.15	7.85	0.10	-4856.8	4765.3	-3422.0	3517.2	-2202.6	2612.8	-1312.5	1823.6
49313.6	5.36	0.11	5.87	0.08	-5448.0	5293.0	-3905.5	3929.2	-2576.9	2910.4	-1576.6	2007.6
49317	4.03	0.02	6.64	0.02	-5590.6	4940.7	-4176.2	3482.7	-2992.4	2152.4	-2160.9	1068.2
49324	4.65	0.12	7.20	0.11	-4976.4	5180.2	-3463.1	3742.2	-2176.5	2668.3	-1237.3	1835.6
49325	5.44	0.13	7.01	0.11	-5490.4	4801.9	-4208.5	3600.8	-3038.3	2762.9	-2216.5	2165.8
49326	5.31	0.26	7.15	0.24	-6194.2	5193.5	-4693.0	3761.1	-3416.8	2691.2	-2368.6	1980.0
49327	5.66	0.20	6.99	0.17	-5965.5	5019.4	-4337.5	3699.0	-2935.0	2742.3	-1996.2	1788.6
49327.6	5.63	0.27	6.49	0.24	-5991.9	5186.5	-4486.7	3632.1	-2973.9	2679.4	-1922.0	1848.3
49328	5.07	0.05	6.70	0.04	-5784.1	4927.7	-4142.9	3597.8	-2847.0	2634.3	-1900.9	1793.7
49329	5.05	0.12	6.60	0.10	-6016.9	5030.6	-4513.3	3597.5	-3234.9	2764.6	-2301.8	2052.5
49330	4.65	0.12	7.09	0.10	-5925.7	4918.1	-4417.2	3720.3	-3134.7	2884.6	-2198.4	2408.2
49331	4.50	0.14	7.68	0.14	-5432.3	5068.2	-4154.3	3750.4	-2987.7	2914.7	-2168.3	2438.3
49332	5.25	0.13	6.68	0.12	-4798.2	5236.2	-3751.5	3799.2	-2818.1	2844.9	-2116.0	2368.9
49332.6	4.65	0.15	6.21	0.14	-5900.7	4943.2	-4275.8	3745.3	-2992.8	2909.7	-2056.2	2195.2
49333	5.73	0.04	6.76	0.03	-5303.5	4866.6	-3770.4	3652.1	-2585.6	2925.8	-1634.4	2321.8
49339	5.72	0.03	7.44	0.03	-6138.9	5056.4	-4747.7	3858.1	-3583.4	3141.4	-2648.7	2664.6
49339.7	5.61	0.15	6.09	0.11	-6274.1	4935.9	-4764.8	3616.3	-3364.7	2660.2	-2427.6	1945.0
49343.1	4.84	1.00	5.68	0.89	-6096.2	5074.6	-4447.0	3712.0	-3010.2	2807.0	-2011.5	2130.0
49364.6	5.21	0.16	6.26	0.14	-5612.7	4887.8	-4182.3	3979.7	-2966.6	3187.4	-1857.1	2622.7
49365.6	5.49	0.02	5.79	0.01	-5082.3	4687.0	-3790.2	3478.5	-2256.0	2635.4	-1307.8	1674.7

Note: (1) Julian dates of IAW watch data in the form “*.1” are used to artificially make a difference between two different spectra under the same MJD on IAW watch web site (as for example 48325.0 and 48325.1)

(2) File names differs according to the observatory/monitoring campaign:

PTG* : Crimean Astrophysical Observatory data

n* : AGN watch data

5* : SAO/GHO data

A* : Asiago data

Continued on next page

Table 2 – continued from previous page

JD-2400000	Flux Hb	Err.	Fl. 5100	Err.	B25%	R25%	B50%	R50%	B75%	R75%	B90%	R90%
49367	5.21	0.81	5.10	0.58	-5445.4	4805.3	-3918.3	3595.2	-2619.9	2751.0	-1672.1	2029.3
49370	4.81	0.07	4.57	0.03	-4723.6	5050.2	-3509.1	3634.4	-2289.6	2638.9	-1228.6	1977.1
49371	7.58	0.24	5.19	0.11	-4851.0	5418.5	-3474.9	3834.8	-2092.4	2921.6	-539.6	2259.3
49372.1	5.50	0.50	5.41	0.35	-5704.9	5457.6	-4332.3	3706.7	-3278.2	2793.6	-2546.3	2131.2
49372	8.86	0.67	7.78	0.46	-5580.2	5920.2	-4288.0	3750.9	-3234.0	2754.9	-2339.2	2175.5
49374	8.38	0.37	7.00	0.22	-5686.8	5378.4	-4036.4	3902.0	-2598.6	2771.1	-1599.1	1869.5
49375	8.54	0.10	7.28	0.03	-5695.7	5890.6	-4322.4	3637.2	-3105.3	2723.9	-2291.1	2144.1
49387	7.41	0.29	5.45	0.17	-5666.9	5166.4	-4212.6	3666.0	-2913.8	2752.7	-1772.8	2172.9
49389.1	7.92	6.55	7.80	3.90	-5319.1	7210.7	-3862.4	3945.8	-2643.0	2865.3	-1663.8	2285.1
49390	5.16	0.22	5.08	0.17	-5251.6	5260.6	-3709.3	3898.0	-2380.8	2993.0	-934.9	2428.7
49394	5.02	0.33	4.96	0.26	-4868.9	5240.9	-3491.9	3740.0	-2189.9	2743.6	-1127.9	2163.8
49395.1	4.76	0.14	6.85	0.11	-4877.9	4897.7	-3257.2	3731.0	-1627.5	2900.4	-153.2	2320.3
49395	3.64	0.08	3.78	0.04	-4590.6	5444.0	-3131.1	3942.3	-1746.0	2945.3	-764.5	2365.2
49395.61	4.26	0.11	5.99	0.11	-4467.1	5335.6	-3406.8	3760.0	-2342.6	2915.1	-1036.9	2313.0
49397.6	4.13	0.27	4.54	0.19	-5258.9	4874.0	-3731.3	3784.8	-2432.5	2940.3	-1365.6	2458.9
49400	4.27	0.19	4.33	0.16	-4493.9	5376.1	-3277.9	3874.8	-2138.4	2961.0	-92.6	2380.9
49403.8	5.36	0.19	6.03	0.16	-5052.1	5138.5	-3675.4	3804.1	-2455.3	2973.0	-1312.0	2392.6
49403.8	5.89	1.67	7.26	1.38	-6043.4	5113.8	-4425.1	3562.4	-3147.4	2730.3	-2098.0	2137.3
49409	5.09	0.15	7.32	0.15	-5851.9	5211.0	-4230.0	3895.2	-2599.2	3060.8	-724.4	2466.2
49415.9	7.51	0.09	7.49	0.07	-5847.0	4890.9	-4103.4	3572.3	-2701.1	2855.6	-1409.8	2259.5
49416.9	5.34	0.14	7.71	0.14	-6199.0	5117.5	-4585.3	3700.3	-3288.0	2869.6	-2148.1	2289.6
49416.9	8.22	0.08	7.79	0.06	-5457.1	5304.3	-3709.7	3743.2	-2187.0	3025.4	-774.4	2428.5
49420.9	5.38	0.11	6.40	0.01	-5988.7	5919.7	-4293.3	3915.9	-3076.2	3001.8	-1854.1	2421.6
49422	5.70	0.15	7.00	0.01	-5587.6	4831.0	-3889.8	3581.5	-2426.7	2751.3	-956.4	2254.3
49428.6	5.09	0.27	6.97	0.27	-5775.8	4887.5	-3997.8	3637.7	-2372.2	2724.4	-737.6	2227.4
49429.8	4.62	0.10	7.25	0.05	-5183.6	4955.4	-3655.0	3623.9	-2000.1	2900.1	-260.8	2298.2
49429.8	9.06	0.02	7.39	0.01	-4787.6	5155.7	-3387.2	3714.9	-1862.7	2877.7	616.7	2519.5
49429.9	4.61	0.36	5.25	0.17	-6159.6	5405.5	-4222.5	3571.5	-2761.3	2658.6	-801.7	2079.1
49436.9	7.30	0.05	7.57	0.00	-5475.2	4924.3	-4043.1	3902.0	-1937.6	3109.3	71.0	2544.3
49443.91	5.80	0.30	6.21	0.24	-5649.6	5443.1	-4372.7	4004.0	-2271.1	3048.4	-861.8	2333.7
49443.9	4.71	0.36	5.15	0.29	-5021.6	5417.1	-3401.7	3832.2	-1854.6	2918.4	-545.5	2338.3
49443.9	6.35	0.15	7.54	0.12	-5801.7	6467.1	-4295.4	3949.2	-2664.6	2995.4	152.1	2400.8
49447	6.64	0.30	7.32	0.19	-5255.9	5336.4	-3475.9	3919.0	-1685.0	3005.4	-47.6	2425.4
49447.91	6.02	0.06	6.93	0.04	-5717.7	4776.7	-3940.1	3278.6	-2151.7	2366.7	-434.5	1870.5
49448.9	5.34	0.10	6.78	0.05	-5993.6	5296.4	-4343.6	3819.2	-2684.5	3026.8	213.6	2462.0
49452.5	6.29	0.13	7.44	0.07	-5590.9	4410.6	-4217.3	3412.0	-2755.8	2748.0	271.1	2251.0
49452.8	5.40	0.37	7.00	0.34	-5613.1	4471.8	-4239.4	3389.8	-2859.3	2643.0	166.8	2146.1
49454.4	6.45	0.13	7.18	0.09	-5078.3	4691.0	-3668.5	3723.8	-1659.7	3000.4	-590.7	2398.9
49457.9	8.29	0.11	7.79	0.07	-5665.3	6275.0	-4139.8	3727.9	-2133.0	2763.2	245.4	2282.0
49461	5.17	0.14	4.92	0.10	-5952.8	5531.7	-4439.1	3606.9	-2800.2	2768.7	149.1	2171.3
49464	6.62	0.10	6.82	0.07	-5417.3	4872.2	-3984.8	3736.6	-2100.8	2831.1	-428.6	2266.6
49471	5.40	0.20	6.80	0.18	-5707.3	4959.2	-4190.0	3635.0	-2664.8	2795.4	-184.4	2190.0
49475	5.69	0.13	6.52	0.10	-5378.6	5065.4	-4092.9	3739.9	-2801.6	2899.4	-1268.3	2300.5
49476	4.97	0.17	6.28	0.10	-5450.3	4807.1	-3994.8	3391.3	-2532.1	2478.8	3.9	1982.2
49477	5.40	0.09	6.13	0.02	-5557.8	4860.9	-4184.1	3611.4	-3048.0	2781.2	-2070.7	2284.2
49478	5.65	0.12	7.12	0.10	-5807.7	4688.7	-4515.7	3522.7	-3380.5	2775.4	-2485.5	2278.3
49481	4.87	0.19	6.18	0.17	-5736.8	5309.6	-4334.3	3740.9	-3042.7	2899.5	-1863.7	2419.8
49482	5.01	0.29	5.53	0.24	-4735.6	5714.5	-3439.0	4127.8	-2218.3	3047.0	-992.5	2383.8
49483	4.46	0.37	5.85	0.32	-4912.3	5699.5	-3697.6	3946.3	-2070.1	2949.0	634.7	2368.8
49485	6.14	0.17	7.79	0.14	-5061.9	5714.4	-3604.0	4127.4	-2138.9	3046.2	-420.5	2465.7
49486	5.61	0.23	7.07	0.22	-5290.5	5278.6	-4121.4	3831.7	-3065.4	2990.9	-1887.5	2511.4
49487	5.87	0.34	6.74	0.29	-5409.6	4970.2	-4352.5	3758.7	-2345.2	2913.6	-562.8	2431.7
49488	5.25	0.02	5.67	0.01	-5743.7	5210.5	-4337.5	3879.6	-2806.6	3035.7	-1030.2	2434.3
49489	4.66	0.05	4.92	0.03	-5275.1	5991.8	-3818.8	3987.3	-2029.1	2990.0	840.5	2409.8
49489	5.65	0.18	6.87	0.17	-5214.7	5134.6	-3433.4	3800.5	-1804.6	2803.8	-577.1	2141.1
49490	7.25	0.20	7.26	0.13	-5779.1	4939.2	-4254.5	3729.3	-2840.2	2885.1	-348.8	2403.9
49491	4.91	0.36	5.46	0.28	-6240.6	6082.7	-4611.1	3913.4	-3207.1	2954.2	-1914.3	2236.8
49491	5.10	0.32	7.48	0.32	-5187.0	5329.5	-3730.3	3828.3	-2184.9	2831.5	-57.0	2251.6
49491	8.57	0.18	8.23	0.12	-5834.0	5860.5	-4426.4	3799.1	-2893.9	2954.3	195.0	2352.3
49498	6.04	0.07	9.67	0.07	-4504.7	5160.8	-3446.1	3709.1	-2383.7	2865.5	-723.4	2384.5
49504	7.30	0.18	8.07	0.13	-4933.7	5134.0	-3883.6	3692.1	-2947.1	2854.1	-2242.8	2376.3
49505	6.21	0.17	7.61	0.12	-5843.6	5059.2	-4229.4	3643.4	-2850.3	2647.9	-1791.4	1986.1
49506	5.74	0.03	7.71	0.02	-5948.7	5276.9	-4437.3	3835.6	-3152.3	2878.5	-329.4	2281.9
49506	6.77	0.35	8.69	0.26	-5792.6	4456.3	-4581.2	3457.2	-3446.0	2709.9	-2551.1	2212.8
49506	7.42	0.26	8.82	0.19	-5817.8	4511.7	-4444.8	3346.3	-3065.5	2599.5	-1107.2	2019.9
49507	7.18	0.25	8.28	0.18	-4848.9	5456.0	-3745.9	3864.9	-2749.6	2959.5	-1861.3	2394.9
49508	6.49	0.06	8.44	0.05	-5622.4	4629.3	-4248.7	3463.6	-2950.0	2716.5	-6.9	2136.8
49509	6.90	0.08	7.97	0.05	-5610.1	4725.0	-4236.4	3559.0	-3019.1	2811.7	-1878.3	2314.6

Note: (1) Julian dates of IAW watch data in the form “*.1” are used to artificially make a difference between two different spectra under the same MJD on IAW watch web site (as for example 48325.0 and 48325.1)

(2) File names differs according to the observatory/monitoring campaign:

PTG* : Crimean Astrophysical Observatory data

n* : AGN watch data

5* : SAO/GHO data

A* : Asiago data

Continued on next page

Table 2 – continued from previous page

JD-2400000	Flux Hb	Err.	Fl. 5100	Err.	B25%	R25%	B50%	R50%	B75%	R75%	B90%	R90%
49513	6.84	0.52	9.05	0.46	-5573.0	4598.1	-4117.9	3432.4	-2899.8	2685.3	-1840.1	2105.6
49513.7	6.20	0.18	6.84	0.12	-4969.3	5098.4	-3685.4	3656.5	-2278.4	2938.1	555.7	2340.7
49514.7	7.50	0.19	8.18	0.14	-5509.3	4495.0	-4135.3	3412.9	-2836.2	2749.0	-138.7	2169.2
49515.7	8.55	0.18	7.23	0.11	-5275.0	4403.9	-4061.9	3405.3	-2925.2	2658.5	100.0	2161.6
49518.7	6.60	0.26	6.92	0.18	-5199.7	7414.3	-3824.1	3815.6	-889.9	2735.9	423.5	2156.2
49519.4	6.27	0.34	7.30	0.28	-5556.5	4839.1	-4124.9	3590.6	-2797.3	2798.8	323.6	2347.2
49519.5	6.63	0.15	6.79	0.10	-5873.3	4623.0	-4095.4	3207.7	-2632.7	2461.1	-425.1	1964.3
49519.7	9.56	0.21	8.62	0.13	-5406.3	4517.3	-4031.9	3435.3	-2651.0	2688.5	-198.4	2108.9
49520.4	6.52	0.47	8.11	0.41	-5896.7	4927.7	-4281.7	3428.5	-2820.6	2433.1	-779.3	1854.0
49520.7	7.43	0.18	8.05	0.13	-5000.7	4657.2	-3825.1	3448.0	-2053.0	2724.7	-31.7	2123.3
49520.7	8.68	0.47	8.21	0.28	-5257.4	5070.0	-3854.0	3624.3	-2561.6	2784.1	40.0	2305.1
49527.7	7.23	0.24	8.53	0.19	-4462.0	4968.6	-3402.6	3516.9	-2339.3	2673.3	753.9	2312.5
49535.4	9.15	0.24	9.27	0.16	-5845.0	4957.6	-4458.0	3645.4	-3180.8	2813.3	-1781.2	2220.3
49536.3	7.19	0.14	8.87	0.12	-5772.8	5433.1	-4365.5	3737.4	-2951.5	2893.1	16.2	2411.8
49537.7	6.05	0.18	6.90	0.13	-5667.8	4803.8	-4026.3	3595.3	-2612.0	2872.5	-1.5	2271.5
49538.7	7.30	0.20	7.00	0.12	-4795.5	4982.8	-3580.5	3815.8	-1380.7	2902.0	-69.4	2239.1
49539.7	7.46	0.74	8.00	0.46	-5424.4	5585.2	-3887.8	3833.0	-2180.2	2919.2	605.5	2421.9
49545.6	6.76	0.39	6.29	0.22	-5163.1	5356.3	-3868.3	3771.4	-2486.3	2857.6	543.9	2360.3
49548.8	7.03	0.70	7.77	0.50	-5402.9	4860.0	-3784.4	3443.5	-1993.7	2613.3	136.5	2116.3
49553.4	7.23	0.22	10.22	0.18	-5388.1	4779.0	-3956.7	3644.8	-2407.4	2966.3	603.4	2402.0
49556.3	7.14	0.33	8.43	0.26	-4971.6	4436.5	-3914.7	3229.2	231.8	2627.3	828.9	2146.7
49568.4	6.46	0.18	8.90	0.11	-5550.7	4958.6	-3898.3	3709.6	-2791.6	2804.5	-118.5	2240.2
49568.8	6.99	0.83	6.93	0.55	-5066.6	4352.9	-3772.7	3264.8	-2354.7	2541.5	501.7	2060.3
49579.3	9.39	0.10	9.89	0.05	-4477.3	4470.5	-3417.6	3262.0	-2354.1	2659.6	979.0	2298.6
49597.3	7.32	0.33	9.52	0.27	-5204.6	4747.5	-3661.0	3726.0	-2664.4	2933.9	-661.0	2482.1
49597.71	8.32	0.75	8.64	0.50	-5392.9	4294.5	-3877.9	3335.5	-2589.9	2618.3	-352.0	2021.9
49597.7	8.79	0.06	9.25	0.03	-5507.8	5833.2	-4098.8	3651.3	-2683.1	2807.0	168.8	2325.6
49599.3	6.87	0.46	9.39	0.37	-4495.8	4917.8	-3438.2	3589.2	-2376.9	2867.0	949.6	2386.5
49601	8.01	0.35	8.36	0.24	-4607.9	4936.4	-3549.3	3606.0	-2723.3	2762.4	-1894.9	2401.6
49603	7.63	0.27	8.81	0.19	-5319.6	4338.5	-4026.2	3370.7	-2727.2	2767.4	-1303.5	2285.6
49604	7.73	0.31	7.33	0.19	-5401.1	4239.9	-4009.5	3285.6	-2728.1	2571.8	-737.0	2096.9
49608.7	7.30	0.12	8.43	0.08	-5282.0	4893.8	-3738.9	3758.6	-2742.7	3079.5	-628.5	2514.7
49622.6	6.98	0.09	7.78	0.06	-5259.5	4182.1	-3862.2	3224.5	-2692.7	2508.3	133.0	2031.7
49626.6	5.14	3.26	3.86	2.23	-4981.6	4337.1	-3934.5	3141.4	-2883.8	2426.3	-1829.3	1950.4
49626.6	7.36	0.04	6.38	0.02	-5580.9	4932.3	-4038.4	3569.6	-3042.5	2777.5	-2265.6	2325.7
49679	7.12	0.10	8.09	0.08	-5245.1	5617.8	-3922.5	3685.5	-2926.6	2893.4	-1927.4	2441.6
49686	6.60	0.10	8.62	0.08	-5002.9	4682.5	-3488.2	3484.5	-1965.8	2768.0	865.5	2410.3
49713.6	6.53	0.11	8.34	0.10	-4682.9	4653.7	-3517.0	3455.7	-2463.9	2739.1	955.3	2381.5
49743.6	5.86	0.26	8.70	0.24	-4665.2	4530.6	-3486.9	3441.2	-1947.9	2837.6	1154.0	2476.0
49744.5	6.42	0.24	8.67	0.23	-4454.8	4748.4	-3511.7	3416.3	-2684.1	2812.8	1129.1	2330.7
49750.1	7.99	0.22	9.05	0.14	-4785.5	4770.6	-3489.5	3559.4	-2187.9	2955.6	1031.4	2473.4
49751	8.77	0.20	8.44	0.12	-4945.1	5412.8	-3811.8	3911.1	-2755.5	2997.0	-1613.8	2582.5
49752	6.77	0.27	9.56	0.22	-5060.8	5625.9	-3766.0	3707.3	-2465.5	2959.9	646.2	2545.4
49753.6	6.32	0.15	9.50	0.10	-6938.8	5939.3	-4267.3	3654.4	-2863.9	2936.4	-2042.1	2578.0
49758.9	6.71	0.26	10.32	0.24	-4544.3	4899.9	-3483.4	3566.9	-2418.6	2842.4	1158.4	2480.7
49765.9	6.70	0.13	9.19	0.05	-4358.7	4887.1	-3306.4	3446.1	-2015.1	2728.1	940.6	2369.8
49772.5	6.71	0.41	8.94	0.36	-5348.7	5145.5	-3838.7	3470.3	-2554.9	2874.3	856.4	2398.2
49772.9	9.20	0.05	9.53	0.03	-6060.2	5845.4	-3856.5	3688.9	-2456.2	2973.4	1192.1	2497.3
49773.1	6.90	0.76	7.89	0.58	-4661.2	4538.4	-3482.3	3327.6	-1942.8	2724.1	1040.4	2362.5
49775	7.91	0.21	8.38	0.10	-5079.9	4871.2	-3647.0	3623.3	-2539.9	2944.8	1142.8	2606.1
49779	6.87	0.11	7.82	0.08	-5084.0	5199.6	-3979.2	3681.8	-2870.3	2925.7	856.2	2548.4
49779	9.97	0.08	9.75	0.04	-5460.8	4546.2	-3843.2	3463.9	-2705.5	2799.8	816.1	2385.4
49781	8.21	0.27	8.87	0.16	-5283.6	6234.7	-3908.4	3562.9	-2771.1	2898.6	-1792.7	2484.1
49782	8.05	0.09	7.90	0.05	-5291.1	5222.6	-3753.7	3555.4	-2452.8	2808.2	577.4	2393.8
49783.5	7.15	0.13	9.42	0.11	-4972.6	4702.9	-3676.9	3491.5	-2612.6	2887.5	-949.3	2405.2
49783.5	7.42	0.44	9.52	0.36	-5215.5	5133.9	-3921.0	3633.4	-2620.8	2968.9	1066.6	2554.4
49784.5	7.80	0.24	10.50	0.15	-5168.5	4763.3	-3793.0	3514.1	-2573.9	2850.0	-1268.0	2435.6
49784.5	8.28	0.12	13.79	0.00	-6572.0	5379.8	-5145.3	3675.3	-3822.1	2883.2	-2825.9	2431.5
49784	7.80	0.21	10.53	0.13	-4686.9	5027.3	-3402.0	3705.8	-2229.0	2987.4	1198.9	2628.9
49784.9	6.67	0.19	8.24	0.14	-5967.9	5436.0	-4538.5	3731.5	-3434.2	2939.4	-2436.9	2487.7
49788.5	7.39	0.24	11.31	0.15	-5814.0	7428.3	-4383.5	3892.7	-3056.9	3100.0	-1835.6	2648.0
49794	6.69	0.08	10.47	0.06	-5408.7	5222.3	-4307.3	3745.2	-3201.8	2952.8	-2092.2	2500.9
49802	8.00	0.03	9.57	0.02	-4686.9	4524.8	-3521.7	3327.9	-2351.8	2731.2	1185.4	2373.8
49808.9	11.02	0.11	11.74	0.06	-5406.4	4769.4	-3863.3	3634.1	-2756.2	2955.1	1151.6	2503.2
49810.8	8.10	0.02	10.05	0.01	-5078.6	5534.2	-3685.2	3620.0	-2402.1	2905.2	1007.4	2429.6
49810.9	13.96	0.03	10.78	0.01	-4956.4	4735.8	-3660.5	3320.0	-2277.4	2656.1	1002.6	2324.7
49811.8	12.30	0.09	10.56	0.04	-5759.0	6260.2	-3862.3	3697.6	-2689.0	2947.9	1156.4	2499.0
49813.6	7.98	0.40	11.51	0.35	-4972.8	4716.8	-3677.2	3467.6	-2539.0	2803.5	819.8	2306.3

Note: (1) Julian dates of IAW watch data in the form “*.1” are used to artificially make a difference between two different spectra under the same MJD on IAW watch web site (as for example 48325.0 and 48325.1)

(2) File names differs according to the observatory/monitoring campaign:

PTG* : Crimean Astrophysical Observatory data

n* : AGN watch data

5* : SAO/GHO data

A* : Asiago data

Continued on next page

Table 2 – continued from previous page

JD-2400000	Flux Hb	Err.	Fl. 5100	Err.	B25%	R25%	B50%	R50%	B75%	R75%	B90%	R90%
49813	8.28	0.48	10.21	0.34	-5905.7	5916.8	-4048.5	3498.2	-2668.3	2834.4	851.7	2420.3
49818.8	10.93	0.03	12.29	0.01	-4633.6	4565.9	-3454.7	3355.2	-2152.6	2751.6	1068.0	2390.1
49830	11.92	0.05	11.12	0.02	-5320.1	5168.7	-3927.2	3375.2	-2644.5	2660.7	881.8	2304.0
49833.8	9.78	0.14	11.21	0.09	-4717.1	5253.6	-3613.2	3549.9	-2505.3	2871.0	955.9	2419.3
49839.8	10.59	0.04	11.99	0.03	-5007.5	4411.3	-3846.3	3336.8	-2797.3	2622.6	844.5	2266.2
49845.4	8.75	0.31	10.50	0.23	-4515.0	4696.7	-3583.2	3380.4	-2765.4	2784.0	1001.7	2307.7
49846.8	8.89	0.12	11.01	0.09	-4669.9	4166.0	-3727.2	3198.1	-2899.8	2474.3	911.8	2113.0
49853.3	9.27	0.19	10.15	0.13	-4466.6	4488.3	-3536.5	3294.7	-2603.5	2699.6	1157.9	2343.1
49860.8	10.92	0.07	10.61	0.03	-4696.6	4609.9	-3650.9	3296.7	-2718.3	2582.8	1041.7	2226.4
49861.9	7.82	1.15	7.64	0.75	-4865.5	5159.6	-3819.9	3246.9	-3004.0	2532.7	636.4	2057.5
49862.3	7.85	0.09	8.54	0.07	-4774.7	4737.3	-3560.6	3489.2	-2896.3	2697.7	-2341.6	2359.1
49868.8	9.22	0.01	10.56	0.01	-4637.5	4560.2	-3576.9	3349.7	-2749.5	2625.7	823.3	2264.4
49870.4	9.50	0.06	9.74	0.04	-4561.9	4639.5	-3619.0	3428.5	-2791.5	2704.2	-2080.4	2342.7
49871.4	9.04	0.09	9.51	0.06	-4495.8	4335.0	-3553.6	3367.7	-2608.4	2644.3	843.2	2283.2
49871.7	8.09	0.02	9.03	0.01	-4968.0	4708.4	-3688.0	3272.8	-2870.6	2557.5	-2285.4	2200.5
49874.7	8.68	0.07	9.41	0.00	-5724.1	6775.8	-4109.0	3601.9	-3135.6	2689.2	-2484.9	2192.6
49875.4	8.72	0.07	9.58	0.01	-4736.9	4455.7	-3676.9	3245.8	-2849.9	2522.2	-2139.1	2161.1
49878.4	9.35	0.06	9.40	0.04	-4835.2	4706.9	-3673.5	3393.2	-2740.9	2679.0	-2039.5	2322.5
49880	8.57	0.04	9.48	0.02	-4772.1	4659.2	-3830.4	3328.2	-2885.8	2604.6	-2175.4	2123.2
49881.7	9.40	0.03	11.78	0.01	-4743.0	4572.7	-3682.8	3241.3	-2737.3	2638.1	715.8	2156.4
49889.4	6.54	0.04	8.20	0.00	-4841.3	4940.3	-3563.2	3506.3	-2630.2	2791.8	-1928.6	2435.2
49889.7	8.18	0.02	9.14	0.01	-5401.3	6284.4	-3892.7	3528.9	-2960.4	2695.1	-2259.3	2338.5
49891.4	7.67	0.04	8.68	0.02	-4304.4	4291.1	-3361.5	3323.9	-2652.3	2720.9	-2060.0	2239.4
49895.7	8.05	0.01	9.13	0.00	-4648.4	4665.3	-3588.5	3455.1	-2761.4	2851.7	-1932.1	2369.9
49903.3	8.30	0.36	9.54	0.28	-5327.3	5417.7	-3699.2	3619.9	-2647.8	2784.6	1002.3	2427.3
49903.7	7.23	3.17	6.87	2.24	-4989.9	4589.0	-3823.8	3150.5	-2770.4	2553.2	-1948.5	2076.1
49905.8	9.95	0.15	9.38	0.09	-4750.6	4676.4	-3573.6	3345.9	-2628.6	2622.7	702.5	2261.8
49910.7	8.20	0.10	9.95	0.07	-4728.6	5812.1	-3514.2	3538.3	-2516.8	2859.5	-1293.2	2407.8
49917.7	7.56	0.10	9.19	0.08	-4938.6	4621.8	-3658.1	3424.9	-2606.3	2709.1	-1668.2	2351.8
49923.7	7.78	0.09	9.98	0.07	-4758.9	4569.0	-3594.2	3372.1	-2542.0	2656.3	755.6	2299.0
49923.8	8.35	2.84	11.08	2.49	-4800.6	4665.4	-3516.6	3346.1	-2344.6	2628.8	843.1	2270.8
49930.8	7.83	0.14	10.36	0.12	-4909.9	4943.3	-3585.2	3467.3	-2476.8	2788.4	648.8	2336.7
49935.3	7.18	0.27	8.69	0.21	-4787.9	5520.9	-3463.2	3702.6	-2465.9	2910.4	-1576.5	2571.6
49937.7	7.36	0.04	9.01	0.01	-4477.9	4366.8	-3416.1	3277.0	-2350.5	2552.8	629.8	2191.3
49953.3	6.38	0.23	8.14	0.20	-4454.3	4727.0	-3349.6	3479.0	-2351.9	2687.5	886.0	2348.8
49953.7	6.46	0.10	6.86	0.04	-4454.6	4512.7	-3289.9	3317.4	-2003.5	2721.5	1177.7	2364.5
49954.7	7.22	0.71	8.16	0.50	-4231.1	4495.8	-3168.9	3164.5	-2102.8	2561.2	758.8	2199.9
49958.7	8.18	0.61	10.34	0.50	-4521.7	4883.6	-3306.8	3521.9	-2420.0	2956.3	1265.8	2504.5
49966.6	6.50	0.13	8.27	0.08	-4305.0	5021.0	-3257.1	3585.7	-2205.5	2870.5	1090.0	2513.6
49972.6	6.74	0.10	8.81	0.08	-4642.8	4663.7	-3480.7	3350.5	-2430.9	2755.4	-1142.7	2399.0
49981.3	6.32	0.38	9.40	0.36	-4634.6	4693.3	-3353.1	3257.7	-2183.3	2542.4	761.5	2185.4
49981.6	6.53	0.06	10.00	0.06	-4503.1	4824.8	-3221.7	3269.8	-2051.8	2673.8	1011.4	2316.8
49985.6	7.50	0.02	9.98	0.01	-4440.4	4886.1	-3142.6	3432.3	-2076.5	2708.0	-1125.8	2346.5
49986.6	11.36	0.07	9.92	0.03	-4940.4	4623.7	-3542.7	3306.9	-2372.9	2591.0	-1198.4	2114.7
50008.2	6.83	0.07	9.14	0.06	-3769.3	4828.3	-2896.0	3440.0	-2140.4	2351.4	-1565.9	1436.8
50044	7.62	0.12	9.49	0.10	-4028.2	4442.2	-3085.8	3355.2	-2021.8	2632.7	714.4	2272.1
50048.6	10.24	0.09	9.05	0.01	-4158.3	4464.5	-3225.4	3268.6	-2289.6	2672.4	1009.3	2196.3
50052	9.78	0.65	8.02	0.35	-4159.6	4800.8	-3216.5	3349.1	-2270.4	2746.3	586.0	2264.9
50061	7.38	0.13	6.50	0.08	-4140.4	4473.8	-3091.7	3398.4	-2039.3	2683.5	1022.1	2326.7
50064.6	6.69	0.21	5.86	0.15	-4335.4	4367.2	-3174.1	3176.4	-2125.0	2582.7	926.6	2108.6
50069	5.58	0.03	5.02	0.02	-4012.0	4461.9	-3187.2	3253.8	-1649.2	2651.6	135.3	2290.8
50074	4.92	0.02	4.42	0.01	-4461.7	4151.7	-3246.3	3132.1	-2248.2	2567.2	878.6	2115.9
50075	6.28	0.31	5.69	0.22	-4362.1	4440.6	-2980.8	3107.9	-1756.6	2526.6	789.5	2112.1
50078	6.14	0.08	4.93	0.04	-4314.4	4658.0	-3258.3	3240.9	-2116.8	2493.4	673.8	2078.8
50080	4.61	0.04	4.62	0.02	-4436.5	4786.2	-3217.7	3201.6	-2157.3	2453.9	304.2	2039.3
50081	5.44	0.18	5.28	0.13	-4274.7	4532.7	-2974.2	3365.5	-1667.8	2700.6	1127.3	2368.7
50087	6.56	0.02	6.15	0.02	-4552.3	4832.3	-3334.2	3414.1	-2274.4	2500.0	-1456.7	1919.8
50095	5.39	0.07	4.84	0.04	-4975.3	5181.3	-3462.0	3504.3	-2292.6	2788.5	-1353.8	2312.2
50096	5.50	0.18	5.22	0.13	-4686.0	5197.1	-3305.6	3610.5	-2327.3	2861.9	-1591.5	2363.8
50097	5.31	0.14	5.20	0.09	-4916.9	5128.3	-3374.5	3625.0	-2232.9	2793.0	-1414.7	2377.9
50098.1	4.90	0.10	4.31	0.05	-4976.6	5067.4	-3515.7	3647.6	-2292.9	2815.5	-1392.9	2400.3
50101.9	5.13	0.29	7.35	0.31	-5059.7	4981.7	-3517.9	3645.5	-2295.0	2896.5	-1558.8	2398.2
50102	4.65	0.38	5.01	0.28	-4259.6	5190.0	-3094.6	3753.5	-1807.8	2918.7	546.2	2442.7
50104	5.81	0.21	6.33	0.15	-5230.8	4971.4	-3852.5	3552.1	-2712.7	2886.4	-1732.2	2471.2
50105	5.73	0.16	6.73	0.05	-4998.6	5128.5	-3537.9	3625.0	-2315.1	2876.1	-1251.2	2460.8
50107	6.08	0.21	5.86	0.13	-4697.7	5102.1	-3480.0	3682.4	-2502.3	2933.5	-1521.3	2518.3
50108	6.66	0.29	6.71	0.20	-5119.7	5168.2	-3659.9	3748.2	-2437.9	2999.1	-1456.7	2500.7
50109	7.07	0.17	6.03	0.09	-4740.9	5056.3	-3523.5	3637.0	-2382.8	2888.3	-1319.6	2473.2

Note: (1) Julian dates of IAW watch data in the form “*.1” are used to artificially make a difference between two different spectra under the same MJD on IAW watch web site (as for example 48325.0 and 48325.1)

(2) File names differs according to the observatory/monitoring campaign:

PTG* : Crimean Astrophysical Observatory data

n* : AGN watch data

5* : SAO/GHO data

A* : Asiago data

Continued on next page

Table 2 – continued from previous page

JD-2400000	Flux Hb	Err.	Fl. 5100	Err.	B25%	R25%	B50%	R50%	B75%	R75%	B90%	R90%
50110	6.26	0.34	5.93	0.23	-5240.6	5880.5	-3618.9	3706.5	-2315.2	2957.5	-1169.6	2459.3
50111	5.54	0.16	5.83	0.08	-5348.1	4935.2	-3807.7	3515.9	-2504.2	2767.1	-1604.8	2269.0
50112	6.03	0.24	5.98	0.16	-4872.8	4922.4	-3330.2	3586.7	-2270.2	2921.1	-1534.1	2422.8
50119	6.23	0.14	7.30	0.09	-4934.0	5022.8	-3555.0	3687.1	-2414.5	3021.5	-1515.4	2606.2
50122.9	9.06	0.10	8.19	0.02	-4903.3	4555.3	-3503.4	3356.6	-2449.2	2759.0	-1744.4	2401.0
50124	7.84	0.44	7.70	0.30	-4968.3	5559.3	-3570.3	3639.4	-2400.2	2922.5	663.6	2445.6
50124.9	7.57	0.30	6.92	0.18	-4531.8	5110.2	-3475.7	3690.0	-2415.8	2857.6	539.1	2359.3
50126	7.59	0.27	6.85	0.16	-4994.6	4882.3	-3615.1	3463.2	-2474.2	2797.7	809.9	2382.5
50127.6	8.15	0.17	6.11	0.09	-5001.0	4958.8	-3784.2	3456.1	-2562.4	2707.6	390.6	2209.6
50128.4	6.79	0.15	7.64	0.11	-5439.7	4959.8	-3897.2	3484.3	-2679.5	2805.7	-1790.8	2354.2
50128	7.11	0.18	6.12	0.11	-4567.2	4773.0	-3400.9	3455.0	-2230.0	2738.5	-1054.5	2380.8
50129	6.72	0.26	6.12	0.16	-4764.3	5105.2	-3452.5	3643.3	-2244.8	2859.0	518.2	2411.7
50130	7.52	0.60	6.30	0.35	-4762.1	4871.1	-3462.9	3368.9	-2321.5	2703.6	799.0	2288.5
50131	7.81	0.49	6.71	0.29	-4691.3	5029.5	-3554.4	3526.2	-2494.8	2694.3	624.4	2279.2
50132	6.42	0.17	5.63	0.09	-4768.3	5200.8	-3469.0	3530.0	-2490.8	2781.2	-1427.4	2366.0
50133	7.10	0.16	6.76	0.09	-4821.6	4727.7	-3441.1	3309.1	-2299.4	2726.9	-1153.2	2311.8
50134	7.55	0.36	6.58	0.22	-4838.9	4791.6	-3621.4	3456.3	-2643.8	2707.7	-1826.7	2292.7
50134.9	7.23	0.24	5.61	0.14	-4445.0	4778.5	-3388.9	3443.4	-2329.1	2778.0	1038.5	2363.0
50135.5	6.24	0.40	6.33	0.29	-4914.3	4715.1	-3615.6	3296.7	-2393.0	2631.4	562.1	2216.4
50136.9	6.02	0.09	7.05	0.07	-4367.2	4696.2	-3308.2	3487.9	-2245.3	2885.6	-822.2	2404.6
50137	6.30	0.45	5.18	0.24	-4159.9	4582.8	-3110.2	3386.4	-1939.4	2670.8	1007.7	2313.6
50142.9	8.52	0.10	6.95	0.06	-4957.4	4671.0	-3577.5	3252.7	-2436.3	2670.6	1013.7	2338.5
50149.9	6.07	0.16	6.44	0.11	-4980.6	5296.1	-3467.3	3499.0	-2415.1	2783.2	645.7	2306.8
50155	5.46	0.22	7.66	0.22	-4984.7	4691.8	-3471.4	3375.5	-2184.8	2659.9	405.1	2183.8
50155.5	5.30	0.22	7.11	0.21	-4380.8	4684.4	-3203.6	3475.9	-2140.1	2753.1	356.2	2392.4
50161.5	6.10	0.27	8.37	0.26	-4604.9	4699.0	-3310.2	3490.0	-2246.7	2766.9	-1298.2	2285.8
50164.8	6.27	0.15	7.96	0.13	-4338.9	5091.7	-3161.5	3640.0	-2097.8	2796.4	518.5	2435.6
50167	7.18	0.18	7.91	0.14	-4815.1	4736.5	-3419.2	3540.8	-2133.8	2825.6	-960.4	2349.7
50168.9	6.15	0.28	8.51	0.26	-4787.6	5084.4	-3490.1	3499.6	-2186.8	2668.8	601.8	2337.1
50169	6.08	0.14	7.03	0.11	-4289.2	4920.6	-3124.2	3485.2	-1720.1	2770.1	989.6	2413.2
50170	5.81	0.21	6.68	0.16	-4721.9	4817.3	-3342.8	3566.6	-2120.6	2901.7	-319.0	2486.9
50171	6.47	0.16	7.13	0.13	-4532.2	4596.2	-3152.2	3346.3	-1847.4	2681.8	944.4	2267.2
50175.9	9.30	0.01	8.70	0.00	-4491.1	4723.9	-3192.0	3473.3	-2132.2	2808.4	822.4	2393.5
50185.9	7.54	0.07	9.87	0.05	-5369.3	5375.7	-3741.2	3458.4	-2338.5	2742.6	-1046.9	2385.3
50186	8.51	0.32	9.08	0.20	-4594.6	4784.0	-3296.0	3533.1	-2073.3	2868.1	634.4	2370.3
50188.4	6.69	0.17	8.85	0.13	-4782.3	4870.7	-3272.6	3557.7	-1989.1	2843.9	594.5	2368.9
50188.8	7.59	0.58	10.95	0.52	-4678.2	5113.9	-3298.8	3612.1	-1994.7	2781.0	630.8	2366.3
50189	8.30	0.27	9.30	0.20	-4285.4	4899.1	-3108.4	3569.7	-1689.9	2726.8	1048.0	2366.3
50190	8.38	0.16	9.22	0.11	-4612.5	4848.1	-3232.7	3430.7	-1764.7	2766.0	945.5	2351.3
50191.1	8.22	0.26	9.02	0.17	-4242.6	4839.0	-2962.0	3405.5	-1793.0	2691.3	913.2	2334.9
50191	8.23	0.19	10.02	0.15	-4780.1	4762.0	-3319.2	3344.5	-1851.2	2679.7	859.2	2265.0
50192	8.67	0.18	9.10	0.12	-4367.6	4852.2	-3149.2	3434.4	-1844.0	2686.5	866.1	2271.8
50193	7.94	0.30	9.02	0.21	-4570.4	4892.4	-3190.3	3391.5	-1803.8	2726.7	906.3	2312.1
50194	7.73	0.29	8.25	0.19	-4350.7	4701.9	-3132.3	3451.3	-1663.5	2786.4	1048.0	2371.6
50198.1	7.38	0.12	7.42	0.07	-4190.0	4920.9	-3022.3	3602.3	-1732.6	2885.5	863.8	2408.6
50198	8.03	0.09	9.79	0.01	-4631.0	4583.4	-3332.0	3249.7	-2027.2	2585.0	847.1	2170.3
50199	8.85	0.21	7.82	0.12	-4292.3	4428.9	-3073.5	3262.4	-1686.2	2597.9	943.0	2266.2
50200.4	7.84	0.04	8.39	0.02	-4454.9	4679.4	-3236.7	3345.5	-1686.5	2597.8	860.2	2266.1
50211.3	7.94	0.31	8.12	0.23	-4257.8	4693.6	-3197.7	3363.9	-1896.8	2761.5	722.0	2280.4
50212.9	9.43	0.15	8.45	0.02	-3952.0	4658.4	-2787.1	3464.2	499.3	2868.9	1208.2	2393.5
50213.1	8.35	0.26	8.06	0.18	-4405.3	4562.8	-3187.0	3229.5	-1718.4	2565.1	827.8	2233.4
50213.4	8.11	0.26	7.48	0.15	-4012.2	4461.7	-2951.2	3133.2	-936.8	2531.2	852.0	2170.6
50215.4	7.72	0.44	7.77	0.32	-4172.9	4410.0	-3113.4	3323.6	-1813.3	2601.6	565.0	2121.2
50216.9	7.32	0.07	8.78	0.05	-4084.1	4389.8	-3023.1	3181.8	-56.0	2579.6	780.1	2098.7
50218	6.41	0.10	6.39	0.06	-4022.1	4327.4	-3079.6	3120.3	-1423.0	2518.6	481.6	2158.2
50219	7.63	0.20	6.97	0.12	-4425.1	4376.5	-3206.8	3293.3	-1819.9	2545.6	231.4	2131.1
50220.1	7.35	0.13	6.03	0.06	-5242.0	4625.1	-3852.2	2957.9	-2572.5	2127.8	356.5	1772.7
50220.8	8.75	0.03	7.83	0.00	-4164.4	4643.1	-3026.7	3226.4	-1393.7	2562.1	907.5	2147.6
50221	7.25	0.12	7.08	0.08	-4607.8	4523.8	-3227.2	3190.3	-1922.0	2525.8	623.3	2111.2
50222	6.97	0.10	6.37	0.06	-4291.8	4681.6	-3154.2	3347.6	-1767.0	2682.7	861.9	2267.9
50223	7.34	0.19	6.88	0.12	-4487.2	4397.9	-3268.9	3231.2	-2127.3	2566.5	746.2	2151.9
50224.4	7.04	0.48	7.01	0.34	-4411.6	4559.1	-3274.3	3225.4	-1969.3	2560.8	905.6	2229.0
50225	6.56	0.03	5.41	0.01	-4263.8	4562.8	-3204.2	3234.2	-1666.8	2512.0	-121.4	2151.6
50226.4	6.68	0.03	5.73	0.01	-4554.1	4577.4	-3254.9	3244.0	-2031.8	2579.4	841.9	2164.8
50226	6.66	0.27	7.36	0.21	-4489.7	4393.5	-3271.6	3143.9	-2130.2	2479.6	660.2	2065.1
50227.8	6.55	0.18	7.48	0.14	-4258.5	4327.9	-3198.6	3120.6	-1898.0	2398.5	720.3	2038.1
50230	7.94	0.22	6.41	0.13	-4235.4	4709.4	-3073.7	3279.3	-1439.5	2685.3	1028.6	2211.1
50231	6.77	0.21	6.06	0.13	-4638.3	4658.7	-3258.0	3241.5	-1707.7	2411.0	427.0	1996.6

Note: (1) Julian dates of IAW watch data in the form “*.1” are used to artificially make a difference between two different spectra under the same MJD on IAW watch web site (as for example 48325.0 and 48325.1)

(2) File names differs according to the observatory/monitoring campaign:

PTG* : Crimean Astrophysical Observatory data

n* : AGN watch data

5* : SAO/GHO data

A* : Asiago data

Continued on next page

Table 2 – continued from previous page

JD-2400000	Flux Hb	Err.	Fl. 5100	Err.	B25%	R25%	B50%	R50%	B75%	R75%	B90%	R90%
50233.8	6.99	0.09	7.23	0.06	-4852.0	4608.8	-3390.8	3108.2	-2085.9	2443.6	293.9	1946.2
50240	6.64	0.12	6.18	0.06	-4679.5	4765.4	-3281.7	3329.6	-2228.9	2733.4	833.3	2257.2
50241.8	6.10	0.38	8.34	0.36	-4913.5	4796.1	-3534.0	3377.8	-2393.1	2546.6	-1247.7	2049.0
50242	6.96	0.14	6.35	0.07	-4350.0	5087.2	-3303.1	3652.7	-2135.5	2818.9	685.6	2343.6
50245.4	6.05	0.30	7.40	0.27	-4876.7	4915.3	-3497.3	3330.3	-2356.6	2499.5	-1211.4	2084.9
50247.4	6.15	0.31	7.59	0.27	-4847.1	4945.2	-3630.4	3609.8	-2490.2	2695.2	-1673.1	2197.5
50247	7.17	0.10	7.23	0.07	-4266.5	4686.7	-3206.1	3356.8	-2023.5	2513.5	-955.2	2032.7
50248.8	6.59	0.23	8.18	0.19	-4497.2	4693.0	-3319.5	3362.8	-2255.6	2639.7	-1306.7	2158.6
50250	6.63	0.10	7.33	0.01	-4675.8	4741.8	-3398.3	3429.3	-2349.0	2597.0	-1413.2	2122.4
50251	7.70	0.67	7.23	0.43	-4781.4	5089.6	-3321.4	3588.2	-2344.1	2840.2	-1363.5	2342.6
50252	7.68	0.10	7.92	0.02	-4878.5	5158.3	-3337.3	3489.8	-2278.3	2659.0	344.8	2161.6
50253	6.79	0.12	8.70	0.10	-4805.0	5321.7	-3506.9	3485.3	-2611.2	2571.2	504.0	2156.6
50253.8	7.83	0.17	7.33	0.09	-4635.3	5052.6	-3237.1	3615.2	-2184.0	2779.9	-891.9	2184.6
50254	7.77	0.17	7.75	0.11	-4858.3	5178.6	-3479.8	3510.1	-2421.3	2679.3	694.6	2264.7
50256.5	7.40	0.37	8.77	0.30	-4877.9	5242.9	-3499.3	3490.7	-2440.8	2659.9	510.3	2162.5
50256.9	8.31	0.10	7.71	0.07	-4749.0	5125.8	-3369.8	3540.5	-2310.7	2709.5	394.7	2129.2
50258.1	6.30	0.08	9.26	0.08	-4838.4	5451.7	-3378.2	3531.7	-2400.8	2617.8	-1583.8	2203.2
50258	8.47	0.05	8.42	0.00	-4725.2	4981.4	-3508.7	3646.7	-2450.3	2815.6	-1388.1	2235.1
50259	6.79	0.29	7.38	0.22	-4195.2	4868.5	-3136.1	3539.6	-2191.5	2817.3	660.4	2336.6
50262	7.69	0.10	10.53	0.08	-4619.3	4429.6	-3482.8	3179.5	-2505.1	2431.9	-211.3	1934.5
50262.8	7.77	0.48	8.12	0.36	-4226.0	5251.1	-3088.3	3331.6	-1700.7	2583.9	681.2	2169.2
50270	9.06	0.27	8.81	0.17	-4292.7	5286.4	-3009.7	3608.9	-2073.1	2773.5	872.8	2297.2
50273	7.49	0.08	10.30	0.02	-4771.7	4689.9	-3554.4	3272.4	-2577.0	2524.6	-1596.4	2027.1
50273.8	7.96	0.29	9.07	0.21	-4666.4	5464.7	-3449.1	3627.4	-2553.3	2713.0	562.4	2215.3
50275.3	6.46	0.05	8.69	0.05	-4845.4	5796.5	-3300.7	3637.8	-2303.4	2620.6	820.7	2169.7
50275.3	7.59	0.07	7.99	0.05	-4237.9	4704.8	-3060.9	3376.4	-2115.9	2654.4	-454.9	2173.9
50275	9.39	0.39	12.29	0.33	-4049.9	4576.3	-2999.8	3499.3	-2180.4	2902.7	882.8	2426.2
50276.4	6.95	0.20	10.58	0.18	-4640.2	5291.0	-3372.1	3612.7	-2462.3	2684.3	836.1	2313.8
50277.4	6.70	0.22	9.07	0.19	-3912.9	4434.9	-2970.6	3348.5	-2143.6	2626.5	351.2	2146.0
50280	10.41	0.07	11.49	0.02	-4472.5	4112.1	-3412.8	3266.7	-2586.0	2423.6	-806.5	1822.8
50280.7	10.09	0.19	10.27	0.12	-4021.1	4742.5	-3085.9	3543.2	-2147.9	2706.6	92.0	2229.5
50281	9.86	0.51	9.69	0.32	-4566.7	4982.8	-3430.2	3564.2	-2371.0	2732.8	499.5	2318.0
50282	8.97	0.37	9.87	0.26	-4690.0	4857.1	-3472.5	3355.6	-2413.3	2607.7	704.7	2193.0
50283	9.51	0.58	9.50	0.36	-4351.3	4620.7	-3213.9	3370.1	-2072.1	2622.1	554.2	2207.4
50284.4	9.82	0.66	10.22	0.42	-4477.7	4658.6	-3422.0	3241.3	-2444.2	2410.6	426.3	1996.1
50285.4	7.20	0.03	9.11	0.00	-4416.9	4971.4	-3361.1	3469.5	-2383.2	2721.2	817.5	2306.4
50285	6.54	0.27	9.09	0.25	-4147.8	4317.6	-3087.9	3351.7	-2379.2	2509.1	-362.0	1788.8
50286.4	7.97	0.33	10.43	0.28	-4009.1	4347.2	-3065.8	3380.4	-2119.6	2657.3	-217.9	2056.0
50287	9.19	0.44	9.57	0.29	-4142.2	4568.7	-3081.9	3360.4	-2136.2	2637.8	241.3	2157.0
50288	9.52	0.18	9.63	0.12	-4327.2	4646.6	-3352.4	3312.4	-2455.9	2647.6	-1474.9	2149.9
50289	9.08	0.38	10.01	0.27	-4285.3	4773.9	-3310.2	3272.7	-2413.6	2607.9	952.2	2193.1
50315.3	7.61	0.25	8.95	0.21	-4119.5	4730.9	-3124.3	3256.5	-2237.0	2578.4	889.8	2127.2
50336.6	8.73	0.76	10.66	0.55	-4208.9	4263.4	-3148.2	3055.5	-2320.5	2453.4	-658.3	1972.6
50339.2	7.85	0.08	10.13	0.06	-4114.8	4963.1	-3119.6	3374.4	-2232.2	2583.1	-1453.6	2131.9
50344.2	7.27	0.19	10.10	0.17	-4028.2	4559.8	-3086.1	3352.3	-2140.9	2509.9	-1074.1	2029.5
50350.6	8.26	0.08	11.57	0.06	-3992.6	4597.2	-2932.2	3268.9	-2104.9	2546.8	-1156.6	2186.4
50358.6	8.52	0.00	10.95	0.00	-4001.9	4479.9	-3071.3	3049.5	-2254.6	2336.9	-1552.8	1981.2
50362.2	8.06	0.06	11.23	0.05	-4008.1	4731.8	-2901.8	3257.4	-2124.9	2466.5	1115.4	2128.1
50372.2	8.53	0.12	11.75	0.09	-3915.0	4437.8	-2972.2	3109.7	-2144.7	2267.7	-1077.4	1907.5
50373.2	8.79	0.24	12.02	0.20	-3787.9	4326.2	-2962.7	3119.2	-2135.2	2277.1	-1305.5	1796.9
50434	9.06	0.16	9.19	0.10	-4032.8	4434.2	-3208.6	3227.2	-2500.4	2505.3	-1908.8	2144.9
50437	8.25	0.11	8.48	0.07	-4638.1	3956.5	-3340.9	2748.0	-2512.5	2025.2	-1919.4	-13.3
50451	9.69	0.21	6.61	0.03	-4234.3	4164.0	-3097.7	2767.2	-2299.5	1955.4	-1728.0	108.0
50458	5.78	0.07	5.62	0.03	-4280.3	4607.9	-3305.7	3025.1	-2572.6	2195.4	-2082.9	1367.9
50459	6.67	0.24	5.62	0.15	-3998.5	4060.2	-3023.3	2812.6	-2289.9	2232.2	-1718.1	1818.2
50465	6.87	0.22	6.16	0.14	-4135.4	4085.9	-3160.7	2755.2	-2346.0	2092.1	-1774.4	1678.4
50479	11.88	0.14	6.90	0.06	-4010.5	4213.3	-3035.6	2716.3	-2220.6	2136.2	-1730.5	1805.1
50480	4.81	0.12	4.56	0.06	-4293.1	5235.3	-3286.6	2939.1	-2389.1	2139.6	-1826.7	1569.7
50481	4.71	0.08	4.74	0.05	-3791.3	3939.7	-3059.7	2692.6	-2244.7	2112.4	872.8	1864.1
50482.1	8.09	1.17	7.69	0.80	-3901.5	3993.0	-3088.8	2745.8	-2355.5	2165.5	-1947.3	1751.6
50482	6.64	0.19	5.27	0.12	-3744.6	4071.6	-3012.8	2823.9	-2279.2	2243.4	-1707.4	1912.2
50483	5.22	0.20	4.82	0.14	-4189.7	4395.4	-3129.9	3067.8	-2421.3	2346.1	-1948.0	1985.9
50485	5.39	0.18	4.58	0.12	-3777.8	4038.7	-2964.6	2790.9	-2230.8	2210.4	-1658.8	1879.1
50486	9.83	0.05	5.98	0.01	-3847.9	4213.5	-2953.8	2965.5	-2220.3	2302.0	-1648.5	1970.9
50487	4.77	0.22	4.19	0.15	-5355.7	4824.3	-3644.8	2830.7	-2613.5	2130.1	-2039.1	1664.0
50490	4.34	0.16	4.51	0.13	-3794.5	4186.1	-2981.6	2772.0	-2248.0	2191.7	-1594.4	1860.6
50493	5.07	0.71	5.06	0.59	-3662.5	4153.7	-2930.8	2906.0	-2278.8	2242.6	-1788.8	1911.5
50494	4.07	0.04	4.11	0.01	-4265.3	4227.7	-3202.0	2775.3	-2253.7	2172.2	-1778.3	1810.9

Note: (1) Julian dates of IAW watch data in the form “*.1” are used to artificially make a difference between two different spectra under the same MJD on IAW watch web site (as for example 48325.0 and 48325.1)

(2) File names differs according to the observatory/monitoring campaign:

PTG* : Crimean Astrophysical Observatory data

n* : AGN watch data

5* : SAO/GHO data

A* : Asiago data

Continued on next page

Table 2 – continued from previous page

JD-2400000	Flux Hb	Err.	Fl. 5100	Err.	B25%	R25%	B50%	R50%	B75%	R75%	B90%	R90%
50495	6.11	0.28	5.03	0.19	-3963.1	3847.7	-2987.7	2766.8	-2172.4	2186.3	-1600.3	1855.2
50499	6.98	0.34	5.32	0.21	-4234.4	4469.6	-3056.9	2901.0	-2111.6	2299.9	-1519.2	1819.8
50506	5.00	0.13	6.50	0.13	-5237.8	4479.4	-3983.2	2954.9	-2952.7	1903.9	-2263.7	508.2
50509.1	5.35	0.34	6.06	0.32	-3860.7	4537.6	-2721.8	2955.3	-1905.7	2125.9	-1251.2	1546.6
50509	3.83	0.18	4.51	0.13	-4425.1	5071.3	-3358.4	3366.4	-2406.9	2517.5	-1691.3	2154.4
50514	9.57	0.23	5.12	0.09	-4581.5	5209.3	-3522.4	3756.5	-2696.1	2791.8	-1986.0	2190.4
50519	3.86	0.03	4.87	0.00	-6156.8	6221.4	-3996.0	3049.6	-2508.3	1766.8	-1589.1	953.3
50520.1	4.20	0.26	4.75	0.12	-4783.6	5245.0	-3289.0	3235.9	-2365.6	2295.1	-1671.1	1708.5
50520	5.80	0.04	6.11	0.03	-3912.9	4570.8	-2773.8	3237.1	-1875.8	2323.7	-1302.8	1826.6
50521	3.50	0.05	4.72	0.04	-4134.5	5006.9	-2996.8	2840.6	-2018.2	2177.2	689.8	1846.0
50522	5.75	0.10	5.44	0.08	-4213.0	4592.8	-2994.1	3010.2	-1933.6	2097.8	-1279.1	1683.9
50527	7.28	0.11	5.23	0.05	-4388.0	5156.7	-2975.6	3223.4	-1911.9	2261.3	-1081.9	1302.3
50534	8.60	0.30	7.36	0.13	-6145.8	5502.2	-3875.1	3042.9	-2504.3	2111.3	-1701.7	719.1
50548	5.13	0.12	4.69	0.07	-5389.8	6970.5	-3901.1	3185.4	-2866.0	2129.3	-2058.5	1544.2
50549.1	5.96	1.77	5.89	1.09	-5394.7	6348.2	-3564.9	3163.9	-2415.5	2343.8	-1608.3	943.0
50549	5.98	0.04	7.13	0.03	-4210.0	4848.2	-3235.0	3097.8	-2420.1	2267.7	-1848.4	1853.6
50550	6.69	0.79	5.98	0.49	-4043.7	5518.0	-3068.6	3182.1	-2253.6	2352.1	451.9	1855.3
50551	5.88	0.14	5.25	0.01	-4188.2	4953.6	-3213.3	3202.7	-2480.0	2372.4	306.7	1875.3
50552	6.95	0.11	5.50	0.07	-4236.1	5321.5	-3098.7	3152.8	-2283.6	2405.6	-1629.8	1991.4
50553	5.91	0.08	5.55	0.06	-4578.2	5638.7	-3198.0	2968.7	-2464.6	2304.9	-1893.0	1973.5
50555	8.35	0.13	6.64	0.05	-6153.5	5128.8	-4166.6	2893.8	-2804.3	2060.0	-1983.8	675.3
50567	5.14	0.13	5.00	0.09	-4586.3	7152.5	-3291.4	3148.4	-2464.4	2305.8	-1753.7	1945.4
50568	5.82	0.11	4.99	0.08	-4304.9	5085.3	-3248.8	3084.0	-2515.5	2336.9	-1943.9	1922.6
50569	5.19	0.14	4.20	0.08	-4383.8	5422.2	-3246.7	2919.9	-2431.8	2256.0	-1860.0	1924.7
50574	4.90	0.17	5.16	0.15	-4436.1	5787.7	-3217.8	2866.6	-2321.1	2202.9	-1585.5	1954.4
50575.1	6.76	0.15	5.58	0.10	-5881.9	5319.9	-3834.7	2859.1	-2576.7	1926.9	-1773.3	649.8
50575	7.75	1.28	5.00	0.68	-4304.7	4521.9	-3127.1	2832.0	-2299.9	1990.6	-1589.1	673.1
50576.1	7.14	0.04	5.71	0.02	-4060.0	4921.1	-3165.8	2754.3	-2187.2	2090.7	933.0	1759.5
50576	4.26	0.95	4.77	0.79	-4475.4	5434.7	-3180.7	2776.0	-2117.2	2054.9	-1524.8	737.4
50577	5.62	0.09	5.69	0.07	-4991.1	5863.3	-3464.4	2962.4	-2639.0	2121.5	-2048.1	1522.3
50578	5.28	0.05	5.97	0.00	-4594.0	5960.6	-3213.5	2954.5	-2480.1	2207.6	-1990.1	1793.5
50580	5.40	0.17	5.50	0.08	-4360.4	5364.2	-3141.6	2612.8	-2407.9	2032.4	-1999.6	1618.5
50581	5.69	0.08	5.93	0.06	-4369.4	5605.2	-3150.8	2851.9	-2417.2	2188.2	-1927.1	1774.1
50582	5.92	0.19	6.40	0.14	-4698.4	5766.3	-3399.9	2679.8	-2585.6	1933.8	-2095.8	1602.8
50585	7.17	0.03	6.56	0.01	-4545.9	6008.6	-3246.8	3002.6	-2431.9	2172.8	-1778.4	1841.6
50591	7.89	0.34	7.60	0.23	-5293.9	5377.7	-3694.3	2908.3	-2776.4	2089.5	-2086.1	-5.6
50598.1	5.74	0.07	6.45	0.05	-4215.0	5012.2	-3158.5	3094.1	-2261.6	2098.1	-1607.6	610.3
50598	5.17	0.04	5.01	0.03	-5004.3	6023.8	-3519.0	2848.2	-2601.3	1913.6	-2141.3	-525.9
50600	5.72	0.05	6.19	0.04	-4386.6	4797.9	-3091.6	2866.2	-2146.3	1905.0	-1435.4	707.7
50601	5.46	0.29	6.16	0.24	-4132.5	4703.0	-3071.8	3011.4	-2244.1	1928.9	-1651.5	491.6
50602	6.36	0.05	5.78	0.01	-4157.7	4791.8	-3097.7	3100.9	-2152.4	1898.9	-1560.1	701.6
50603	6.12	0.22	6.34	0.17	-4416.1	5558.0	-3197.6	2971.0	-2300.8	2141.2	-1810.5	241.2
50604.1	5.91	0.09	6.28	0.07	-4751.8	5286.0	-3486.6	2921.6	-2563.0	1863.6	-1868.4	341.9
50604	8.02	0.07	7.08	0.04	-4076.4	5071.0	-3019.4	3069.5	-2285.5	2073.7	-1713.3	174.2
50605.1	5.80	0.20	6.35	0.15	-4147.0	4913.8	-3090.4	3245.9	-2275.0	2083.9	-1702.9	596.4
50605	5.27	0.17	5.50	0.13	-4214.2	4596.6	-3238.9	3013.1	-2423.7	2183.0	-1933.5	117.7
50608	6.40	0.21	7.35	0.17	-4675.7	5067.3	-3350.6	3025.5	-2463.9	2009.7	-1797.1	324.2
50609	5.47	0.09	5.81	0.06	-4435.2	5787.7	-3216.9	3033.0	-2483.6	2369.0	-1993.7	1789.1
50610	5.42	0.38	5.77	0.27	-4185.6	4875.1	-3210.4	3124.2	-2395.3	2128.1	-1823.3	1714.1
50615	8.09	0.05	7.09	0.03	-4180.4	5044.5	-3124.2	3542.7	-2390.7	2379.8	-1819.0	1965.5
50623	9.38	0.04	6.54	0.02	-5072.7	4545.5	-3586.6	2901.4	-2553.3	1849.2	-1862.5	451.9
50627	5.29	0.40	4.79	0.26	-4769.3	4633.5	-3509.6	2987.2	-2590.1	1816.7	-2013.9	301.8
50628.1	9.60	0.59	7.62	0.35	-4203.0	5526.8	-3146.5	3272.6	-2412.8	2442.0	-1922.7	1944.6
50628	6.75	0.18	5.69	0.11	-4035.3	4778.3	-3059.7	3194.3	-2325.9	2363.9	-1835.6	1535.9
50630	5.84	0.20	5.14	0.13	-4722.0	5544.3	-3310.5	3125.3	-2602.2	2283.3	-2129.1	1563.3
50631	4.77	0.13	5.01	0.08	-4262.6	4627.3	-3125.0	3044.2	-2309.7	2214.3	-1737.7	149.4
50633	5.62	0.12	5.50	0.08	-4142.8	4501.7	-3167.4	2918.9	-2352.2	2006.3	-1780.1	1675.2
50635.1	5.14	0.06	4.96	0.02	-5045.5	4910.8	-3561.6	3033.3	-2644.7	2098.9	-1955.2	702.8
50635	9.21	0.06	6.58	0.02	-4106.9	4621.2	-3131.6	2954.9	-2316.3	2290.9	-1744.2	143.0
50636	6.21	0.18	5.80	0.13	-4144.2	4667.3	-3087.4	3000.6	-2271.9	2087.8	-1699.7	1673.8
50637	5.31	0.06	5.08	0.04	-4165.0	4729.8	-3189.7	3228.9	-2537.7	2481.3	-1966.0	1983.9
50639	5.67	0.17	5.60	0.11	-4065.7	4665.3	-3008.5	2998.5	-2274.4	2085.6	-1702.2	185.7
50641.1	8.52	0.57	7.36	0.36	-4155.2	4738.7	-3098.5	3154.9	-2446.4	2324.6	-1956.4	1579.3
50641	6.78	0.13	5.53	0.07	-4248.2	4712.5	-3142.7	3125.0	-2366.4	2221.5	-1810.7	1658.2
50642	6.89	0.43	5.21	0.11	-4503.9	5273.0	-3328.6	3099.4	-2621.2	2258.4	-2030.4	1778.8
50643	6.90	0.03	5.35	0.01	-4208.2	5354.6	-3314.4	3267.9	-2744.2	2354.2	-2336.3	1857.0
50655	7.55	0.40	5.96	0.26	-4213.8	5011.9	-3157.5	3094.1	-2423.9	2264.1	-1933.9	-212.5
50659	6.13	0.06	4.14	0.01	-4514.3	5276.4	-3337.4	3099.8	-2628.9	2257.5	-2155.7	1657.3

Note: (1) Julian dates of IAW watch data in the form “*.1” are used to artificially make a difference between two different spectra under the same MJD on IAW watch web site (as for example 48325.0 and 48325.1)

(2) File names differs according to the observatory/monitoring campaign:
 PTG* : Crimean Astrophysical Observatory data

n* : AGN watch data
 5* : SAO/GHO data
 A* : Asiago data

Continued on next page

Table 2 – continued from previous page

JD-2400000	Flux Hb	Err.	Fl. 5100	Err.	B25%	R25%	B50%	R50%	B75%	R75%	B90%	R90%
50664.1	4.63	0.11	4.08	0.07	-4247.7	4810.7	-3109.9	3060.2	-2294.6	2131.0	-1477.0	1898.8
50664	4.44	0.24	4.46	0.16	-4310.5	4824.4	-3086.2	3111.7	-2416.3	2202.2	-1968.9	1408.6
50687	4.94	0.19	6.10	0.17	-4459.0	5177.4	-3243.6	3021.8	-2356.6	2118.6	-1800.8	1105.9
50697.1	6.34	0.03	6.02	0.02	-4147.9	4798.0	-3088.4	3469.2	-2261.8	2026.1	-1669.9	351.3
50697.2	4.68	0.09	6.53	0.08	-4344.4	5295.6	-3239.3	3478.6	-2352.3	2235.7	-1796.5	773.3
50699	6.28	0.48	7.32	0.41	-3856.5	4620.8	-3031.3	3412.3	-2322.1	2328.7	-1729.9	650.9
50714	6.29	0.15	7.60	0.13	-4626.6	5275.6	-3686.3	3823.7	-2861.1	2619.0	-2270.3	1778.6
50729	5.77	0.23	7.80	0.22	-4361.8	4591.5	-3183.4	3140.9	-2355.7	1817.3	-1763.1	260.6
50775	9.87	0.04	9.29	0.02	-3914.4	4315.8	-2971.7	2988.6	-2262.7	1907.0	-1789.1	709.7
50777	7.40	0.08	9.46	0.07	-4819.8	4293.2	-3320.2	2873.1	-2509.5	1577.1	-1929.1	-64.2
50806	6.21	0.17	6.82	0.12	-3980.5	4377.5	-3037.0	2807.6	-2209.0	1845.6	-1734.9	288.8
50814	8.89	0.15	9.26	0.09	-4205.4	4268.4	-3149.1	3019.5	-2415.5	1941.1	-1843.8	454.4
50815	8.33	0.10	9.11	0.06	-4217.8	4841.5	-3080.0	3007.7	-2346.2	2012.1	-1856.0	195.3
50816	7.24	0.11	8.12	0.06	-4190.8	4785.2	-3052.9	3118.1	-2319.1	2122.2	-1828.8	222.5
50828	10.05	0.03	9.18	0.01	-4348.9	4455.4	-3130.2	2956.2	-2233.3	1960.8	-1742.9	144.4
50834.1	9.92	0.30	8.98	0.18	-4193.6	4448.5	-3055.7	3032.3	-2240.2	2036.7	-1668.0	384.5
50834	6.84	0.05	8.67	0.04	-5000.1	4537.3	-3393.2	3122.5	-2471.0	1714.3	-1777.5	196.2
50837	9.18	0.68	9.86	0.44	-4545.7	4946.5	-3208.0	3115.2	-2312.9	2203.7	-1752.0	162.8
50838.1	9.00	0.15	10.02	0.09	-4998.6	5485.7	-3276.6	3359.4	-2238.5	2067.3	-1660.3	547.4
50838	8.99	0.07	11.06	0.04	-4436.4	4954.8	-3298.8	3202.6	-2565.2	2288.9	-2075.2	1377.9
50839	8.98	0.16	9.15	0.10	-4064.7	4914.6	-2926.3	3163.7	-2273.9	2167.7	-1783.6	21.0
50840	9.03	0.07	9.51	0.05	-4326.1	4645.7	-3107.3	3228.7	-2292.0	2232.4	-1801.7	496.9
50841	10.02	0.20	10.04	0.13	-4194.1	4781.5	-3056.2	3197.6	-2240.8	2118.6	-1750.5	466.1
50842.1	10.16	3.71	11.17	2.36	-4340.0	5049.7	-3121.2	3214.7	-2387.6	2218.5	-1897.4	71.1
50842	9.64	0.25	10.56	0.16	-4208.0	5017.9	-2988.7	3183.2	-2336.5	2270.0	-1846.3	-42.1
50843	8.18	0.26	9.54	0.18	-4170.5	4903.9	-2954.2	3315.9	-2066.5	2299.3	-1621.6	276.4
50845	7.69	0.15	9.42	0.10	-4173.0	4554.3	-3034.8	2971.3	-2219.2	1975.7	-1646.9	323.6
50847	8.18	0.25	9.34	0.18	-4029.0	4700.5	-3053.4	3283.3	-2238.1	2038.3	-1584.1	633.6
50867.1	10.23	0.29	8.12	0.16	-4008.2	4555.0	-2951.1	3138.5	-2217.1	2308.3	-1726.7	654.8
50867	8.17	0.38	8.91	0.28	-4134.4	4508.9	-2996.3	3092.5	-2262.4	2096.7	-1690.3	361.9
50868.1	8.00	0.43	9.36	0.34	-3975.8	4590.1	-2918.4	3006.8	-2265.8	2259.7	-1775.4	-52.7
50868	7.84	0.47	8.41	0.31	-4573.4	4574.6	-3123.9	2973.4	-2228.4	2176.0	-1667.4	135.2
50870	6.71	0.11	9.42	0.08	-3680.9	4555.9	-2737.4	3107.1	-2146.3	2265.2	-1553.9	230.2
50871	7.26	0.27	10.11	0.21	-3661.9	4408.6	-2766.8	3076.1	-2114.1	2246.3	-1623.7	346.2
50872	10.17	0.22	9.24	0.11	-3895.1	3918.7	-3000.7	3003.5	-2348.6	2505.4	-1940.3	2173.9
50874	10.85	1.52	11.29	0.97	-4392.2	4745.1	-3092.2	3244.4	-2358.4	2331.0	-1868.2	1337.6
50875.1	10.05	0.06	9.32	0.04	-4454.8	4391.6	-3190.5	2977.3	-2267.6	1921.0	-1689.4	518.3
50875	11.06	0.06	10.42	0.03	-4317.4	5490.2	-3098.7	3236.7	-2365.1	2489.3	-1956.8	1992.0
50876.1	9.87	0.10	10.67	0.06	-4458.3	4761.3	-3402.6	3426.9	-2506.4	2595.7	-1853.0	2015.3
50876	8.96	0.37	9.95	0.23	-4125.0	4687.0	-2905.3	3020.1	-2089.3	2107.3	-1598.6	866.9
50877	7.10	0.08	8.90	0.04	-3850.2	4627.1	-2788.8	3177.5	-1960.7	2214.9	-1486.4	1135.6
50878	7.81	0.23	10.26	0.18	-4110.4	4283.6	-2972.1	3034.4	-2238.1	2204.5	-1665.9	1211.6
50885	9.42	0.12	12.19	0.04	-4214.4	4431.5	-3157.4	3014.7	-2341.8	2184.4	-1769.5	1604.6
50892	8.82	0.31	9.81	0.22	-5833.9	4912.0	-3326.6	3035.7	-2409.6	2218.4	-1835.0	11.2
50893	9.07	0.11	9.43	0.07	-3964.7	4601.6	-2907.3	3101.4	-2173.0	2188.2	-1600.6	370.2
50903	7.04	0.27	9.02	0.20	-3906.1	4661.6	-2848.4	3244.3	-2195.7	2247.9	-1705.2	1007.0
50905.7	8.90	0.82	9.15	0.51	-4435.5	4622.1	-3379.2	3204.4	-2319.2	2456.5	718.6	2124.7
50905	7.94	0.43	9.94	0.35	-3900.5	4582.4	-2843.0	3165.7	-2108.7	2335.5	-1536.3	1342.2
50906.1	8.22	0.49	10.39	0.40	-4145.1	4665.7	-2925.5	3082.2	-2109.6	2169.2	-1537.2	763.6
50906	8.80	0.40	9.20	0.24	-3550.2	4683.2	-2725.1	3235.1	-2016.1	2393.5	-1424.0	1674.0
50924	8.50	0.29	12.29	0.25	-3799.3	4674.5	-2738.4	3225.5	-2028.9	2383.4	-1555.0	1663.4
50926	12.24	0.04	12.71	0.02	-3889.0	4584.8	-2828.1	3256.3	-2000.3	2293.7	-1407.5	1094.8
50930	10.26	0.16	11.54	0.10	-4481.0	4838.2	-3101.5	3186.4	-2293.9	2129.2	-1715.6	1075.7
50931	8.71	0.29	12.22	0.21	-3980.7	4666.8	-2842.1	3333.0	-2107.7	2336.4	-1535.4	1508.4
50932	9.16	0.22	11.51	0.16	-4391.7	4745.7	-3254.5	3411.4	-2357.9	2663.4	-1786.0	2165.8
50933	9.59	0.48	11.21	0.22	-3908.3	4658.6	-2850.7	3241.5	-2034.7	2328.1	-1544.0	1252.1
50934	6.58	0.07	12.77	0.06	-4238.6	4988.2	-3019.2	3402.9	-2285.2	2488.9	-1713.0	1991.5
50935	8.92	0.46	11.85	0.35	-3538.9	4368.0	-2670.6	2947.0	-1974.2	2239.1	-1450.8	476.3
50936.1	8.18	0.21	12.79	0.19	-3823.8	4745.3	-2766.0	3327.8	-2031.4	2414.2	-1458.9	1420.5
50936	9.21	0.47	12.13	0.34	-3766.2	4722.5	-2789.5	3221.7	-2054.9	2308.2	-1564.2	1562.8
50937	10.05	0.35	12.66	0.25	-3719.2	4277.2	-2775.6	3311.2	-2065.9	2588.7	-1591.8	1747.9
50938	11.51	0.06	11.94	0.03	-4041.0	4688.8	-2984.0	3354.8	-2168.3	2524.0	-1596.0	1612.7
50940	9.55	0.32	12.02	0.22	-4367.4	4787.5	-3028.7	3299.3	-2245.0	2387.1	-1683.9	1704.8
50941	10.77	0.26	12.61	0.18	-4271.8	4542.3	-3156.2	3283.6	-2260.7	2371.4	-1587.3	1462.0
50949	10.26	0.36	12.40	0.24	-4136.5	4566.2	-3020.5	3193.3	-2236.8	2281.4	-1675.7	1372.3
50951	10.57	0.43	13.43	0.30	-4217.4	4510.3	-3079.2	3176.6	-2263.5	2263.1	-1773.0	1352.3
50955	12.88	0.07	15.59	0.04	-4225.1	4670.4	-3086.9	3252.6	-2352.8	2338.8	-1780.5	1593.1
50961	11.86	0.10	15.02	0.07	-3767.8	4862.5	-2846.8	3446.1	-2038.5	2505.4	-1575.6	1567.7

Note: (1) Julian dates of IAW watch data in the form “*.1” are used to artificially make a difference between two different spectra under the same MJD on IAW watch web site (as for example 48325.0 and 48325.1)

(2) File names differs according to the observatory/monitoring campaign:

PTG* : Crimean Astrophysical Observatory data

n* : AGN watch data

5* : SAO/GHO data

A* : Asiago data

Continued on next page

Table 2 – continued from previous page

JD-2400000	Flux Hb	Err.	Fl. 5100	Err.	B25%	R25%	B50%	R50%	B75%	R75%	B90%	R90%
50962	11.38	0.52	13.97	0.35	-3963.1	4686.8	-2905.7	3435.8	-2171.4	2521.6	-1680.8	1775.8
50963	10.79	0.19	12.89	0.09	-4307.6	4583.5	-3088.5	3249.6	-2272.9	2335.9	-1618.8	1259.7
50964	11.49	0.28	13.19	0.17	-4121.5	5027.8	-3064.3	3525.2	-2330.2	2610.5	-1839.8	1947.0
50965	10.40	0.24	12.71	0.16	-4282.7	4776.9	-3144.8	3358.8	-2247.6	2527.8	-1675.3	1781.8
50966.1	9.51	0.38	13.73	0.31	-3728.1	4595.3	-2832.8	3427.7	-2098.2	2513.5	-1525.6	1602.0
50966	9.82	0.59	12.68	0.42	-3974.1	4510.4	-2834.9	3343.0	-2018.5	2428.9	-1527.6	939.1
50980	9.56	0.07	11.30	0.04	-3692.6	4527.5	-2751.0	3442.5	-1924.7	2481.3	-1451.5	1523.2
50980	9.95	0.25	10.21	0.15	-3910.9	5071.1	-2990.1	3418.0	-2182.1	2360.0	-1719.4	1539.7
50981	12.13	0.03	11.84	0.00	-3911.3	4406.3	-2935.1	3239.6	-2200.8	2408.9	-1628.5	1663.3
50982	10.51	0.38	11.11	0.24	-3746.5	4660.0	-2932.7	3325.7	-2198.3	2411.8	-1707.8	1748.8
50982	11.52	0.12	10.56	0.06	-4022.6	4627.5	-2965.1	3293.3	-2230.8	2379.3	-1740.2	1633.6
50982.1	8.45	0.37	13.21	0.30	-3958.6	4444.6	-2990.3	3310.6	-2296.7	2462.8	-1740.7	1758.1
50982.2	12.95	0.47	15.05	0.33	-3722.6	4142.8	-2685.7	3258.6	-1992.5	2377.1	-1471.5	796.7
50982.3	9.65	0.35	11.46	0.24	-3700.9	4164.5	-2664.0	3280.3	-1970.8	2398.8	-1449.8	818.4
50982.4	7.92	0.14	10.58	0.10	-3801.8	4426.6	-2859.3	3340.5	-2150.5	2498.4	-1677.0	1778.5
50983.1	13.16	0.62	14.04	0.42	-3839.2	4649.4	-2944.1	3314.9	-2291.4	2483.9	-1800.9	1737.9
50983	11.96	0.01	10.21	0.01	-3706.8	4289.7	-2881.2	3323.6	-2171.8	2360.7	-1816.5	1760.4
50983.2	9.47	0.47	11.59	0.35	-3809.5	4679.1	-2914.4	3344.7	-2261.6	2513.6	-1771.2	1767.6
50984	11.17	0.07	10.83	0.04	-3828.1	4289.4	-2884.4	3202.4	-2174.7	2479.9	-1700.6	1759.1
50984.3	11.96	0.82	13.71	0.59	-4037.9	4523.1	-2981.1	3273.2	-2247.2	2525.7	-1757.0	1862.9
50985	9.57	0.06	9.60	0.03	-4621.7	4458.0	-3158.0	3331.3	-2423.5	2395.7	-1687.1	1276.6
50986	10.68	0.56	10.71	0.34	-3891.8	4509.7	-2997.0	3342.5	-2344.6	2428.7	-1854.3	1848.5
50987	9.53	0.88	10.12	0.51	-3995.0	4406.4	-3018.7	3239.3	-2366.1	2325.5	-1875.7	1662.5
50988	10.53	0.22	10.22	0.12	-3809.4	4512.1	-2832.8	3344.8	-2179.9	2430.8	-1771.1	1850.6
50989	13.11	0.04	10.01	0.01	-3957.8	4525.5	-2981.8	3358.3	-2329.3	2527.4	-1839.0	1947.0
50990.1	12.13	0.09	9.56	0.04	-3858.5	4461.7	-2882.0	3211.4	-2147.5	2297.8	-1656.8	1552.3
50990	9.80	0.26	9.51	0.15	-3863.8	4790.6	-2968.8	3289.3	-2234.5	2375.4	-1744.0	1547.0
50991.1	11.34	0.16	11.24	0.10	-3816.1	4420.5	-2839.6	3253.7	-2105.1	2340.1	-1614.5	1429.3
50991	9.58	0.41	9.70	0.25	-4063.4	4602.1	-3050.2	3332.3	-2372.9	2412.2	-1807.2	1609.4
50992	8.79	0.21	8.85	0.13	-4668.0	4906.0	-3206.3	3289.0	-2416.2	2368.9	-1963.7	1566.1
50993	12.08	1.49	11.42	0.84	-3803.2	4351.2	-2826.6	3267.8	-2173.7	2437.0	-1683.1	1773.9
50994.1	13.22	0.03	11.26	0.01	-4103.2	4372.1	-2965.3	3122.9	-2231.4	2292.9	-1741.1	1547.9
50994	9.47	0.46	10.69	0.31	-3875.6	4832.0	-2933.6	3383.2	-2225.2	2421.2	-1751.9	1701.6
50994	9.91	0.02	9.14	0.01	-3892.3	4843.9	-2916.0	3342.4	-2263.4	2511.4	-1854.7	2013.9
50995.1	8.71	0.21	10.40	0.15	-3742.6	4329.5	-2847.3	3163.0	-2112.8	2415.5	-1622.1	1504.3
50995	9.09	0.41	10.05	0.28	-3804.4	4540.3	-2862.4	3213.5	-2272.2	2372.3	-1799.1	1653.1
50996	9.97	0.04	8.57	0.00	-3693.1	4063.1	-2749.3	2977.2	-2039.4	2135.2	-1565.3	577.8
51008	9.66	0.07	9.87	0.04	-3676.9	4479.6	-2863.0	3229.5	-2128.6	2398.9	-1638.0	1653.4
51009	10.31	0.37	10.72	0.19	-4488.1	4404.5	-3083.0	3323.4	-2201.4	2425.4	-1671.1	1530.1
51010	10.00	0.17	9.53	0.10	-4300.0	4592.1	-3080.7	3258.0	-2183.4	2261.3	-1610.9	607.5
51011	9.48	0.13	10.03	0.08	-4561.7	4489.1	-3017.8	3238.7	-2120.3	2325.1	-1547.8	1166.2
51012	9.24	0.61	10.08	0.36	-4366.8	4756.4	-2954.0	3306.9	-2245.0	2404.5	-1712.2	1504.8
51013.1	8.30	0.07	9.74	0.04	-4198.0	4863.7	-2896.9	3362.1	-2080.8	2448.1	-1590.0	1454.1
51013	8.54	1.61	8.86	1.10	-4506.2	4630.2	-3124.9	3296.0	-2146.0	2465.1	-1573.5	1802.0
51015	8.96	0.23	9.64	0.15	-3814.9	4537.9	-2754.0	3330.3	-2044.5	2367.7	-1570.7	1528.0
51017	9.26	0.09	10.70	0.07	-3869.3	4365.8	-2729.9	3199.2	-1913.4	2202.8	-1422.5	549.5
51018	8.65	0.43	9.61	0.30	-4778.8	5188.2	-2900.5	3371.9	-2123.6	2242.2	-1567.4	667.7
51019	9.48	0.08	9.76	0.03	-4053.4	4511.0	-2833.2	3094.3	-2016.9	1849.7	-1444.2	857.7
51020.703	12.55	0.01	11.90	0.00	-6063.8	6123.8	-3643.7	3850.2	-2426.2	3058.5	-1537.5	2607.0
51020	8.66	0.30	9.55	0.20	-4312.9	4810.9	-2900.0	3180.5	-2191.1	2278.6	-1658.2	1559.0
51021.1	9.01	0.02	10.08	0.01	-4021.3	4545.0	-2719.3	3127.9	-1902.6	2048.8	-1411.5	560.9
51021.712	9.63	0.17	10.46	0.11	-4149.7	4863.3	-2934.0	3389.4	-2102.3	2316.8	-1546.5	1416.6
51021	9.19	0.40	9.65	0.26	-4048.0	4599.9	-2827.8	3182.8	-2011.6	2186.4	-1520.7	863.1
51022	9.33	0.27	11.13	0.21	-4211.0	4803.8	-2965.2	3343.2	-2072.1	2433.8	-1714.1	1527.2
51024	7.93	0.11	10.43	0.08	-4176.4	5053.6	-2956.6	3301.3	-2140.7	2304.5	-1650.0	1393.6
51040	7.44	0.03	10.06	0.01	-3662.1	4456.9	-2718.3	3249.1	-1890.0	2286.3	-1415.6	967.5
51052	7.80	0.22	10.87	0.17	-3679.1	4315.7	-2617.5	3229.4	-1907.7	2026.8	-1314.8	829.1
51056	8.03	0.03	9.22	0.00	-3845.3	4262.3	-2784.7	3056.3	-1957.2	2094.8	-1364.8	658.4
51067	9.42	0.15	11.83	0.09	-4022.0	4263.5	-2804.8	3243.6	-2027.6	2227.0	-1471.2	989.2
51074	8.60	0.18	11.52	0.14	-4118.8	4359.8	-2817.4	3110.1	-1919.4	2362.8	-1428.4	1369.1
51077	11.35	0.18	12.52	0.11	-4058.9	4282.1	-2763.5	3076.3	-2054.5	2235.1	-1462.4	1396.2
51085	10.53	0.06	12.95	0.04	-4337.5	5188.6	-3010.9	3259.2	-2234.3	2355.4	-1678.3	1904.5
51142	10.32	0.04	8.85	0.02	-4064.7	5490.8	-2886.8	3193.8	-2059.5	2111.8	-1467.1	1153.2
51143	8.54	0.02	8.79	0.00	-5086.7	4622.3	-3080.6	3134.4	-2072.3	1653.8	-1398.3	519.8
51153	7.60	0.05	8.37	0.03	-4382.7	5257.2	-3277.6	3440.3	-2279.5	2761.7	847.3	2310.1
51170	8.80	0.11	10.07	0.04	-4208.9	4833.0	-2534.2	3345.1	-1749.5	1978.1	-1187.7	730.4
51176	7.65	0.19	8.76	0.13	-3870.5	4697.3	-2812.9	2947.5	-2078.4	1703.8	-1587.8	135.8
51185	8.23	0.05	9.23	0.04	-3864.1	4706.8	-2724.5	3122.7	-1989.6	1216.0	-1498.7	143.7

Note: (1) Julian dates of IAW watch data in the form “*.1” are used to artificially make a difference between two different spectra under the same MJD on IAW watch web site (as for example 48325.0 and 48325.1)

(2) File names differs according to the observatory/monitoring campaign:

PTG* : Crimean Astrophysical Observatory data

n* : AGN watch data

5* : SAO/GHO data

A* : Asiago data

Continued on next page

Table 2 – continued from previous page

JD-2400000	Flux Hb	Err.	Fl. 5100	Err.	B25%	R25%	B50%	R50%	B75%	R75%	B90%	R90%
51186	8.96	0.06	9.53	0.04	-4999.6	5301.0	-2967.7	3328.1	-2173.8	1713.0	-1605.3	450.0
51188	6.68	0.19	8.67	0.15	-4860.3	5560.7	-2940.9	3354.9	-2146.9	1970.0	-1578.5	362.3
51189.1	8.05	0.36	8.47	0.25	-3857.0	4463.2	-2717.5	2880.3	-1982.6	1471.1	-1409.7	480.2
51189	8.29	0.43	8.58	0.30	-3609.6	4630.9	-2632.7	3214.0	-1897.8	1638.2	-1406.9	399.9
51190.5	9.62	0.17	9.60	0.12	-3890.2	4960.6	-2784.3	3259.9	-1952.0	1681.2	-1395.9	670.7
51190	6.76	0.26	7.64	0.19	-3918.9	4369.7	-2701.2	3010.0	-1923.7	1431.4	-1367.2	420.9
51191	11.81	0.07	9.55	0.04	-3559.6	4433.5	-2500.6	3017.2	-1765.3	1442.2	-1274.1	369.2
51191.952	8.87	0.12	9.70	0.09	-3799.7	4940.7	-2748.7	3240.0	-1971.9	1717.6	-1415.8	706.8
51192	7.68	0.28	8.16	0.20	-4724.7	4988.3	-2949.7	3347.5	-2058.2	1534.8	-1343.0	632.5
51193.1	7.46	0.07	8.68	0.05	-3705.2	4367.5	-2646.8	2868.4	-1830.0	1542.1	-1257.0	633.7
51193	6.50	0.31	7.80	0.22	-3761.0	4476.1	-2702.9	2976.7	-1968.2	1567.4	-1395.4	494.1
51194	7.19	0.16	7.55	0.11	-3902.6	5104.6	-2835.9	3463.3	-2122.7	2192.9	-1586.6	207.2
51195	6.35	0.11	7.34	0.07	-3726.2	4347.1	-2667.7	3014.1	-1932.7	1438.8	-1359.8	365.7
51196	7.24	0.07	7.67	0.04	-3772.8	4548.3	-2388.3	2882.2	-1652.7	1142.6	-1243.3	153.0
51197	7.42	0.13	8.17	0.08	-3741.8	4498.6	-2683.3	2998.6	-1948.3	1423.2	-1457.2	350.1
51198	7.14	0.12	7.50	0.08	-3797.5	4606.8	-2739.4	3106.5	-2004.7	1779.2	-1431.9	540.1
51199	8.74	0.76	9.00	0.52	-3710.1	4528.6	-2733.3	3195.2	-1916.9	1784.8	-1426.0	545.8
51200	8.30	0.13	10.62	0.09	-3789.1	5029.3	-2813.0	3194.9	-2078.7	1785.1	-1588.3	381.8
51201	6.98	0.28	8.25	0.19	-3545.5	4717.7	-2503.2	2940.5	-1806.3	1349.9	-1282.6	469.8
51203	6.33	0.31	9.19	0.23	-3668.8	4487.0	-2692.0	3070.7	-2039.0	1826.5	-1466.4	669.9
51215	6.98	0.14	8.83	0.10	-3541.7	4721.5	-2499.4	2944.3	-1802.6	1706.4	-1278.9	473.6
51217	6.90	0.10	8.45	0.03	-3886.8	4681.5	-2747.5	3180.9	-1931.1	1853.3	-1358.3	614.0
51219	6.47	0.25	9.76	0.23	-4162.5	4481.8	-2779.8	3065.3	-1881.7	1655.4	-1390.6	499.2
51220	6.90	0.28	9.10	0.22	-3597.1	4404.1	-2534.7	2955.3	-1824.3	1513.5	-1231.0	556.0
51221	8.10	0.44	9.59	0.33	-4095.4	4718.8	-2956.8	3301.0	-2140.8	2138.5	-1568.3	815.3
51223	7.65	0.33	8.67	0.24	-4239.4	5404.2	-2912.3	3699.8	-2024.2	2230.4	-1579.2	543.7
51224	8.95	0.05	9.34	0.01	-3968.2	4766.2	-2584.5	3098.7	-1767.5	1605.7	-1194.2	449.6
51225	6.18	0.09	8.54	0.03	-3947.8	5288.7	-2645.7	3285.5	-1910.7	1957.3	-1501.5	140.6
51227	7.07	0.14	9.30	0.03	-4030.3	4701.3	-2647.0	3367.0	-1830.2	1459.2	-1339.1	303.8
51228	7.51	0.35	8.89	0.21	-3908.5	4994.9	-2769.2	3326.2	-2116.2	2080.6	-1625.5	666.3
51230	7.23	0.15	9.04	0.09	-4122.6	4774.3	-2739.6	3439.5	-1841.3	1613.8	-1350.1	457.7
51231	9.61	0.74	9.85	0.48	-3882.8	4769.2	-2662.0	3101.9	-1845.4	1443.7	-1354.3	370.8
51232	7.26	0.28	8.65	0.22	-3901.8	5671.3	-2599.4	3332.6	-1946.0	1838.6	-1455.1	269.6
51233	9.89	0.05	8.49	0.03	-3809.1	4927.5	-2588.2	3342.8	-1853.2	1766.3	-1362.2	280.3
51247	7.88	0.19	9.71	0.14	-4599.7	4919.3	-2941.7	3217.5	-2053.7	1300.2	-1497.3	290.1
51248	8.14	0.12	9.10	0.08	-4328.9	4895.8	-3191.3	3394.1	-2294.3	2148.3	-1640.3	907.6
51248	8.23	0.23	8.61	0.13	-4123.9	4688.2	-2659.5	3270.8	-1842.8	1446.3	-1269.8	455.8
51250.1	7.89	0.20	10.00	0.13	-3827.2	4828.7	-2687.4	3077.6	-1952.4	1419.1	-1461.4	346.0
51250	7.35	0.15	9.90	0.08	-4256.8	4802.4	-2874.6	3134.9	-1976.7	1641.9	-1322.0	650.7
51252	11.19	0.05	11.25	0.03	-3788.1	5185.9	-2681.0	3482.8	-1903.5	2127.2	-1346.9	441.1
51260	9.37	0.11	10.72	0.02	-3955.3	6002.6	-2706.2	3619.0	-1990.0	1979.8	-1272.1	711.0
51261	9.56	0.02	10.38	0.02	-4064.6	5331.7	-2763.5	3412.2	-2029.1	2249.7	-1620.3	185.0
51262.1	8.67	0.18	10.94	0.14	-4017.7	5127.3	-2798.1	3458.9	-2063.9	2048.0	-1491.6	891.0
51262	8.59	0.21	10.25	0.14	-4101.0	5546.2	-2881.4	3458.8	-2147.3	2047.4	-1656.8	148.4
51267	8.89	0.04	9.14	0.03	-3598.9	4933.3	-2581.9	3593.4	-1853.4	1963.8	-1415.4	342.9
51277	7.19	0.25	9.66	0.20	-4653.7	4918.6	-3192.1	3417.1	-2289.2	1923.0	-1723.4	208.2
51278.1	7.91	0.31	10.86	0.26	-3984.6	4827.4	-2764.8	3493.2	-2030.5	2082.0	-1540.0	265.5
51278	8.27	0.18	10.35	0.12	-3752.9	4484.2	-2694.8	3317.3	-1960.0	1906.5	-1551.1	172.7
51279.1	7.21	0.33	11.81	0.30	-3799.8	4852.7	-2660.5	3351.6	-1925.8	1940.8	-1435.0	289.3
51279	8.68	0.30	10.99	0.22	-3786.3	4425.5	-2727.9	3341.7	-2020.2	1902.5	-1429.1	232.1
51280	9.29	0.31	11.76	0.23	-3696.3	4700.8	-2659.4	3285.0	-1792.6	2227.4	-1271.3	647.9
51281	6.35	0.03	10.18	0.03	-3981.2	4998.8	-2924.3	3247.7	-2190.3	1837.6	-1618.2	434.0
51282	8.07	0.30	11.33	0.19	-3447.0	4317.0	-2620.5	3350.6	-1910.2	1307.1	-1554.4	-7.8
51283	8.38	0.13	12.04	0.07	-4135.6	4757.2	-2834.7	3339.9	-2018.7	2012.0	-1528.1	277.9
51284	8.74	0.25	11.45	0.19	-3869.7	4614.2	-2812.1	3280.5	-2077.7	1787.1	-1587.1	136.4
51285	10.86	0.02	11.11	0.01	-4070.0	4658.7	-2850.2	3324.8	-2034.1	1914.0	-1543.5	262.6
51286	8.50	0.54	10.88	0.41	-3873.0	4945.4	-2733.8	3443.8	-1835.7	1370.4	-1262.8	545.1
51287	9.39	0.44	12.20	0.34	-4040.6	4690.0	-2820.5	3522.3	-2167.7	1779.2	-1677.2	293.0
51288	8.47	0.05	10.55	0.04	-3948.5	4866.8	-2728.3	3448.9	-1993.7	2037.6	-1503.0	220.9
51290	8.55	0.22	11.63	0.16	-4081.9	4397.1	-2780.4	3313.7	-1964.1	1323.6	-1391.4	333.5
51291	9.24	0.58	12.42	0.45	-3911.6	4821.8	-2772.6	3320.8	-2038.1	1910.0	-1629.3	588.2
51293	11.30	0.04	11.36	0.01	-3882.1	4685.0	-2824.5	3434.2	-2008.4	1940.1	-1435.9	453.3
51309	9.12	0.39	11.54	0.30	-4343.4	4614.0	-2906.0	3479.6	-2017.9	1336.0	-1350.1	437.9
51310	9.09	0.04	10.67	0.02	-3574.2	4672.5	-2747.9	3463.2	-2037.8	2499.3	-1563.4	341.6
51319	9.01	0.40	12.16	0.33	-4001.5	4743.2	-2894.6	3607.8	-2117.3	2476.6	-1672.2	226.9
51322	8.84	0.40	11.69	0.31	-3677.4	4678.7	-2734.1	3591.3	-1906.3	2628.0	-1432.2	710.5
51342	6.97	0.21	9.12	0.15	-3548.9	4689.4	-2605.3	3602.0	-1895.6	2398.3	-1302.9	840.6
51344	7.44	0.05	8.74	0.04	-3777.2	4300.8	-2735.9	3234.7	-1865.3	1995.8	-1341.7	410.2

Note: (1) Julian dates of IAW watch data in the form “*.1” are used to artificially make a difference between two different spectra under the same MJD on IAW watch web site (as for example 48325.0 and 48325.1)

(2) File names differs according to the observatory/monitoring campaign:

PTG* : Crimean Astrophysical Observatory data

n* : AGN watch data

5* : SAO/GHO data

A* : Asiago data

Continued on next page

Table 2 – continued from previous page

JD-2400000	Flux Hb	Err.	Fl. 5100	Err.	B25%	R25%	B50%	R50%	B75%	R75%	B90%	R90%
51346	7.36	0.44	8.12	0.25	-3917.5	4297.4	-2708.2	3236.1	-1667.8	2354.5	-972.1	1475.5
51348	7.76	0.30	8.81	0.23	-4507.7	4755.8	-3300.6	3515.9	-2435.3	2457.1	-1741.3	1226.5
51367	7.28	0.32	8.49	0.25	-3803.2	4547.9	-2860.5	3461.1	-2151.5	2618.6	-1559.4	1898.2
51368	10.43	0.49	8.12	0.26	-3652.7	4471.3	-2708.3	3262.7	-1879.5	1698.8	-1286.1	620.8
51376.1	7.59	0.09	8.06	0.06	-4583.0	4592.4	-3012.7	2981.8	-2163.6	1748.7	-1555.7	520.6
51376	9.61	0.06	8.47	0.02	-4128.1	4835.9	-2911.4	3247.8	-1912.1	1555.5	-1355.6	656.7
51377	10.92	0.01	8.54	0.01	-5051.5	4978.3	-3241.8	3242.1	-2150.6	1515.7	-1421.0	656.2
51399	7.53	0.86	8.33	0.59	-4684.1	4363.5	-2993.2	3124.8	-2022.7	1276.3	-1414.5	540.0
51400	6.05	0.03	6.19	0.02	-4601.3	4202.5	-2970.2	2717.2	-2060.2	1239.1	-1512.8	319.0
51407	9.54	0.01	6.65	0.01	-3764.8	4460.7	-2704.7	3134.2	-1877.5	1574.0	-1285.3	617.9
51408	5.87	0.02	6.49	0.01	-4834.4	5465.6	-3068.4	3083.3	-2070.4	1393.0	-1403.2	495.4
51425	8.45	0.01	8.01	0.00	-3771.2	4817.1	-2711.0	3127.8	-1883.8	1807.2	-1410.2	492.3
51426	7.79	0.12	7.88	0.08	-4219.7	5818.3	-2924.2	3277.3	-1978.4	1235.8	-1385.8	399.1
51431	6.19	0.00	6.32	0.00	-4524.9	5353.7	-2999.1	3664.5	-2056.2	1148.3	-1465.3	433.2
51456	6.36	0.07	8.47	0.02	-4508.3	5006.1	-3072.6	3418.2	-2185.7	2063.7	-1518.7	491.2
51517	6.50	0.12	8.60	0.07	-4014.0	4688.3	-2718.8	3722.3	-1891.6	2879.5	-1417.9	484.5
51548	6.37	0.06	7.38	0.05	-3766.3	4475.5	-2704.1	3629.0	-1875.3	2784.9	-1400.7	505.5
51557	6.46	0.05	6.54	0.03	-3433.0	4447.2	-2488.8	3360.4	-1778.7	2397.7	-1304.3	1198.5
51570	10.54	0.88	6.46	0.42	-3422.3	4461.1	-2477.7	3494.5	-1767.3	2410.7	-1292.7	1091.3
51570.5	7.55	0.12	6.52	0.07	-3604.7	4799.5	-2608.5	3325.9	-1775.9	2084.5	-1163.8	1184.9
51571	9.15	0.11	6.90	0.05	-4377.8	5177.8	-2787.3	3428.3	-1988.8	2267.5	-1417.1	1111.2
51586	5.13	0.16	5.03	0.12	-4403.8	5261.4	-2928.3	3396.3	-2016.6	2120.7	-1445.4	850.5
51588.1	6.02	0.14	6.40	0.10	-3234.0	4306.2	-2367.0	3242.7	-1671.5	1654.3	-1148.8	600.1
51588	4.16	0.12	6.73	0.11	-3483.7	4401.3	-2538.9	3193.3	-1828.3	1870.0	-1353.7	672.0
51600	7.86	0.03	5.51	0.01	-3979.5	4782.8	-3114.7	3363.6	-2421.1	2479.9	-2073.7	-505.2
51600.898	5.41	0.02	5.10	0.01	-3713.6	5312.8	-2662.5	3497.1	-1885.5	2198.7	-1329.3	1186.5
51601	8.00	0.04	5.12	0.01	-3975.3	6475.0	-2731.3	3452.1	-1823.2	1951.9	-1254.3	802.9
51632	3.95	0.11	4.35	0.08	-4438.9	6288.6	-2962.3	3483.5	-2049.9	2090.6	-1478.3	934.7
51658.5	3.85	0.27	3.17	0.13	-4074.7	5453.8	-2858.5	3806.9	-2026.5	2563.4	-1470.5	1493.6
51659	6.52	0.84	4.02	0.46	-3665.6	5425.8	-2558.0	3834.7	-1780.3	2477.5	-1112.0	1351.2
51659.839	4.83	0.06	3.42	0.04	-3876.5	5543.3	-2715.1	3782.9	-1882.7	2088.8	-1326.5	796.5
51660	6.34	0.02	3.84	0.01	-4976.5	5496.2	-3047.7	3628.2	-2021.5	1887.4	-1335.4	617.2
51676	2.79	0.14	5.23	0.16	-4807.9	5555.6	-2991.6	3570.6	-2079.2	1829.7	-1393.1	674.8
51686.35	4.05	0.03	3.67	0.03	-4493.1	5362.5	-3057.4	3942.7	-2170.5	2868.2	-1592.2	1572.4
51686	4.51	0.31	7.34	0.12	-4949.7	5362.9	-3399.4	3766.8	-2188.0	2531.2	-1319.7	1651.6
51689	6.16	0.13	4.08	0.08	-4905.9	5051.3	-3700.8	3457.0	-2490.8	2046.9	-1797.1	1168.9
51690	6.99	1.42	4.99	0.90	-5379.4	5771.0	-3227.9	3903.1	-2089.1	2509.7	-1403.8	892.1
51690.835	3.86	0.10	4.12	0.09	-4370.2	5429.2	-3176.3	3866.5	-2250.4	2477.9	-1595.1	1371.6
51691	3.08	0.04	3.93	0.04	-5652.4	6544.5	-3616.0	4321.6	-2478.6	3042.1	-1679.8	2114.9
51706	3.57	0.13	5.16	0.15	-3682.7	4552.4	-2621.3	3586.0	-1793.2	2142.1	-1318.9	585.7
51721.1	6.27	0.08	4.19	0.05	-4389.5	4254.4	-3088.4	3253.9	-2190.5	932.1	-1617.7	189.6
51721	2.97	0.20	2.94	0.18	-4465.0	4967.6	-3051.2	3636.4	-1986.4	2551.5	-1036.8	1710.4
51722	2.74	0.88	3.48	1.19	-5018.3	8731.1	-3347.7	4116.3	-2340.7	2631.5	-1779.8	1153.8
51729	2.79	0.04	3.64	0.05	-4451.9	5329.4	-3276.0	3878.0	-2450.1	3034.6	-1858.8	160.5
51730	3.28	0.23	4.33	0.24	-3852.9	4628.7	-2714.1	3628.2	-1898.0	2713.9	-1407.2	399.1
51732	3.10	0.09	4.44	0.09	-4241.5	4939.6	-2947.0	3490.3	-2002.0	2407.8	-1409.9	492.9
51734	2.98	0.54	4.25	0.69	-3965.3	4738.8	-2787.8	3531.5	-1960.8	2809.4	-1487.2	176.4
51750	4.58	0.35	5.26	0.32	-4359.2	5276.4	-3222.4	3940.4	-2407.8	3274.6	-1836.2	2859.2
51753	4.33	0.05	5.80	0.02	-3753.6	4481.9	-2810.3	3636.1	-1982.4	2792.6	-1389.7	395.6
51754	4.11	0.04	6.10	0.05	-3766.3	4351.5	-2822.6	3505.7	-2112.9	2782.6	-1638.7	-92.7
51755	3.69	0.15	6.00	0.14	-6502.2	5687.5	-4103.8	3562.4	-2724.5	2153.9	-1859.2	752.0
51756	3.82	0.05	5.79	0.03	-6379.0	5532.3	-3672.1	3668.8	-2582.4	2371.1	-1853.7	343.2
51760	7.20	0.03	4.79	0.01	-3632.1	4266.7	-2724.3	3523.1	-1996.0	2411.2	-1448.6	15.9
51763	5.19	0.05	5.58	0.04	-5313.5	4832.5	-3384.3	3591.8	-2415.0	1371.2	-1685.9	267.1
51781	8.31	0.51	7.56	0.23	-4714.5	4333.1	-3144.7	3465.5	-2174.6	2600.4	-1566.7	387.1
51789	6.70	0.07	5.76	0.02	-5191.0	4586.2	-3018.9	3594.1	-2048.4	3099.2	-1318.4	637.0
51791	4.52	0.06	5.57	0.02	-4465.3	4341.3	-3015.4	3597.5	-1923.4	2855.5	-1314.9	640.4
51878	6.70	0.08	6.52	0.05	-3867.7	4335.7	-2778.7	3591.9	-2050.5	2973.5	-1442.4	2109.7
51900	4.76	0.02	6.11	0.00	-6710.5	5870.4	-3463.6	3757.3	-2130.4	2891.5	-1400.8	799.0
51902	5.51	0.09	6.44	0.08	-5428.0	4713.8	-3499.6	3721.3	-2409.3	2979.0	-1680.2	517.8
51926	6.57	0.04	5.45	0.02	-4347.1	4214.9	-3017.8	3595.2	-2047.3	2853.2	-1439.1	515.5
51931	5.83	0.23	5.72	0.20	-4588.9	4338.2	-3018.6	3346.8	-2048.1	1250.9	-1439.9	392.2
51934	6.67	0.45	4.67	0.28	-4235.6	4214.8	-2814.0	3395.4	-1922.1	1130.7	-1296.1	499.7
51938	4.22	0.06	7.08	0.07	-4823.8	4339.4	-3227.1	3337.7	-2336.3	2429.9	-1711.1	172.2
51944	3.68	0.06	6.68	0.05	-4108.3	4088.4	-2049.7	2850.7	-1197.9	758.2	-832.1	268.0
51957	3.85	0.05	6.92	0.01	-3618.7	4218.9	-2650.1	3228.0	-1921.7	2363.6	-1435.0	274.5
51960	4.54	0.15	5.59	0.15	-4187.7	4377.8	-2979.0	3510.2	-2008.5	2768.5	-1400.3	431.8
51961	4.17	0.12	4.89	0.12	-4290.1	4981.6	-3224.6	3704.5	-2422.9	2795.5	-1887.3	-94.8

Note: (1) Julian dates of IAW watch data in the form “*.1” are used to artificially make a difference between two different spectra under the same MJD on IAW watch web site (as for example 48325.0 and 48325.1)

(2) File names differs according to the observatory/monitoring campaign:

PTG* : Crimean Astrophysical Observatory data

n* : AGN watch data

5* : SAO/GHO data

A* : Asiago data

Continued on next page

Table 2 – continued from previous page

JD-2400000	Flux Hb	Err.	Fl. 5100	Err.	B25%	R25%	B50%	R50%	B75%	R75%	B90%	R90%
51962	4.17	0.07	4.85	0.07	-3958.6	4319.1	-2891.8	3317.3	-2089.2	2318.8	-1552.9	151.7
51969	7.87	0.02	6.04	0.01	-4062.4	4213.0	-2906.8	3302.4	-2104.2	2485.2	-1567.9	136.7
51981	4.39	0.16	6.16	0.15	-6151.6	5207.7	-3624.2	3346.2	-2413.0	2234.8	-1683.9	391.5
51999	2.77	0.08	4.04	0.06	-4344.8	5086.9	-3257.6	3597.4	-2409.3	2485.2	-1801.9	27.9
52013	3.70	0.09	6.13	0.08	-4217.6	4099.8	-2766.5	3356.6	-1916.8	769.6	-1430.1	157.0
52030.1	2.98	0.01	3.90	0.02	-7708.8	6826.7	-3748.4	3590.4	-2295.0	2848.4	-1565.6	388.2
52030	3.05	0.08	4.22	0.00	-6279.8	5453.1	-2419.8	2970.7	-1568.7	631.1	-1081.2	140.9
52034	2.29	0.02	4.18	0.00	-5667.7	4838.6	-2530.2	2855.9	-1436.4	395.7	-948.9	28.4
52041	1.98	0.03	4.72	0.00	-5803.2	4947.4	-3635.5	3458.6	-2303.0	2716.9	-1695.3	135.3
52041.5	2.39	0.06	4.21	0.01	-5196.6	5431.1	-3874.8	3841.2	-2713.4	2428.6	-1825.5	1359.4
52043	2.05	0.03	4.24	0.01	-4472.2	5453.6	-3264.5	3714.4	-2416.1	2725.1	-1808.7	265.9
52043.859	2.78	0.02	3.54	0.02	-7102.7	6468.5	-3643.1	3342.7	-2425.4	2439.4	-1703.5	248.9
52045	2.84	0.01	3.84	0.01	-5172.3	4853.5	-3363.3	3365.2	-2272.6	2500.5	-1664.9	165.6
52048	2.64	0.01	4.07	0.00	-5923.4	5071.7	-3514.8	3087.3	-1695.4	2100.0	-1208.4	135.1
52051	2.15	0.14	4.12	0.25	-5566.3	4695.6	-2548.8	2960.8	-1211.4	499.6	-845.6	132.1
52053	2.13	0.02	3.86	0.03	-5603.8	4911.5	-3476.8	3542.6	-2229.0	2815.1	-1513.6	282.4
52058	3.08	0.20	5.83	0.29	-5289.3	4415.8	-3070.7	3048.9	-1999.8	2685.5	-1373.3	2413.2
52060	1.99	0.35	3.65	0.54	-5626.5	4796.9	-3766.3	3246.5	-2430.4	2428.9	-1626.0	1613.6
52074	3.42	0.07	5.54	0.03	-4719.1	4001.9	-2138.3	3000.1	-1063.9	555.1	-704.8	194.6
52074.772	3.43	0.05	4.52	0.03	-5737.8	5268.1	-3977.4	3735.7	-2428.4	2549.1	-1317.1	1648.2
52075	3.25	0.02	5.93	0.03	-5073.0	5454.7	-3505.3	3963.5	-2536.3	3096.9	-1807.5	2479.5
52075.738	2.52	0.10	4.19	0.12	-5638.7	4973.2	-3712.0	3668.5	-2217.1	2933.5	-1550.3	67.3
52076	2.67	0.07	5.17	0.00	-5921.1	5073.9	-4116.5	3708.3	-2786.1	3089.6	-1786.4	2595.6
52078	3.19	0.13	4.77	0.10	-5075.2	4333.4	-3628.3	3465.8	-2538.5	2847.6	-1931.3	2230.7
52086	3.61	0.02	5.42	0.00	-4914.7	4888.8	-3317.8	3702.7	-2337.6	2975.1	-1712.2	352.0
52087	4.45	0.29	6.78	0.36	-5003.3	4285.1	-3313.8	3417.5	-2222.7	2799.3	-1614.7	216.6
52101.1	4.29	0.03	5.38	0.01	-4530.2	4920.5	-3287.3	3734.2	-2396.2	3006.4	-1770.9	2280.5
52101	4.59	0.43	6.53	0.52	-5572.0	5124.6	-3889.6	3846.2	-2822.2	3209.1	-2108.4	2845.6
52102	4.76	0.06	6.03	0.03	-4715.1	4332.4	-3266.5	3588.6	-2175.3	2970.2	-1567.4	508.9
52103	5.36	0.04	6.29	0.04	-4599.6	4079.4	-2908.1	3212.5	-1450.6	626.6	-963.1	136.6
52112	4.39	0.07	8.99	0.10	-4966.0	4322.4	-3276.5	3454.8	-2185.3	2836.6	-1577.4	253.9
52113	6.31	0.02	4.71	0.01	-4112.5	4704.9	-3145.5	3712.4	-2296.9	3217.3	-1810.8	2846.5
52114	2.79	0.11	7.20	0.10	-5443.1	4705.5	-3395.1	3534.9	-2251.2	2834.6	-1562.8	512.2
52115	3.41	0.19	4.41	0.14	-4501.8	4428.3	-3458.1	3475.7	-2643.8	2881.9	-1827.3	2526.1
52117	3.52	0.33	8.32	0.48	-4493.0	4308.3	-3030.4	3558.0	-2051.3	2975.7	-1478.7	328.1
52137	3.46	0.05	5.41	0.05	-4465.3	5186.9	-3421.0	3635.9	-2489.7	2804.0	557.5	2329.7
52147	3.76	0.19	6.21	0.24	-4221.6	4492.9	-3042.8	3404.7	-2214.8	2922.4	-1621.9	2440.8
52174	2.51	0.06	5.39	0.07	-4486.5	4823.0	-3544.9	3492.5	-2718.6	2769.3	-1652.8	2408.3
52338.78	3.44	0.02	3.44	0.01	-4565.7	5802.6	-3130.0	3530.4	-2132.1	2908.5	-1464.8	2513.4
52369.85	3.31	0.02	2.63	0.01	-5028.0	6465.5	-3096.7	3451.8	-2154.1	2830.0	-1542.5	2322.2
52370.78	2.25	0.04	2.45	0.00	-4353.0	4484.6	-3138.0	3521.2	-2251.2	2955.9	-1640.0	2617.2
52439.5	1.17	0.14	3.29	0.03	-5130.4	6297.5	-3863.6	4532.8	-2868.4	2947.6	-2092.0	1876.6
52665.924	2.23	0.03	3.82	0.04	-6282.7	5617.2	-4745.2	3685.8	-3586.9	2668.3	-2812.1	2104.5
52666.926	2.16	0.03	3.71	0.04	-6162.2	8145.8	-4734.3	3526.9	-3631.2	2735.7	-2856.6	2284.4
52667.901	3.35	0.11	4.92	0.05	-5421.6	5368.8	-4266.3	3665.9	-3272.4	2592.4	-2497.1	1972.6
52667.93	2.88	0.05	3.55	0.05	-6766.8	7735.9	-4957.7	3520.5	-3745.4	2729.5	-2916.0	2278.5
52725.893	1.74	0.01	2.32	0.00	-5214.4	6264.2	-3838.0	3537.0	-2787.6	2915.5	-2011.2	2520.6
52782.728	3.08	0.05	2.69	0.05	-5137.0	6216.8	-3817.0	3323.8	-2767.8	2703.4	-2047.8	290.5
52782.75	4.21	0.01	4.82	0.00	-5239.8	4363.0	-3697.5	3287.0	-2646.3	2609.4	-1924.9	249.7
52995.604	0.93	0.03	3.88	0.05	-4739.2	5107.1	-3912.6	3066.7	-3194.3	199.4	-2696.0	-861.8
53031.969	1.51	0.09	2.74	0.17	-6240.6	9235.8	-4541.8	5405.3	-3275.0	1790.7	-2445.9	446.3
53054.015	0.63	0.06	1.25	0.05	-5613.2	8752.3	-4460.4	5664.7	-3468.8	2664.4	-2750.5	-194.8
53065.54	1.79	0.01	2.62	0.01	-6668.0	8977.0	-5050.3	3863.4	-3873.4	2540.9	-3142.5	-655.1
53083.862	2.51	0.10	3.29	0.12	-6317.5	8721.5	-5166.0	5516.6	-4175.5	2401.3	-3458.0	1894.6
53107.894	1.79	0.05	4.79	0.08	-5796.6	5778.8	-4807.7	3337.3	-3981.1	2546.7	-3373.4	2152.1
53140.504	1.80	0.13	5.07	0.23	-5601.2	7176.1	-4557.1	5122.3	-3730.2	2969.3	-3067.0	-231.7
53144.756	1.48	0.03	1.96	0.03	-5919.7	8142.9	-4658.3	4437.7	-3722.5	2686.4	-3060.2	-897.3
53167.751	1.31	0.04	1.93	0.07	-6106.8	7757.8	-4518.5	4514.2	-3583.4	2370.8	-2921.5	1753.2
53171.406	1.12	0.06	4.08	0.14	-5247.6	5374.2	-4367.5	3671.9	-3540.1	2824.4	-2876.6	2429.7
53198.356	1.31	0.24	4.07	0.11	-5450.9	4481.4	-4626.5	2615.0	-3910.3	2164.3	-3413.4	-1862.1
53199.331	1.01	0.04	3.43	0.05	-5581.5	6281.3	-4427.3	3723.9	-3489.5	1580.9	-2825.8	-435.3
53355.995	4.07	1.95	6.18	2.05	-5896.9	7288.8	-4631.8	3413.7	-3582.6	2622.0	-2862.5	2170.5
53386.96	1.51	0.10	1.58	0.13	-5629.3	7474.6	-4476.5	3268.6	-3540.0	2310.5	-2821.9	1916.9
53389.929	1.82	0.01	2.34	0.01	-5620.2	8361.5	-4504.3	4540.2	-3567.9	2337.8	-2905.2	2000.4
53415.861	1.06	0.03	1.56	0.06	-5910.6	9295.4	-4759.6	6659.8	-3769.4	2974.0	-3052.2	2242.2
53417.569	1.34	0.11	5.14	0.27	-5160.9	6548.2	-4115.2	4725.7	-3287.0	3027.0	-2622.8	1169.3
53447.797	1.84	0.03	2.49	0.01	-5656.1	9443.3	-4559.3	6978.5	-3568.8	3911.0	-2906.5	-242.7
53451.563	1.50	0.07	4.29	0.09	-5358.1	7600.7	-4423.3	5487.3	-3651.3	3445.0	-3098.6	-654.5

Note: (1) Julian dates of IAW watch data in the form “*.1” are used to artificially make a difference between two different spectra under the same MJD on IAW watch web site (as for example 48325.0 and 48325.1)

(2) File names differs according to the observatory/monitoring campaign:

PTG* : Crimean Astrophysical Observatory data

n* : AGN watch data

5* : SAO/GHO data

A* : Asiago data

Continued on next page

Table 2 – continued from previous page

JD-2400000	Flux Hb	Err.	Fl. 5100	Err.	B25%	R25%	B50%	R50%	B75%	R75%	B90%	R90%
53477.785	1.36	0.00	1.68	0.00	-5476.3	6941.6	-4268.5	4043.2	-3331.8	2407.3	-2668.8	-336.7
53478.437	1.51	0.03	5.48	0.06	-4785.7	5800.8	-3959.1	4152.1	-3240.8	2568.6	-2742.5	-126.7
53502.783	2.85	0.04	3.67	0.04	-5691.3	7031.2	-4591.9	4409.4	-3709.4	2091.4	-3045.8	-41.2
53507.487	1.91	0.12	6.41	0.22	-5146.1	5601.5	-4320.3	3840.0	-3602.7	1807.2	-3049.5	-993.6
53508.515	2.34	0.16	4.46	0.17	-5736.2	8021.0	-4581.5	3063.6	-3698.6	2048.0	-3034.8	-1034.3
53509.483	1.98	0.05	4.71	0.06	-5665.0	7346.2	-4675.6	3813.7	-3848.5	2062.8	-3240.5	-1241.9
53530.753	2.21	1.02	2.92	1.27	-6366.7	8346.6	-4663.1	4515.3	-3724.6	2307.1	-3171.2	-1281.9
53538.428	1.44	0.10	3.67	0.15	-5772.0	6771.8	-4618.2	4663.5	-3625.6	2400.6	-2906.6	266.4
53560.391	1.57	0.10	3.93	0.17	-5489.9	6039.3	-4500.1	3879.1	-3672.7	1172.2	-3064.5	-730.6
53786.962	3.77	0.05	4.44	0.01	-5887.9	7971.2	-4459.0	4205.2	-3078.4	1607.7	-1747.0	821.6
53787.539	2.63	0.28	5.30	0.37	-5979.7	6892.9	-4662.1	3820.8	-3062.2	2183.7	-1398.0	1340.4
53788.567	3.03	0.16	5.02	0.14	-5684.6	8117.1	-4420.9	4578.7	-3262.3	2373.8	-2210.2	1979.7
53816.542	2.97	0.06	3.54	0.05	-5744.6	7832.6	-4535.5	4352.2	-3487.3	2260.4	-2767.9	1810.0
53843.803	1.97	0.07	3.99	0.08	-5592.7	6557.9	-4328.0	3375.0	-3223.8	1908.6	-2226.6	1121.8
54156.565	3.58	0.14	6.58	0.17	-5304.0	5832.4	-4258.5	3843.6	-3319.9	1699.1	-2655.5	72.6
54157.604	3.46	0.13	6.13	0.16	-5357.1	5494.3	-4201.4	3677.2	-3207.1	1927.2	-2486.9	523.3
54182.522	3.42	0.21	4.82	0.16	-5299.1	6695.8	-3867.2	2550.2	-2927.2	1536.6	-2261.8	-312.8
54183.467	2.68	0.03	4.35	0.02	-4993.2	5813.4	-3780.9	2750.5	-2840.8	1230.5	-2175.3	277.5
54184.901	3.91	0.08	3.62	0.05	-5450.8	6535.1	-4075.2	2618.1	-3080.7	314.4	-2471.3	-468.3
54216.521	1.92	0.04	4.52	0.06	-5977.9	7589.2	-4824.7	4735.7	-3832.6	2302.8	-3169.4	-613.3
54241.756	1.80	0.02	2.25	0.02	-6019.9	8748.1	-4702.1	5713.5	-3544.2	2201.4	-2658.9	796.7
54243.43	1.26	0.05	6.71	0.16	-5010.9	5231.9	-4129.2	3528.7	-3411.0	1666.2	-2857.2	-576.2
54244.399	1.65	0.10	5.53	0.15	-5466.3	8188.7	-4475.9	5157.4	-3648.1	2945.9	-3039.5	-1094.8
54275.395	1.67	0.50	5.61	0.88	-5809.1	5367.5	-3883.2	3268.3	-2998.6	846.7	-2610.7	-1221.4
54303.331	2.21	0.08	4.59	0.08	-5678.4	8538.6	-4633.9	5333.7	-3751.4	-27.3	-3143.2	-1088.1
54510.605	1.92	0.03	5.02	0.02	-5465.6	6294.1	-4530.7	4472.2	-3648.1	2661.2	-3039.7	188.7
54624.45	3.07	0.11	5.57	0.08	-7436.9	8525.0	-6289.5	6119.0	-5247.6	2996.8	-4532.5	-1766.0
54866.564	3.32	0.29	6.73	0.37	-5639.1	5486.8	-4539.5	3783.0	-3546.3	2088.7	-2771.6	627.9
54881.596	4.35	0.10	6.82	0.08	-5409.8	6637.8	-4309.4	4473.1	-3426.0	1817.0	-2761.8	-257.8
54882.563	5.09	0.13	6.01	0.09	-7854.7	7802.2	-4953.5	4718.7	-3464.5	935.7	-2744.9	-742.9
54968.419	5.00	0.10	6.31	0.07	-6033.9	8397.1	-4384.9	5535.0	-3390.9	1572.7	-2781.9	-556.7
54969.41	4.99	0.11	6.95	0.03	-5636.7	6573.3	-4592.2	4579.3	-3709.7	2372.8	-2990.8	-97.4
55250.556	7.91	0.33	12.49	0.28	-5653.5	6266.4	-4664.4	4502.0	-3782.4	2691.3	-3119.2	219.2
55251.574	10.06	0.18	12.48	0.11	-6257.7	8269.5	-4775.8	5353.1	-3728.6	2182.7	-3009.9	-285.3
55275.51	9.21	0.09	10.04	0.05	-6533.2	7294.9	-4722.4	4217.1	-3674.7	1788.3	-3011.1	-788.4
55306.462	8.11	0.10	9.65	0.07	-5589.0	7479.6	-4489.4	4229.9	-3606.7	1744.8	-2943.0	-664.1
55939	6.58	0.02	6.49	0.00	-7327.4	6186.9	-5053.8	3565.4	-3783.1	2263.2	-3018.0	-582.2
55978	5.14	0.03	5.83	0.02	-7363.2	6805.9	-5470.3	4179.6	-4074.3	2744.8	-3055.0	411.4
55979	4.21	0.02	5.42	0.01	-6461.5	6687.1	-4944.3	4455.5	-3801.3	2890.0	-2909.3	815.1
55986	3.99	0.14	5.77	0.11	-5999.3	6244.6	-4987.4	4539.4	-3972.0	2973.9	-3080.7	1805.0
55987	4.84	0.05	5.76	0.03	-6517.5	7283.3	-5127.8	4917.1	-3858.7	2829.0	-2967.1	755.3
56014.519	4.70	0.26	7.26	0.21	-5258.8	6336.1	-4268.2	4684.6	-3329.6	3268.0	-2609.8	2195.9
56016.497	3.52	0.29	5.42	0.01	-5273.8	7064.4	-4228.1	5124.3	-3344.6	3309.6	-2680.3	2631.9
56657.094946	7.59	0.12	8.13	0.07	-6719.6	8073.8	-5435.4	5815.1	-4281.7	3573.0	-3259.9	2180.0
57127.811272	4.90	0.10	6.62	0.07	-6528.3	6501.3	-5263.4	4137.5	-3993.0	2702.0	496.7	2181.6

Note: Julian dates of IAW data in the form “*.1” are used to artificially make a difference between two different spectra under the same mjd on the IAW web site (as for example, 48325.0 and 48325.1)

Table 3: Results from the periodicity analysis on light curves of continuum at 5100Å H β fluxes, and radial velocity curves of half widths of broad H β emission line measured at blue and red side of 25%, 50%, 75% and 90% of maximum intensity. Note: In the table are given period and the formal false alarm probability (P-value) for Lomb-Scargle periodogram of 80 day binned data series, where we present longest significant periods.

Curve:	L-S	P-val.
LC C. 5100Å	5490	$< 10^{-7}$
LC H β	5710	$< 10^{-8}$
RV 25% blue	5798	$< 10^{-8}$
RV 25% red	5670	< 0.09
RV 50% blue	5920	$< 10^{-8}$
RV 50% red	5730	$< 10^{-2}$
RV 75% blue	5740	$< 10^{-8}$
RV 75% red	5740	$< 10^{-8}$
RV 90% blue	5950	$< 10^{-8}$
RV 90% red	6240	$< 10^{-7}$
FW50%	2960	< 0.002
FW25%	3430	$< 10^{-8}$
FW75%	3302	< 0.0005

A. Appendix: [O III] calibration of slit spectra

NGC 5548 hosts a very compact narrow line region (NLR) structure (see Kramer et al. 1998; Schmitt et al. 2003; Peterson et al. 2013). The [O III] emission is so tightly concentrated that there is no position angle (PA) effect if the slit is wide enough, as can be seen in Schmitt et al. (2003). For a 1 – 2'' slit the effect is small but appreciable. It is about 4% for a 1'' slit, as can be seen by comparing the total flux within the slit at position angles 0° and –45°. This is shown in column 1 of Table 4, where the total [O III] flux within the slit F_{tot} (column 3) is compared to the unresolved core flux within the slit F_{slit} (column 4). The measurements were carried out on a narrow band WFPC2 image with angular resolution 0.1'' (see Fig. 10), available in digital format at NED⁶ and originally published by Schmitt et al. (2003). The total emission measured on the image is 4.30×10^{-13} , assuming zero background in the image. The average background is actually slightly less than zero ($\approx -5 \times 10^{-17}$) but it is difficult to estimate it accurately.

⁶[http://ned.ipac.caltech.edu/ing/2003ApJS..148..327S/NGC_5548:I:O III:sda2003.fits.gz](http://ned.ipac.caltech.edu/ing/2003ApJS..148..327S/NGC_5548:I:OIII:sda2003.fits.gz)

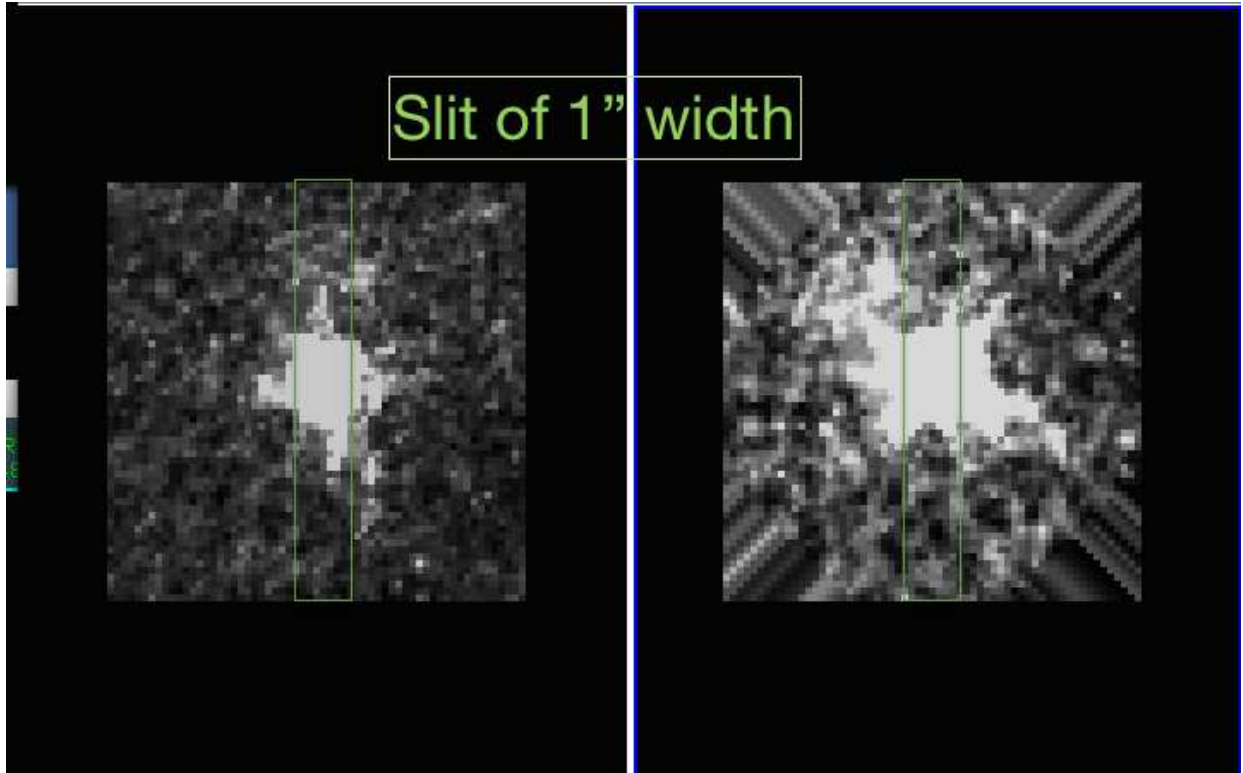


Fig. 10.— Slit size and position angle influence on flux calibration using [O III] emission (see Table 4). Left panel: PA=0, Right panel: same image rotated clockwise by 45 degrees.

Table 4: Slit size and position angle influence on flux calibration using [O III] emission.

PA	Col. range	F_{tot}	F_{slit}
2 arcsec virtual slit			
0	23-42	4.28E-13	4.01E-13
-45	23-42	4.19E-13	4.12E-13
1 arcsec virtual slit			
0	28-37	4.03E-13	3.86E-13
-45	28-37	3.90E-13	3.85E-13

REFERENCES

- Anderson, K., S., 1971, *ApJ*, 169, 449
- Arav, N., Chamberlain, C., Kriss, G. A., et al. 2015, *A&A*, 577, A37
- Armitage, P. J., Zurek, W. H., & Davies, M. B. 1996, *ApJ*, 470, 237
- Begelman, M. C., Blandford, R. D., & Rees, M. J. 1980, *Nature*, 287, 307
- Bentz, M. C., Denney, K. D., Cackett, E. M., et al. 2007, *ApJ*, 662, 205
- Bentz, M. C., Walsh, J. L., Barth, A. J., et al. 2009, *ApJ*, 705, 199
- Bentz, M. C., Denney, K. D., Grier, C. J., et al. 2013, *ApJ*, 767, 149
- Bentz, M. C., & Katz, S. 2015, *PASP*, 127, 67
- Bogdanović, T., S., Britton D., Sigurdsson, S., Eracleous, M., 2008, *ApJS*, 174 , 455
- Bogdanović, T., Eracleous, M., & Sigurdsson, S. 2009, *New A Rev.*, 53, 113
- Bogdanović, T. 2015, *Astrophysics and Space Science Proceedings*, 40, 103
- Bon, E., Jovanović, P., Marziani, P. et al. 2012, *ApJ*, 759, 118
- Bon, N., Popović, L. Č., & Bon, E. 2014, *Advances in Space Research*, 54, 1389
- Bon et al. 2016. in preparation.
- Bouchard, A., Prugniel, P., Koleva, M., Sharina, M., 2010, *A&A*, 513, 54
- Chen, X., Sesana, A., Madau, P., & Liu, F. K. 2011, *ApJ*, 729, 13
- Chakrabarti, S. K., & Wiita, P. J. 1993, *ApJ*, 411, 602
- Chakrabarti, S. K., & Wiita, P. J. 1994, *ApJ*, 434, 518
- Cherepashchuk, A. M., & Lyutyi, V. M. 1973, *Astrophys. Lett.*, 13, 165
- Clavel, J., Reichert, G. A., Alloin, D., et al. 1991, *ApJ*, 366, 64
- Cuadra, J., Armitage, P. J., Alexander, R. D., & Begelman, M. C. 2009, *MNRAS*, 393, 1423
- Czerny, B., Schwarzenberg-Czerny, A., & Loska, Z. 1999, *MNRAS*, 303, 148
- Czerny, B. 2006, *Astronomical Society of the Pacific Conference Series*, 360, 265

- Czerny, B., & Hryniewicz, K. 2011, *A&A*, 525, L8
- De Paolis, F., Ingrosso, G., Nucita, A. A., & Zakharov, A. F. 2003, *A&A*, 410, 741
- Denney, K. D., Peterson, B. M., Pogge, R. W., et al. 2009, *ApJ*, 704, L80
- Denney K., D., 2010, ProQuest Dissertations And Theses; Thesis (Ph.D.)–The Ohio State University, Vol.: 71-11, 101
- Denney, K. D., De Rosa, G., Croxall, K., et al. 2014, *ApJ*, 796, 134
- De Rosa, G., Peterson, B. M., Ely, J., et al. 2015, *ApJ*, 806, 128
- Deuch, A. N. 1966, *IAU Symposium* 29
- Dibai, É. A., Esipov, V. F., & Pronik, V. I. 1968, *Soviet Ast.*, 11, 553
- Dietrich, M., Kollatschny, W., Peterson, B. M., et al. 1993, *ApJ*, 408, 416 optical emission lines of NGC 5548
- Dietrich, M., Bender, C. F., Bergmann, D. J., et al. 2001, *A&A*, 371, 79
- Du, P., Hu, C., Lu, K.-X., et al. 2015, *ApJ*, 806, 22
- Eckart, A., & Genzel, R. 1997, *MNRAS*, 284, 576
- Edelson, R., Gelbord, J. M., Horne, K., et al. 2015, *ApJ*, 806, 129
- Elitzur, M., & Shlosman, I. 2006, *ApJ*, 648, L101
- Elitzur, M. 2008, *New A Rev.*, 52, 274
- Elitzur, M., & Netzer, H. 2016, *MNRAS*, 459, 585
- Elvis, M. 2000, *ApJ*, 545, 63
- Eracleous, M., & Halpern, J. P. 2003, *ApJ*, 599, 886
- Eracleous, M., Boroson, T., A., Halpern, J., P., Liu, J., 2012, *ApJS*, 201, 23
- Fan, J. H., Xie, G. Z., Pecontal, E., Pecontal, A., & Copin, Y. 1998, *ApJ*, 507, 173
- Fausnaugh, M. M., Denney, K. D., Barth, A. J., et al. 2016, *ApJ*, 821, 56
- Flohic, H. M. L. G., & Eracleous, M. 2008, *ApJ*, 686, 138
- Gaskell, C. M. 1983, *Liege International Astrophysical Colloquia*, 24, 473

- Gaskell, C. M. 1988, *ApJ*, 325, 114
- Gaskell, C. M. 2008, *Revista Mexicana de Astronomia y Astrofisica Conference Series*, 32, 1
- Gaskell, C. M., 2009, *New A Rev.*, 55, 140
- Gaskell, C. M. & Klimek, E. S., 2003 *Astronomical and Astrophysical Transactions*, 22, 661
- Gaskell, C. M. & Sparke, L. S. 1986, *ApJ*, 305, 175
- Gezari, S., Halpern, J. P., & Eracleous, M. 2007, *ApJS*, 169, 167
- Gezari, S., Chornock, R., Rest, A., et al. 2012, *Nature*, 485, 217
- Ghez, A. M., Klein, B. L., Morris, M., & Becklin, E. E. 1998, *ApJ*, 509, 678
- Gillessen, S., Eisenhauer, F., Trippe, S., et al. 2009, *ApJ*, 692, 1075
- Goosmann, R. W., Gaskell, C. M., & Marin, F. 2014, *Advances in Space Research*, 54, 1341
- Graham, M. J., Djorgovski, S. G., Stern, D., et al. 2015, *Nature*, 518, 74
- Graham, M. J., Djorgovski, S. G., Stern, D., et al. 2015, *MNRAS*, 453, 1562
- Guo, D., Tao, J., & Qian, B. 2006, *PASJ*, 58, 503
- Guo, D.-F., Hu, S.-M., Tao, J., et al. 2014, *Research in Astronomy and Astrophysics*, 14, 923
- Hayasaki, K., Mineshige, S., Ho, Luis C. 2008, *ApJ*, 682, 1134
- Hayasaki, K., Stone, N. C., & Loeb, A. 2015, *arXiv:1501.05207*
- Hills, J. G. 1975, *Nature*, 254, 295
- Hu, C., Wang, J.-M., Ho, L. C., et al. 2008, *ApJ*, 683, L115
- Ivanov, P. B., Polnarev, A. G., & Saha, P. 2005, *MNRAS*, 358, 1361
- Jovanović, P., Popović, L. Č., Stalevski, M., & Shapovalova, A. I. 2010, *ApJ*, 718, 168
- Kaspi, S., Smith, P. S., Netzer, H., et al. 2000, *ApJ*, 533, 631
- Kaasra, J. S., Kriss, G. A., Cappi, M., et al., 2014, *Science*, 345, 64
- Karas, V., & Šubr, L. 2007, *A&A*, 470, 11

- Katz, J. I. (1997) *ApJ*, 478, 527
- Kieffer, T. F., & Bogdanović, T. 2016, *ApJ*, 823, 155
- Koleva, M., Prugniel, P., Ocvirk, P., Le Borgne, D., Soubiran, C., *MNRAS*, 385, 1998
- Koleva, M., Prugniel, P., Bouchard, A., & Wu, Y. 2009, *A&A*, 501, 1269
- Koleva, M., Prugniel, P., de Rijcke, S., Zeilinger, W. W., 2011, *MNRAS*, 417, 1643
- Koleva, M., Bouchard, A., Prugniel, P., de Rijcke, S., Vauglin, I., 2013, *MNRAS*, 428, 2949
- Kollatschny, W., & Zetzl, M. 2013, *A&A*, 551, L6
- Komossa, S., & Bade, N. 1999, *A&A*, 343, 775
- Komossa S., 2006, *Mem. Soc. Astron. Ital.*, 77, 733
- Komossa, S., Xu, D., Zhou, H., Storchi-Bergmann, T., & Binette, L. 2008, *ApJ*, 680, 926
- Komossa, S. 2015, *Journal of High Energy Astrophysics*, 7, 148
- Komossa, S., & Zensus, J. A. 2016, *IAU Symposium*, 312, 13
- Koratkar, A. P., & Gaskell, C. M. 1991, *ApJ*, 375, 85
- Korista, K. T., Alloin, D., Barr, P., et al. 1995, *ApJS*, 97, 285 ground-based study of NGC 5548
- Kovačević, J., Popović, L. Č., & Dimitrijević, M. S. 2010, *ApJS*, 189, 15
- Koshida, S., Minezaki, T., Yoshii, Y., et al. 2014, *ApJ*, 788, 159
- Kraemer, S. B., Crenshaw, D. M., Filippenko, A. V., & Peterson, B. M. 1998, *ApJ*, 499, 719
- Kun E., Gabányi K. É., Karouzos M., Britzen S., Gergely L. Á., 2014, *MNRAS*, 445, 1370
- Landt, H., Ward, M. J., Steenbrugge, K. C., & Ferland, G. J. 2015, *MNRAS*, 454, 3688
- Lawson, C. L. & Hanson, R. J., *Solving Least Squares Problems*, *Classics in Applied Mathematics* No. 15 (Philadelphia, Penn.: SIAM), 1995
- Le Borgne D., Rocca-Volmerange B., Prugniel P., Lancon A., Fioc M., Soubiran C., 2004, *A&A*, 425, 881
- Lehto, H. J., & Valtonen, M. J. 1996, *ApJ*, 460, 207

- Lewis, K. T., Eracleous, M. & Storchi-Bergmann, T. 2010, *ApJS*, 187, 416
- Li, Y.-R., Wang, J.-M., Ho, L. C., et al. 2016, *ApJ*, 822, 4
- Liu, F. K., Li, S., & Chen, X. 2009, *ApJ*, 706, L133
- Liu, T., Gezari, S., Heinis, S., et al. 2015, *ApJ*, 803, L16
- Liu, J., Eracleous, M., & Halpern, J. P. 2016, *ApJ*, 817, 42
- Lomb, N. R., 1976, *Ap&SS*, 39, 447
- Lyutyi, V. M. 1973, *Astronomicheskij Tsirkulyar*, 777, 1
- Marquardt, D. W., 1963, *SIAM*, 11, 431
- MacFadyen, A. I., & Milosavljević, M. 2008, *ApJ*, 672, 83
- Maoz, D., Smith, P. S., Jannuzi, B. T., Kaspi, S., & Netzer, H. 1994, *ApJ*, 421, 34
- Marziani, P., Sulentic, J. W., Stirpe, G. M., et al. 2016, *Ap&SS*, 361, 3
- Mehdipour, M., Kaastra, J. S., Kriss, G. A., et al. 2015, *A&A*, 575, A22
- Mehdipour, M., Kaastra, J. S., Kriss, G. A., et al. 2016, *A&A*, 588, A139
- Meyer, L., Ghez, A. M., Schödel, R., et al. 2012, *Science*, 338, 84
- Merritt, D. and Milosavljević, M., 2005, *Living Reviews in Relativity*, 8, 8
- Milosavljević, M. and Merritt, D., 2001, *ApJ*, 563, 34
- Magorrian, J., & Tremaine, S. 1999, *MNRAS*, 309, 447
- Nandra, K., George, I. M., Mushotzky, R. F., Turner, T. J., & Yaqoob, T. 1997, *ApJ*, 476, 70
- Netzer, H., Maoz, D., Laor, A., et al. 1990, *ApJ*, 353, 108
- Netzer, H., & Peterson, B. M. 1997, *Astronomical Time Series*, 218, 85
- Netzer, H., & Marziani, P. 2010, *ApJ*, 724, 318
- Netzer, H. 2013, *The Physics and Evolution of Active Galactic Nuclei*, Cambridge, UK: Cambridge University Press
- Netzer, H. 2015, *ARA&A*, 53, 365

- Nikolajuk, M., Papadakis, I. E., & Czerny, B. 2004, MNRAS, 350, L26
- Nguyen, K., & Bogdanovic, T. 2016, arXiv:1605.09389
- Oknyanskij, V. L. 1978, *Peremennye Zvezdy*, 21, 71
- Oknyanskij, V., & Lyuty, V. 2007, *Peremennye Zvezdy Prilozhenie*, 7, 28
- Peterson, B. M., & Gaskell, C. M. 1986, AJ, 92, 552
- Peterson, B. M., Korista, K. T., Cota, S. A., 1987, ApJ, 312, 1
- Peterson, B. M., Balonek, T. J., Barker, E. S., et al. 1991, ApJ, 368, 119 5548 at optical wavelengths
- Peterson, B. M., Alloin, D., Axon, D., et al. 1992, ApJ, 392, 470 5548 at optical wavelengths
- Peterson, B. M. 1997, *An introduction to active galactic nuclei*, Publisher: Cambridge, New York Cambridge University Press, 1997 Physical description xvi, 238 p. ISBN 0521473489
- Peterson, B. M., Barth, A. J., Berlind, P., et al. 1999, ApJ, 510, 659
- Peterson, B. M., Berlind, P., Bertram, R., et al. 2002, ApJ, 581, 197
- Peterson, B. M., Denney, K. D., De Rosa, G., et al. 2013, ApJ, 779, 109
- Pihajoki, P. 2016, MNRAS, 457, 1145
- Plavchan, P., Jura, M., Kirkpatrick, J. D., Cutri, R. M., & Gallagher, S. C. 2008, ApJS, 175, 191
- Popović, L. Č., Shapovalova, A. I., Chavushyan, V. H., et al. 2008, PASJ, 60, 1
- Popović, L. Č., 2012, *New A Rev.*, 56, 74
- Pringle, J. E. 1996, MNRAS, 281, 357
- Ptak, R., L. & Stoner, R., E., 1973, ApJ, 179, 89
- Rees, M. J. 1990, *Science*, 247, 817
- Rieger, F. M., & Mannheim, K. 2000, A&A, 359, 948
- Rix, H.-W., & White, S. D. M., 1992, MNRAS, 254, 389

- Rokaki, E., Collin-Souffrin, S., & Magnan, C. 1993, *A&A*, 272, 8
- Scargle, J. D., 1982, *ApJ*263, 835
- Schmitt, H. R., Donley, J. L., Antonucci, R. R. J., Hutchings, J. B., & Kinney, A. L. 2003, *ApJS*, 148, 327
- Sergeev S. G., 1992, *Ap&SS*, 197, 77
- Sergeev, S. G., Doroshenko, V. T., Dzyuba, S. A., et al. 2007, *ApJ*, 668, 708
- Shapovalova, A. I., Doroshenko, V., T., Bochkarev, N., G., et al., 2004, *A&A*, 422, 925
- Shapovalova, A. I., Burenkov, A. N., Borisov, N., et al., 2006, *Astronomical Society of the Pacific Conference Series*, 360, 239
- Shapovalova, A. I., Popović, L. Č., Collin, S., et al. 2008, *A&A*, 486, 99
- Shapovalova, A. I., Popović, L. Č., Chavushyan, V. H., et al. 2016, *ApJS*, 222, 25
- Shen, Y. & Loeb, A. 2010, *ApJ*, 725, 249
- Sillanpaa, A., Haarala, S., Valtonen, M. J., Sundelius, B., & Byrd, G. G. 1988, *ApJ*, 325, 628
- Slavcheva-Mihova, L., & Mihov, B. 2011, *A&A*, 526, A43
- Smailagić, M., & Bon, E. 2015, *Journal of Astrophysics and Astronomy*, 36, 513
- Smith, H. J., & Hoffleit, D. 1963, *AJ*, 68, 292
- Stalevski, M., Ricci, C., Ueda, Y., et al. 2016, *MNRAS*, 458, 2288
- Steenbrugge, K. C., Kaastra, J. S., Crenshaw, D. M., et al. 2005, *A&A*, 434, 569
- Stellingwerf, R. F. 1978, *ApJ*, 224, 953
- Sudou, H., Iguchi, S., Murata, Y., & Taniguchi, Y. 2003, *Science*, 300, 1263
- Syer, D., Clarke, C. J., & Rees, M. J. 1991, *MNRAS*, 250, 505
- Šubr, L., & Karas, V. 1999, *A&A*, 352, 452
- Torres, G., Andersen, J., & Giménez, A. 2010, *A&A Rev.*, 18, 67

- Tyson, J. A., Fischer, P., Guhathakurta, P., McIlroy, P., Wenk, R., Huchra, J., Macri, L., Neuschaefer, L., Sarajedini, V., Glazebrook, K., Ratnatunga, K., Griffiths, R., 1998, *AJ*, 116, 102
- Ulrich, M. H., 1972, *ApJ*, 174, 483
- Uttley, P., Edelson, R., McHardy, I. M., Peterson, B. M., & Markowitz, A. 2003, *ApJ*, 584, L53
- Valtonen, M., Ciprini, S., 2012, *Mem. Soc. Astron. Italiana*, 83, 219
- Valtonen, M., & Sillanpää, A. 2011, *Acta Polytechnica*, 51, 76
- Valtaoja, E., Teräsranta, H., Tornikoski, M., et al. 2000, *ApJ*, 531, 744
- van der Marel, R. P., 1994, *MNRAS*, 270, 271
- Vaughan, S., Uttley, P., Markowitz, A. G., et al. 2016, *MNRAS*, 461, 3145
- Westman, D. B., MacLeod, C. L., & Ivezić, Ž. 2011, *Astronomical Data Analysis Software and Systems XX*, 442, 159
- Witzel, G., Ghez, A. M., Morris, M. R., et al. 2014, *ApJ*, 796, L8
- Wu, Y., Singh, H. P., Prugniel, P., Gupta, R., Koleva, M., 2011, *A&A*, 525, 71
- Zu, Y., Kochanek, C. S., & Peterson, B. M. 2011, *ApJ*, 735, 80
- Zucker, S., Alexander, T., Gillessen, S., Eisenhauer, F., & Genzel, R. 2006, *ApJ*, 639, L21